On the Digital Re-Design of an Analogue Missile Flight Control System Using the PIM Method

Chuk Man Ng

Department of Mechanical Engineering
McGillUniversity
Montreal, Canada

Final Report

Date delivered: 15th March, 2000

for

Government of Canada
Department of National Defence
Defence Research Establishment Valcartier
Val-Bélair, Québec, Canada

under

PWGSC Contract No. W7701-7-3104/001/XSK

Scientific Authority: Mr. Marc Lauzon

Regional Science Contracting Officer: Ms. Geneviève Arcand
Eastern Quebec Region

Executive Summary

The rapid developments in computer technology over the past decades have fostered the design and production of more effective and robust weapon systems. The advent of powerful processors now extends the capability of weapon control systems through the use of digital processing. Today's design of control systems employs both traditional methods developed originally for analogue controllers as well as new methods developed specifically for digital controller design. A modern digital controller can be developed solely using digital design methods but the preferred approach is often to design an analogue controller and convert it to a digital one before final implementation in the weapon system processor.

The present report explores the Plant-Input Mapping (PIM) method developed by Dr. H. Nori and his colleagues at McGill University for converting an analogue controller realisation to a digital one. One key feature of this method compared to other digital re-design methods is the reduced processing power needed, an advantage that is of primary importance for lower-speed and lower-capacity microprocessors of tactical missiles. The applicability and limitations of the PIM method were specifically demonstrated in the present project, in the conversion of a tactical air-to-air missile analogue autopilot design to a digital realisation. Two versions of the PIM method were initially investigated, namely, the multiple-input multiple-output (MIMO) and the multiple-loop PIM methods. A comparison of these two versions based on design procedure, implementation structure and characteristics of the resulting digital controller showed that they were equally effective. Based on the observed limitations, a weighted reduced-order version of the PIM method was developed that is better suited to the low order digital controller that is used in missile autopilots. The use of a weighting matrix in this version of the PIM method provides an additional degree of freedom to tune the characteristics and performance of the digital realisation.

The three variants of the PIM method investigated in the present research project were found to be suitable for the conversion of the analogue autopilot controller design to a digital realisation. An analysis of the autopilot digital realisations and a comparison with the analogue controller design identified key parameters that influence the performance of the digital controller. Future work is required on the comparison of the PIM method and other analogue-to-digital re-design methods currently in use, to fully identify the applicability and limitations of the PIM method in the design of weapon digital controllers.

Abstract

This research examines some of the ways to design a digital control system with particular reference to the control of yaw plane dynamics of an air-to-air missile model. Specific attention is paid to compare two methods of global digital re-design of validated analogue closed loop control system. These two methods are the multi-input multi-output (MIMO) Plant Input Mapping (PIM) method and multi-loop PIM method. The thesis will first show how a specific class of closed loop MIMO feedback systems with a single-input multi-output (SIMO) plant can be re-structured as multi-loop control systems, which includes the closed loop missile control system. Some special characteristics pertaining to SIMO systems for control system design are explored. The aforementioned two methods of PIM global digital re-design are then applied to the MIMO analogue missile control system and its re-structured multi-loop counterpart. A comparison of the two methods is made on its design procedure, implementation structure and results from computer simulation. The later is carried out by exercising a qualitative comparison of the plant input and closed loop system output signals subjected to a step input, as well as a quantitative comparison of the norms of the resulting plant input errors and closed loop system errors. The investigation shows, by looking into the design procedure associated with the two PIM methods, that the MIMO formulation theoretically gives at least marginally better sampled-data system performance than the multi-loop formulation when the number of system output is greater than two. Results from computer simulation confirms that finding, particularly at lower sampling frequencies.

This thesis also touches upon the topic of controller order reduction, particularly in consideration of the PIM digital re-design of analogue feedback systems. A weighted reduced order PIM formulation is proposed, and some guidelines and practical consideration for the design are given. By prescribing specific feature to the weighting matrix used in the problem formulation, all rapprochement properties of the resultant sampled-data system remain valid. It is shown that this method gives a larger set of stabilizing digital controllers a designer may employ for the PIM method. Therefore, in effect, the addition of the weighting matrix gives the designer an extra degree of freedom to tune the characteristics and performance of the sampled-data system.

Sommaire

Cette recherche examine quelques unes des manières qui permettent la conception d'un système de commande numérique avec application pour la commande du modèle d'un missile. L'emphase est mise sur la comparaison de deux méthodes de reconception numérique globale en rapport avec un système de commande analogue à boucle fermeé. Ces deux méthodes sont la méthode de Correspondance d'Entrée du Système sous Contrôle (CESC ou PIM en anglais) telle qu'appliquée à des systèmes à de multiples entrées et multiples sorties (MEMS) et la méthode CESC à multiples boucles. Cette thèse va premièrement démontrer comment une certaine classe de systèmes à boucle fermée à multiples entrées et sorties, reliés à un système sous contrôle ayant une simple entrée et de multiples sorties (SEMS), peuvent être restructurés en tant que systèmes de commande à multiples boucles. Ces dernières incluent le système de commande pour missile.

L'étude démontre, à partir des procédures de conception associées aux deux méthodes CESC, que la formulation MEMS donne, théoriquement, une performance des systèmes à données échantillonnées supérieure à celle obtenue avec formulations de systèmes à boucles multiples lorsque le nombre de signaux de sortie du système est supérieur à deux. Les résultats obtenus des simulations confirment cette découverte, plus particulièrement a des fréquences d'échantillonnage lentes.

Cette thèse considère aussi le sujet de la réduction de l'ordre du bloc de commande, plus particulièrement en rapport avec la méthode de reconception numérique CESC. Une formulation appelée méthode CESC à ordre réduit avec matrice de calculs est proposée. Quelques régles et considérations pratiques sont établies. En contraignant certaines caractéristiques de la matrice de pondération, toutes les propriétes du système de commande à données échantillonnées restent valables. Il est démontré que cette méthode permet d'obtenir un plus grand groupe de contrôleurs numériques qui stabilisent le système à boucle fermée qu'en stabilisant le système avec la méthode CESC. La matrice de pondération ajoute un degrée de liberté pour améliorer les caractéristique et la performance du système de commande à données échantillonnées.

大衛的詩。

1 耶和華是我的牧者，我必不至缺乏。
2 他使我躺卧在青草地上、領我在可安歇的水邊。
3 他使我的靈魂甦醒、爲自己的名引導我走義路。
4 我雖然行過死蔭的幽谷、也不怕遭害，因爲你與我同在，
你的杖、你的竿、都安慰我。
5 在我敵人面前、你爲我擺設筵席，你用油膏了我的頭、
使我的福杯滿溢。
6 我一生一世必有恩惠慈愛隨著我，我且要住在耶和華的殿中、
直到永遠。

詩篇第二十三篇

Dedicated to my parents

給親愛的父母

Acknowledgment

I would first like to thank my thesis supervisor Prof. Noriyuki Hori wholeheartedly and most sincerely for his much helpful advice and never-ending support throughout this research, as well as for his much patience in helping me to understand difficult concepts during the course of the Master's program. Dr. Hori's often unique prospective in analyzing and solving engineering problem is always refreshing, motivating and enlightening. I would also like to thank Prof. Peter Caines for lecturing a very inspiring non-linear control systems course in my last semester, and Prof. Hannah Michalska for giving several insightful discussions on multivariable control systems in the early stages of this research, and taking me as a teaching assistant for the undergraduate control systems course with the department of electrical engineering which was a splendid experience. I would also like to express much gratitude to Marc Lauzon of Defence Research Establishment Valcartier (DREV), Department of National Defence (DND) Canada. Marc first introduced me to the topic of control systems two year ago during my summer work at DREV. His interest and enthusiasm in the current work gave me much courage to pursue this research.

As I found out, a master's thesis is by all means quite a bold and serious undertaking. Reflecting on two years of work, there has certainly been many moments of triumph and disappointment. On a more personal note, I would like to embrace much encouragement I have received from Vai-Man (Walter) Lei and David Venditti throughout the duration of this research. Indeed, every 0.1N of thrust I gathered helped to push the project forward. I would also like to express much gratitude to Miguell Torre-Torriti, Joel Foucault, Christine Desmarais, Aurelle Larrivé, Duyen Nguyen, Mau Hiep Nguyen, Ziv Lu, David Guo and Nick Pratley, as well as to many brothers and sisters at the Montreal Chinese Alliance Church, particularly to Ian and Ming Lai, Garry Chu and Michelle Kuan, Johnny Wong, Alice Lee, Kit Fong Ng, John Yeong, Joshua Lam, as well as Simon Wong. Their encouragement during the last few weeks of the completion of this thesis provided much comfort in my race towards the checker flag.

These last two years have been a thrilling experience in learning. I discovered control engineering is indeed a very interesting, rich and dynamic subject. Within our control systems research group in the department of mechanical engineering, I thoroughly enjoyed many challenging and stimulating discussions with Dr. C. Alain Rabbath and Mr. K.-K. Ro. These led to new and previously un-thought-of ideas that gave us more theoretical and practical insights into many control related topics. I will surely miss these wonderful times that we fostered together.

I would like to thank the Defence Research Establishment Valcartier (DREV), a Research and Development Branch of National Defence Canada, for providing the financial support for this project during the past two years. Also, I would like to thank Prof. Venkat Krovi of the department of mechanical engineering and Richard Lestage of DREV for reviewing this thesis and providing many constructive suggestions.

Last but not least, I would like to say "thank you" to my parents. Throughout my university studies, they have given me much encouragement and supported me with much persevering love, particularly during the last several months. I can only express my thankfulness with many unspeakable words. This modest thesis is dedicated to them with the most unreserved gratitude.

This thesis contains slightly more than 32,000 words.

Chuk Ng
Montreal, August 1999.

Content

Notation and Symbols

List of Acronyms

Chapter 1
Introduction
1.1 Prologue 1
1.2 Motivation and Previous Work 1
1.3 Objectives 3

Chapter 2
Discrete-Time Control Systems and Missile Dynamics
2.1 Discrete-Time Operators and Systems 8
2.2 Discrete-Time Models 16
2.2.1 Invariant Models 16
2.2.2 Mapping Models 18
2.2.3 Pole-Zero Matching Models 20
2.3 Design Overview 21
2.4 Indirect Design of Discrete-Time Controller 23
2.5 Local Discretization Methods 24
2.5.1 Some issues with Local Discretization 27
2.6 Plant Input Mapping (PIM) Method 28
2.6.1 General Framework 28
2.6.2 PIM method for MIMO systems 30
2.6.3 PIM method for SISO systems 36
2.6.4 PIM method for Multi-Loop systems 40
2.6.5 Reduced Order PIM method for SISO systems 43

2.7 Implementation of Discrete-Time Systems 45
2.7.1 Realization Structure of Digital Controllers 46
2.7.2 Direct Form Structure 47
2.7.3 Cascade Form Structure 48
2.7.4 Parallel Form Structure 48
2.7.5 State Space Form Structure 48
2.7.6 Representation of Numbers 49
2.7.7 Quantization of Digital Controller Coefficients 49
2.7.8 Quantization of Signals 51
2.7.9 Overflow 51
2.7.10 Limit Cycle Oscillation 51
2.8 Overview of Missile Flight Control Systems 52

Chapter 3
PIM Digitally Re-designed Missile Control System
3.1 Analogue Missile Control System 57
3.1.1 Missile Dynamic Model 57
3.1.2 Missile Control System 59
3.2 Characteristics of the continuous-time closed loop system 62
3.3 Comparison of MIMO and Multi-Loop PIM methods 66
3.3.1 A Glimpse of SIMO Systems 66
3.3.2 General Comparison of Multi-Loop PIM method with MIMO PIM method .. 78
3.4 Digital Re-Design: A Case Study 82
3.4.1 Local discretization of missile flight controller 82
3.4.2 Application of MIMO PIM method 85
3.4.3 Application of Multi-Loop PIM method 93
3.4.4 Reduced Order Multi-Loop PIM method 98
3.5 Analysis of Digitally Re-Designed Missile Control Systems 100
3.5.1 Overview of Criterias of Comparison 100
3.5.2 Fairness of Comparison 102
3.5.3 Digital Control of Missile Yaw Plane Dynamics 102

Chapter 4
Controller Order Reduction For PIM Methods: Further Exposition
4.1 Principles of Low Order Controller Design: A PIM Prospective 113
4.2 Reduced-Order PIM method for SISO systems: A re-visit 114

4.2.1 A Modified Reduced-Order PIM Method 115
4.3 Consideration for reduced-order Controller Design 127
4.4 Further Comments 130

Chapter 5
Conclusion
5.1 Research Contribution 132
5.2 Future Research Work 133
5.3 Epilogue 134

Blibliography

Appendix

List of Figures

2.1 : Block diagram of a basic digital control diagram. 7
2.2 : Structure of the invariant model 17
2.3 : Three approaches in designing discrete-time control systems 23
2.4 : A 2-DOF SISO feedback analogue compensator design 25
2.5 : A 2-DOF feedback discrete-time feedback control system 25
2.6 : Continuous-time control system considered for applying PIM digital re-design. 30
2.7 : Sampled-data system results from applying the PIM digital re-design 31
2.8 : An analogue 2-loop feedback SISO system 41
2.9 : Focusing on the innermost loop 41
2.10 : Performing a re-design of the outer loop 42
2.11 : PIM digitally re-designed 2-loop sampled-data system 42
2.12 : A typical air-to-air missile block diagram 53
2.13 : A schematic diagram of missile dynamics 55
3.1 : Configuration of a statically stable, tail-controlled air-to-air missile. 57
3.2 : Step response of the open loop system 59
3.3 : Architecture of the analogue missile flight control system 60
3.4 : Step input response of the closed loop system (with $\bar{rr} = 0$) 63
3.5 : Bode diagram of transfer function from reference input to the actual output of the analogue closed loop system. 63
3.6 : Plot of principal gains for the sensitivity of the analogue system 65
3.7 : Plot of principal gains for the analogue system transfer function 65
3.8 : A simple SIMO system with two feedback loops 67
3.9 : First step in re-structuring the two-loop SIMO system 68
3.10 : The final modified SIMO system 69

3.11 : A re-configured SIMO feedback control system 74
3.12 : A MIMO feedback system with one non-zero reference input 75
3.13 : A re-organized feedback system with the non-zero reference input now corresponds to the first system output 75
3.14 : The final re-organized MIMO system 76
3.15 : Comparison of the Multi-Loop with the MIMO PIM method 79
3.16 : Plot of as a function of frequency 84
3.17 : Digitally re-designed missile control system using MIMO PIM method. 92
3.18 : The re-structured multi-loop analogue missile control system. 93
3.19 : Multi-loop sampled-data system digitally re-designed using PIM method 98
3.20 : Step response of the sampled-data system obtained for T = 0.01 sec. (a) plant input signal u, (b) lateral acceleration of missile 104
3.21 : Step response of the sampled-data system obtained for T = 0.02 sec. (a) plant input signal u, (b) lateral acceleration of missile 105
3.22 : Step response of the sampled-data system obtained for T = 0.1 sec. (a) plant input signal u, (b) lateral acceleration of missile 106
3.23 : (a) and (b) 107
3.24 : Step response of the sampled-data system obtained for T = 0.01 sec. (a) plant input signal u, (b) lateral acceleration of missile 108
3.25 : Step response of the sampled-data system obtained for T = 0.02 sec. (a) plant input signal u, (b) lateral acceleration of missile 109
3.26 : Step response of the sampled-data system obtained for T = 0.1 sec. (a) plant input signal u, (b) lateral acceleration of missile 110
4.1 : Basic approaches in low order controller design 113
4.2 : The sets Π and Πw where 126
4.3 : Step response of the sampled-data system obtained for T = 0.02 secs. using multi-loop PIM digital re-design, (a) plant input signal $\bar{u}$, (b) lateral acceleration of missile 128
4.4 : With n = 2, (a) plant input signal $\bar{u}$, (b) lateral acceleration of missile 128
4.5 : With n = 1, i.e. order of digital controllers is the same as continuous-time system, (a) plant input signal $\bar{u}$, (b) lateral acceleration of missile 129

List of Tables

2.1 : Comparison of properties of the e and z operator 15
2.2 : Several approximations used in mapping models 19
3.1 : Discrete-time Models of expressed in e 83
3.2 : Discrete-time Models of expressed in z 84

Notation and Symbols

$\mathbf{R}$	field of real numbersl
$\mathbf{R}^+$	field of non-negative real numbers
$\mathbb{Z}$	field of integers
$\mathbb{Z}^+$	field of non-negative integers
$\forall$	for any
$\in$	belong to
$\subset$	subset
D	end of definition or theorem
B	end of proof
c	end of remark
$\bar{\sigma}(A)$	largest singular value of A
$\underline{\sigma}(A)$	lowest singular value of A
$\|\cdot\|_{L_2}$	L_2 norm of continuous-time signal
$\|\cdot\|_{L_\infty}$	L_∞ norm of continuous-time signal
$R_p(\rho)$	the set of rational proper transfer function matrices
RH_∞	the set of real proper (transfer) functions that are analytic in $\mathrm{Re}(s) > 0$.

s	variable for the Laplace transform
z	variable for the z-transform
ε	variable for the E-transform
K_a, K_ψ, K_r	gain constants for the analogue missile control law
$\bar{P}_a$	continuous-time actutor dynamic model
$\bar{P}_m$	continuous-time missile yaw-plane dynamic model
$\bar{S}(s)$	continuous-time sensitivity function
$\bar{\Phi}(s)$	continuous-time plant-input transfer function
$\bar{T}(s)$	continuous-time closed loop system transfer function
$\widehat{X}$	least square estimator
$\widehat{X}_w$	weighted least square estimator

List of Acronyms

A/D	Analogue-to-Digital
CG	Centre of Gravity
D/A	Digital-to-Analogue
DC	Direct Current
DERA	Defence Evaluation and Research Agency (U.K.)
DREV	Defence Research Establishment Valcartier (Canada)
DOF	Degrees-of-Freedom
DSP	Digital Signal Processing
FOH	First-Order Hold
FWL	Finite Word length
LTI	Linear, Time-Invariant
MIMO	Multi Input-Multi Output
MPZ	Matched Pole-Zero/Pole-Zero Matching
ORHP	Open Right-Half-Plane
OLHP	Open Left-Half-Plane
PIM	Plant Input Mapping
PITF	Plant Input Transfer Function
SIM	Step Invariant Model
SIMO	Single Input-Multi Output
SISO	Single Input-Single Output
ZOH	Zero-Order Hold

Chapter 1

Introduction

1.1 Prologue

The digital control of dynamic systems is concerned with the control of physical systems with a digital computer or microprocessor. The design of digitally-controlled systems has matured significantly since the dawn of the Apollo space program. During the recent two decades, aided by the rapid increase in processing power from available microprocessors, scientists and engineers have been able to design and implement increasingly sophisticated control algorithms for more complex systems. At the same time, there has been a considerable growth in practical and theoretical knowledge of control systems and theory for continuous-time and discrete-time systems due to progresses made by researchers in industry, government laboratory and educational institution. The availability of convenient and capable software also facilitated these developments. The result is that, today, designers have a rich amount of resources available for their analysis, design and implementation of control systems. Examples of electromechanical servomechanism exist in automobiles, mass-transit vehicles, automated manufacturing systems, food processing plants, oil refineries, as well as in complex aerospace systems such as aircraft, spacecraft, satellites, and missile.

1.2 Motivation and Previous Work

The digital control of dynamic systems is well detailed in texts by Åström et al. [47] and Franklin

et al. [55], as well as in a survey by Hanselmann [11]. A more in-depth study of discrete-time models of continuous-time systems is given by Hori et al. in [30]. There are many different approaches to designing discrete-time controllers for a continuous-time system in a feedback configuration. The simplest and most conventional approach involves the approximation of pre-designed continuous-time controller transfer functions with discrete-time ones using some particular scheme. This process is therefore suitably called *local* discretization, since the discretization is applied locally only to the controller without consideration for the overall closed loop system performance. To account for this, Markazi et al. in [29] and Markazi in [38] proposed a discretization method called the Plant Input Mapping (PIM) method which is directly applicable to single input-single output (SISO) as well as multi input-multi output (MIMO) systems. This method is based on the discretization of the transfer function from the reference input of the closed loop system to the input of the plant using the standard Pole-Zero Matching (MPZ) method. Therefore the PIM method, appropriately termed a *global* digital re-design method, takes into account the continuous-time closed loop system performance in the formulation of a discrete-time closed loop control system. The result guarantees closed loop stability for all non-pathological sampling periods [50].

More recently, Ro et al. in [35] proposed an extension of the PIM method that can be used for multi-loop control systems, and Rabbath et al. in [32] presented a controller order reduction technique applicable to the PIM digital re-design method for SISO systems. Viewing a discrete-time controller as a digital filter, it is well known that numerical inaccuracy increases with the order of the digital filter as a result of finite word length effects [37] & [17]. Therefore, it is desirable to reduce the order of digital controllers during discrete-time control system design in as much to avoid such a problem. However, as in general with controller order reduction, this ordinarily represents a trade-off in the sampled-data system performance. Thus it is necessary to establish some practical guidelines for employing such method in the context of the PIM design for SISO systems. Also, in light of the work published in [35], it is possible to set up a framework such that the controller order reduction technique may be applied to multi-loop control systems in association with the application of the PIM digital re-design method.

In the PIM digital re-design of MIMO systems proposed in [38] and multi-loop systems in [35], it

is possible in general to re-structure strictly single input-multi output (SIMO) systems as multi-loop systems. Hence a SIMO system can be treated as a MIMO system as well as a multi-loop system, when appropriate, for carrying out a digital re-design of the continuous-time system. Each formulation will likely lead to a different, resultant discrete-time control system structure, and thus, two different systems will also likely bear different outputs irrespective of whether the digital controllers are subjected to finite word length floating-point or fixed-point arithmetic. However, a comparison of the implementation of these two different PIM methods have not been studied.

In the automatic control of missile, Garnell [45], Cloutier et al. [8] and Blakelock [46] gave accounts of many different aspects of the design of missile flight control systems. They include exposition of the different elements that comprise a missile flight control system, design of a missile autopilot and guidance system, calculation of an aerodynamic transfer function of a missile, and analysis of different dynamics of a missile. The presentations are addressed exclusively in the continuous-time domain in these works. In a recent technical report published by DERA [42], the effects of some conventional digital implementation methods on a missile flight control system are examined. Unfortunately, there seems to be inaccuracies in the analysis carried out in that report which resulted in an unstable closed loop system and thus most of the investigation is questionable.

More details of previously published work is presented in Chapter 2 and Chapter 3 of this thesis.

1.3 Objectives

This thesis examines and compares the digital re-design of a continuous-time control system using the PIM methods in the MIMO and multi-loop settings. It is organized as follows. First of all, in Chapter 2, an overview of discrete-time control system design is given, along with some relevant previously published results. The different PIM methods investigated by various authors are recapitulated, and some of their theoretical results are presented mostly without proofs. In Chapter 3, the MIMO PIM method and the multi-loop PIM method are applied to a missile

control system. The study outlines the conditions when a SIMO or MIMO system can be represented as a multi-loop system as well as some of its distinctive features and properties. The investigation compares these two different methods of PIM in terms of their design procedure and simulation results. Most commonly used local discretization methods are also applied to the analogue missile control system to enable a more complete understanding of its effect of digital implementation. In addition, a simple framework is proposed in which the method of reduced order PIM can be applied to multi-loop systems.

Chapter 4 looks at several issues with controller order reduction in the context of the PIM methods. Since it is possible for the PIM methods to yield discrete-time controllers with the same number of states as the modelled plant, it is expected that numerical problems due to the finite word length effect may be noticeable under fixed point calculation for plants with a large number of states. A modified reduced-order PIM method for SISO systems which includes a weighting term in the problem formulation is proposed. This modification enlarges the set of lower-order controllers that can bring closed loop stability to the discretized system.

The continuous-time control system considered here is a missile autopilot for controlling the yaw-plane dynamics of a tail-controlled air-to air missile concept. The analogue control law uses the Raytheon 3-loop design to control the lateral acceleration of the missile, and the closed loop system yields desirable performance in the continuous-time domain.

The use of PIM methods to obtain a discrete-time control system for a missile autopilot is worth a special interest in that a PIM digitally re-designed system typically allows the use of a much slower sampling rate to achieve the kind of performance found in other sampled-data systems obtained from local discretization methods. This translates into the possibility of using less powerful and thus cheaper hardware on-board a missile. The irony is that, while an agile missile is usually a piece of sophisticated hardware with complex system integration capable of high performance, it is often used only once during its operation: it strikes and destroys the target. Therefore, it is highly desirable to reduce production cost as much as possible without sacrificing its designed performance and functionality. Hence a PIM based discrete-time control system offers a possible solution, at least for classically designed missile autopilots. Or put another way,

more computational resources can be devoted to other sub-systems of the missile electronic hardware using PIM based discrete-time control systems. A brief description of missile flight control systems is given in Section 2.8.

Chapter 2

Discrete-Time Control Systems and Missile Dynamics

This chapter presents a basic overview of discrete-time control systems and some previously published results related to PIM methods.

To control a system means to alter its dynamics so that a desired behaviour is obtained. This can be done through feedback. A typical block diagram structure of the closed loop feedback control of analogue dynamic system using digital controllers is sketched schematically in Figure 2.1. It typically comprises the following physical elements: (a)"plant", (b)sensor, (c)analogue-to-digital converter, (d)digital controller, (e)digital-to-analogue converter, and (f)control actuator.

The plant is the dynamic system to be controlled, and physical systems are inevitably analogue systems. For example, consider the cruise-control function inside a common automobile: the plant can be a mathematical model of the automobile that describes the input to output relation, the gasoline supply the plant input, and the vehicle speed the plant output. The sensor is used to measure, or "observe", the output of the plant. This analogue signal is fed to the controller via an analogue-to-digital (A/D) converter which converts the analogue sensor output signal to a digital one. It is also called a *sampler*, as it samples the sensor output signal at a certain time interval T, called the *sampling period*. For simplicity, T is assumed to be a constant quantity throughout this thesis. The digital controller can be a hardware device with specifically written software that performs the necessary calculation to generate an input signal to the control actuator, which in turn supplies the actual physical input to the plant so that it behaves in a satisfactory fashion. The

digital controller takes on the form of a digital computer or, in a smaller scale, some microprocessing units or digital signal processing (DSP) microchips.

In between the digital controller and the control actuator, a digital-to-analogue (D/A) converter is used to change the controllers output in a digital signal form back to an analogue one. It is also commonly called the *hold device*. The reason for that is its capability to hold the output signal of the controller at some value in between the sampling instant, when the digital controller output is actually zero, when viewed from the continuous-time domain. In many control system analyses, a zero-order hold (ZOH) device is used, which simply maintains the same control actuator input signal throughout the sampling period. For real-time (on-line) control purposes, there are more advanced hold devices that can be used such as a predictive higher-order hold circuit [47]. Referring back to the automobile cruise control example, the control actuator may be an electric motor with gearing assembly or a miniature hydraulic actuator that regulates the fuel supply (input) to the engine of the car (plant). This sequence of events is illustrated symbolically in a control block diagram in Figure 2.1.

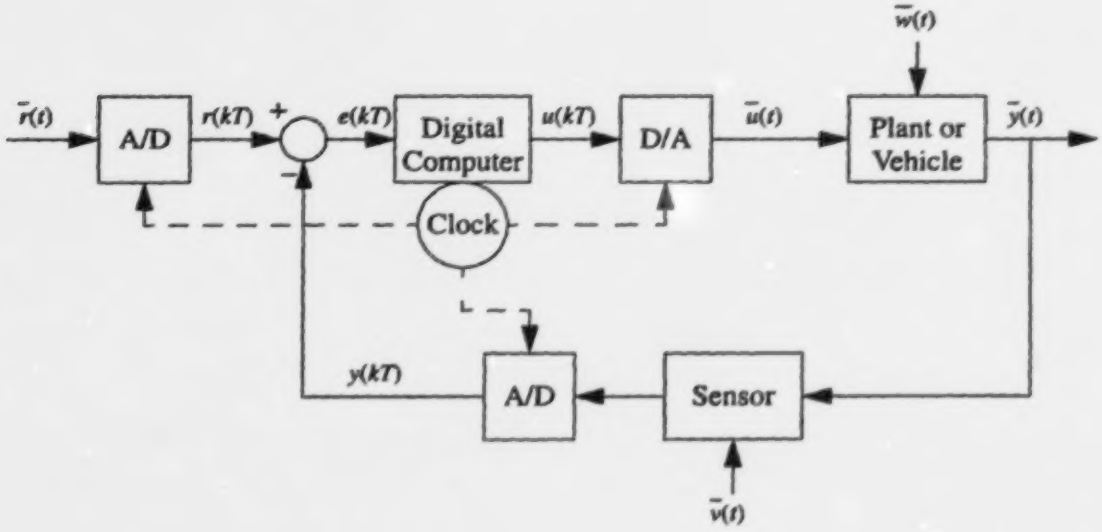

Figure 2.1: Block diagram of a basic digital control diagram

The reference input $\bar{r}$ is the signal in which the output of the closed loop control system y is designed to approach, e.g. the "set" speed of the car, and $\bar{w}$ and $\bar{v}$ are disturbance and noise signals

that appear in real life; they affect the plant and sensor outputs respectively. Figure 2.1 illustrates that discrete-time control systems typically possess both continuous-time and discrete-time signals, thus they are also called *sampled-data systems* because continuous-time data are sampled before being used by digital controllers to calculate control actions [55].

The following two sections present some definitions and features of discrete-time systems, operators and models.

2.1 Discrete-Time Operators and Systems

The systems that this thesis considers are proper, linear, and time-invariant (LTI) systems. Continuous-time LTI systems can be described in a number of ways. For control systems analysis, they are commonly described in the state space form and transfer function form, the latter using the Laplace (differential) operator s [57] & [54]. Discrete-time LTI systems are usually expressed in terms of a set of finite difference equations as well as in the transfer function form. In the later case, a number of discrete-time operators can be used to describe the input to output relation. The shift (q) and z operators[1] are commonly used in control literature [47] & [55]. Their simple relationship with the finite difference equation allows an easy mechanism of constructing a transfer function and implementing the algorithm in hardware and software form. There are extensive studies for the use of the q and z operators in Digital Signal Processing (DSP). However, for control systems application, the drawback in using these operators is that the output of the discrete-time system does not correspond to the continuous-time result when the sampling period of the discrete-time system approaches zero [27].

Another discrete-time operator that can be used is the Euler operator, defined as

$$\varepsilon = \frac{z-1}{T} \quad . \tag{2.1}$$

1. A strict definition refers to q as the shift operator used in difference equation, and z is the corresponding transform variable used in transfer function representation. In practice, they are often used interchangeably. It is referred to as the z operator in this thesis.

This is proposed by Middleton et al. [17][1] & Hori et al. [25] to bridge the gap between continuous-time and discrete-time results. The characteristics of discrete-time systems expressed in the ε operator are shown to approach the continuous-time counterparts as the sampling rate increases. Moreover, the advantages of using the ε operator in discrete-time systems are that it has superior finite word length coefficient representation, superior finite word length error performance and superior numerical properties in calculations with discrete-time models when compared with the z operator. These are highly valued features for the design of practical discrete-time control systems. In addition, in consideration of real-time calculation, a digital controller expressed in the Euler operator only requires past data to calculate the present output, thus making it suitable for on-line control applications.

There are analysis for employing other discrete-time operators in digital control and filtering. The synthesis of digital control law in the w domain[2] is reported by Whitbeck et al. and Ha et al. in [23] & [10] respectively. It is shown that there are many advantages of using the w operator, defined as

$$w = \frac{2}{T} \cdot \frac{z-1}{z+1} \quad . \tag{2.2}$$

For example, the w domain models the sampling and data-hold operations exactly regardless of the sampling rate employed, such that the non-minimum phase effects of the data-hold operation [5] becomes clearly evident. Moreover, the w variable is analogous to the s variable in the sense that all familiar frequency domain design concepts, procedures, and interpretations can be carried over directly. Furthermore, the w variable approaches the continuous-time s variable as the sampling interval approaches zero. These are favourable properties for designing discrete-time control systems. However, since the relative degree of the w operator in z is zero, present-time data is required to compute the present controller output. This creates problems for systems with long computational time when compared with the sampling period. Thus, the designed control algorithm is customarily written in the z operator form for real time computation. A summary of the comparison of the w and other operators are shown by Hori in [27].

---

1. It is referred to as the delta (δ) operator in [17].
2. This is equivalent to the w' operator in older literature.

The discrete-time systems that appear in this thesis are expressed in the Euler and z operators. To facilitate the exposition of some concepts and properties of discrete-time models and their equivalence, the following definitions are given.

Definition 2.1 (Cormier [36] and Mori et al. [24])
A continuous-time signal is a function $\bar{f}(t)$, $\bar{f} : \mathrm{R} \rightarrow \mathrm{R}$, where the time $t \in \mathrm{R}$ is a real and independent variable. A discrete-time signal is a function $f(kT)$ which is defined only at discrete instants kT, where $k \in \mathbb{Z}$ is an integer, and $T \in \mathrm{R}^{+}$ is a discrete-time interval which is positive and real.D

Definition 2.2 (Mori et al. [24])
Assume that a continuous-time system $\bar{S}$ and a discrete-time system S are causal and have zero initial state. Also assume that their respective inputs $\bar{u}(t)$ and $u(kT)$ are zero for $t < 0$ and finite for a finite t. Denote the outputs of the continuous-time and discrete-time systems as $\bar{y}(t)$ and $y(kT)$, respectively. The discrete-time system S is then said to be a discrete-time *model* of the continuous-time system $\bar{S}$ if the following condition is satisfied:
For an arbitrary and fixed $t \in \mathrm{R}$, if

$$\lim_{T \rightarrow 0} |\bar{u}(t) - u(kT)| = 0 \tag{2.3}$$

then it implies

$$\lim_{T \rightarrow 0} |\bar{y}(t) - y(kT)| = 0 \tag{2.4}$$

where $k \in \mathbb{Z}$ is an integer such that $kT \leq t < (k+1)T$.D

Consider the above definition for the input and output of an analogue plant in a closed loop setting. A discrete-time plant is a discrete-time model of the continuous-time system if the output of the digitally controlled plant model approaches its continuous-time value as the plant input supplied by the digital controller also approaches its continuous-time complement, as the sampling period approaches zero.

Theorem 2.3 (Hori et al. [27])

Let a continuous-time system be given in state space form as

$$\begin{aligned} s\bar{x}(t) &= \bar{A}\bar{x}(t) + \bar{B}\bar{u}(t) \;\; ; \;\; \bar{x}(0) = 0 \\ \bar{y}(t) &= \bar{C}\bar{x}(t) + \bar{D}\bar{u}(t) \end{aligned} \tag{2.5}$$

Then, any discrete-time system which can be expressed in the following form is a discrete-time model of the above continuous-time system:

$$\begin{aligned} \varepsilon x(kT) &= (\bar{A} + \Delta\bar{A})x(kT) + (\bar{B} + \Delta\bar{B})u(kT) \;\; ; \;\; \bar{x}(0) = 0 \\ y(kT) &= (\bar{C} + \Delta\bar{C})x(kT) + (\bar{D} + \Delta\bar{D})u(kT) \end{aligned} \tag{2.6}$$

where

$$\lim_{T\to 0} \Delta\bar{A} = 0 \;,\; \lim_{T\to 0} \Delta\bar{B} = 0 \;,\; \lim_{T\to 0} \Delta\bar{C} = 0 \text{ and } \lim_{T\to 0} \Delta\bar{D} = 0 \;. \tag{2.7}$$

The $\Delta\cdot$ terms are independent of ε, but they depend on $\bar{A}$, $\bar{B}$, $\bar{C}$, $\bar{D}$ and T, as well as the method of discretization.D

Theorem 2.3 gives the criteria of connecting a discrete-time model with its continuous-time system in the state-space form. The following theorem provides a description of the similar idea for a SISO system in the transfer function form.

Theorem 2.4 (Mori et al. [24])

Suppose a SISO continuous-time system is given by

$$\begin{aligned} \bar{G}(s) &= \bar{C}(sI - \bar{A})^{-1}\bar{B} + \bar{D} \\ &= \frac{\bar{n}(s)}{\bar{d}(s)} \\ &= \frac{\bar{b}_n s^n + \bar{b}_{n-1}s^{n-1} + \ldots + \bar{b}_1 s + \bar{b}_0}{\bar{a}_n s^n + \bar{a}_{n-1}s^{n-1} + \ldots + \bar{a}_1 s + \bar{a}_0} \end{aligned} \tag{2.8}$$

where $\bar{A} \in \mathrm{R}^{n\times n}$, $\bar{B} \in \mathrm{R}^{n\times 1}$, $\bar{C} \in \mathrm{R}^{1\times n}$, $\bar{D} \in \mathrm{R}^{1\times 1}$. Then, any discrete-time system that can be expressed as

$$
\begin{aligned}
G(\varepsilon) &= C(\varepsilon I - A)^{-1}B + D \\
&= \frac{n(\varepsilon)}{d(\varepsilon)} \\
&= \frac{b_n\varepsilon^n + b_{n-1}\varepsilon^{n-1} + \ldots + b_1\varepsilon + b_0}{a_n\varepsilon^n + a_{n-1}\varepsilon^{n-1} + \ldots + a_1\varepsilon + a_0}
\end{aligned}
\tag{2.9}
$$

where

$$
b_i = \bar{b}_i + \Delta\bar{b}_i \ , \ \ a_i = \bar{a}_i + \Delta\bar{a}_i \ \ ; 0 \le i \le n \tag{2.10}
$$

such that

$$
\lim_{T \to 0} \Delta\bar{b}_i = 0, \ \lim_{T \to 0} \Delta\bar{a}_i = 0 \tag{2.11}
$$

is a discrete-time model of $\bar{G}(s)$.D

Theorem 2.4 relates a discrete-time model with its continuous-time system in transfer function form by the convergence of the transfer function coefficients. To establish an equivalence for MIMO systems however, is not so direct, since it involves the manipulation of coefficients of the elements of transfer function matrices.

Definition 2.5 The Laplace Transform

Consider a continuous-time signal prescribed by Definition 2.1. The one-sided Laplace transform of the signal is defined as

$$
\mathrm{L}_{-}\{\dot{f}(t)\} = \bar{F}(s) \equiv \int_{0^-}^{\infty} \dot{f}(t)e^{-st}dt. \tag{2.12}
$$

D

The lower limit of integration at 0^- allows the use of an impulse function at $t = 0$ [54]. However, this distinction between $t = 0^-$ and $t = 0$ does not usually come up in practice. The one-sided Laplace transform will be used throughout this thesis, and the minus superscript will be dropped on $t = 0$ and $\mathrm{L}(s)$.

Definition 2.6 The z-Transform

Consider a sequence of numbers $\{x(kT); k = 0, 1, 2, \ldots\}$ that forms a discrete-time signal. Such a signal can be thought of as arising from a process whereby a continuous signal prescribed by Definition 2.1 is sampled at times kT, $k = 0, 1, 2, \ldots$ In popular convention used in control

literature, the z-transform of this discrete-time signal is defined as

$$Z\{x(kT)\} = X(z) \equiv \sum_{k=0}^{\infty} x(kT)z^{-k}. \tag{2.13}$$

D

Definition 2.6 is designated as the one-sided z-transform, strictly speaking, and is concerned only with the values of the sequence for positive n. This is sufficient for the present analysis of discrete-time control systems. A more general z-transform can be defined to include both positive and negative integers. For causal discrete-time signals, the two transformations are identical.

Definition 2.7 "T-scaled" z-Transform (Mori et al. [24])

The z-transform used in this thesis is re-defined as

$$Z\{x(kT)\} = X(z) \equiv \sum_{k=0}^{\infty} T \cdot x(kT)z^{-k}. \tag{2.14}$$

D

This definition differs from the conventional one in that the terms inside the summation is scaled by a factor of T. The inclusion of the sampling period explicitly in the definition of the z-transform results in many advantages [24]. For example, the z-transform of a sampled signal approaches the Laplace transform of the continuous-time waveform as the sampling interval approaches zero, i.e.

$$\lim_{T \to 0} f(z)\Big|_{z = e^{sT}} = f(s) \ . \tag{2.15}$$

All properties of the conventional z-transform carry over to the re-defined transform in (2.14) with the exception that the convolution property is re-defined as [37]

$$G_1(z) \cdot G_2(z) = T \sum_{i=0}^{k} g_1(i,T) \cdot g_2(k-i,T). \tag{2.16}$$

Definition 2.8 The Euler Transform

Recall the definition of the Euler operator from (2.1), $\varepsilon = (z-1)/T$. Following earlier discussions on advantages of the ε operator over z, a transform of discrete-time signals can also be defined using the Euler operator. Consider a discrete-time signal $x(kT)$, $k \in \mathbb{Z}^+$ as per Definition

2.1. The Euler transform of this discrete-time signal is defined by Middleton et al. [62][1] as

$$E\{x(kT)\} = X(\varepsilon) \equiv T \cdot \sum_{k=0}^{\infty} x(kT) \cdot [1 + \varepsilon T]^{-k}. \tag{2.17}$$

D

From (2.1), (2.13) and (2.17), the Euler transform of a discrete-time signal is related to its z-transform by

$$E\{x(kT)\} = X(\varepsilon) = X(z)\big|_{z = \varepsilon T + 1} = [Z\{x(kT)\}]\big|_{z = \varepsilon T + 1} \quad . \tag{2.18}$$

If the Euler operator is applied to a discrete-time signal $u(kT)$ as

$$\begin{aligned} y(kT) &= \varepsilon\, u(kT) = \left(\frac{z-1}{T}\right) u(kT) \\ &= \frac{1}{T}\,[u(kT+T) - u(kT)] \end{aligned} \tag{2.19}$$

it immediately reveals that the ε operator is in fact the Euler approximation of differentiation. A similar procedure to evaluate $1/\varepsilon \cdot u(kT)$ would disclose that $1/\varepsilon$ is the Euler approximation of integration [67]. Hence, the Euler operator can be viewed as a discrete-time equivalent to the continuous-time Laplace operator s, making it suitable to relate discrete-time results with continuous-time ones. A comparison of the stability region for s, ε and z is shown in Table 2.1. Further details and properties of the ε-transform and the z-transform are given in Chapter 4 of Middleton et al. [62].

1. This is referred to as the Delta transform in [62].

Transform Variable	Stability Region	Stability Boundary	Illustration
s	$Re\{s\} < 0$	$Re\{s\} = 0$	
ε	$\lvert 1 + \varepsilon T \rvert < 1$	$\lvert 1 + \varepsilon T \rvert = 1$	
z	$\lvert z \rvert < 1$	$\lvert z \rvert = 1$	

Table 2.1: Comparison of properties of the ε and z operator

Theorem 2.9 Shannon's Sampling Theorem (Åström et al. [47], Franklin et al. [55])
A continuous-time signal with a Fourier Transform that is zero outside the interval $(-w_0, w_0)$ is given uniquely by its values in equidistant points if the sampling frequency w_s is higher than $2w_0$.D

Remark 2.9

To re-construct a continuous-time signal with its Fourier Transform values in equidistant points requires the use of non-causal hold function and is not applicable to on-line control. Therefore, in practice, $w_s \gg 2w_0$.c

The sampling theorem states that in order to re-construct an unknown bandwidth continuous signal from samples of that signal, one must use a sample rate at least twice as fast as the highest frequency contained in the unknown signal. In the context of a closed loop digital control system as depicted in Figure 2.1, it is possible to specify the tracking performance in terms of the frequency response from the reference input $\tilde{r}$ to the plant output $\tilde{y}$. Consider $\tilde{r}$ as the unknown

signal that must be followed by the plant output $\bar{y}$. If it is desirable for the system to track $\bar{r}$ up to a certain closed bandwidth w_b, it is assumed that $\bar{r}$ will have a spectral content up to w_b. Based on the sampling theorem, the sampling rate must therefore be at least twice the required closed loop bandwidth of the system, i.e.,

$$\frac{w_s}{w_b} > 2 . \tag{2.20}$$

If a sampling rate is selected based on w_b, but violates the inequality given by (2.20) because the actual $\bar{r}$ has higher frequency spectral content than w_b, then the sampled value for $\bar{r}$ would be aliased, and the resultant system response can be considerably slower or unstable. In practice, this situation is avoided by designing an antialiasing filter for $\bar{r}$ and using a much higher sampling rate of at least ten times the closed loop bandwidth.

2.2 Discrete-Time Models

In the previous section, Theorem 2.3 gave the criteria that defines a discrete-time model of a continuous-time system. Several discrete-time models are described next.

2.2.1 Invariant Models

Invariant models are discrete-time models with outputs that coincide with the continuous-time system at the sampling instants for a particular type of input. The input signals considered are typically impulse, step or ramp waveforms. For example, a step invariant model (SIM) of a continuous-time plant is a discrete-time model with outputs that coincide with that of the continuous-time system at the sampling instants for a step input. Invariant models of a continuous-time system can be represented as a cascade combination of a hold element, the analogue system and the sampler, as shown in Figure 2.2.

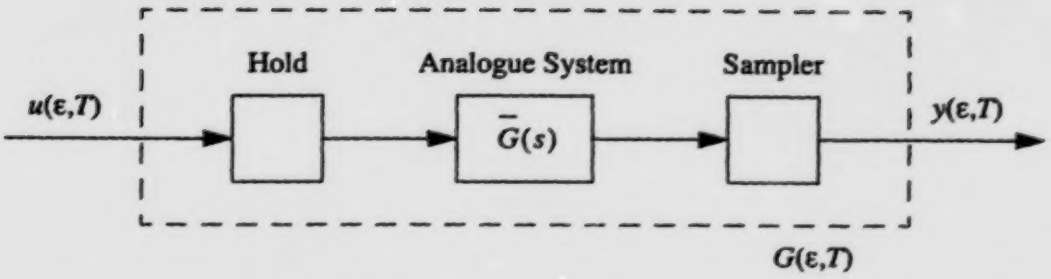

Figure 2.2: Structure of the invariant model

The mathematical representations for a SIM is now given. Consider a continuous-time system represented in the state space form given by (2.5). Inserting a ZOH and a sampler prior to and after the plant, respectively, the SIM model of the plant is represented by

$$x(k+1) = \underbrace{\left\{e^{\bar{A}T}\right\}}_{A} x(k) + \underbrace{\left\{\int_0^T e^{\bar{A}\sigma} d\sigma\, \bar{B}\right\}}_{B} u(k) \quad ; \quad kT \le t < (k+1)T. \tag{2.21}$$

$$y(k) = \bar{C}x(k) + \bar{D}u(k)$$

The discrete-time model represented by (2.21) implicitly uses the z operator, since it can also be written as

$$\begin{aligned} zx(k) &= Ax(k) + Bu(k) \\ y(k) &= \bar{C}x(k) + \bar{D}u(k) \end{aligned} \quad ; \quad kT \le t < (k+1)T. \tag{2.22}$$

To employ the Euler operator in representing the discrete-time model, consider Figure 2.2 again. The output of the sampler is given by

$$[y(t) = L^{-1}\{P(s)H(s)\}]\Big|_{t=kT} \tag{2.23}$$

where $H(s)$ is the transfer function of the hold element in continuous-time. Applying the Euler transform to (2.22), the SIM model of the plant is given by

$$P(\varepsilon,T) = E[L^{-1}\{P(s)H(s)\}] \ . \tag{2.24}$$

A simpler way of representing this in state space form is by substituting $z = \varepsilon T + 1$ in (2.22). After some algebraic manipulation, this is given as

$$\varepsilon x(k) = \underbrace{\frac{e^{\bar{A}T} - I}{T}}_{A} x(k) + \underbrace{\frac{\int_0^T e^{\bar{A}\sigma} d\sigma}{T} \bar{B}}_{B} u(k) \quad ; \quad kT \le t < (k+1)T. \tag{2.25}$$

$$y(k) = \bar{C}x(k) + \bar{D}u(k)$$

Taking the limit of A and B as T approaches 0, it is evident that

$$\lim_{T \to 0} A = \bar{A} \text{ and } \lim_{T \to 0} B = B. \tag{2.26}$$

Therefore, from Theorem 2.3, it is apparent that a SIM is a valid discrete-time model of a continuous-time system. The evaluation of the invariant models of a continuous-time system is usually carried out in the state space form. Details of the SIM of a continuous-time system in transfer function form, as well as properties and representation of the Impulse and Ramp Invariant models are shown in Section 3 of Hori et al. [26].

It is important to note that, from the state space representation of SIM models in ε and z given by (2.25) and (2.23) respectively, a stable continuous-time system will give a stable SIM in discrete-time.

2.2.2 Mapping Models

The mapping models form a class of discrete-time models where the Laplace variable s is substituted by $f(\rho,T)$ and ρ is a discrete-time variable such as ε and z. Using the ε operator, the continuous-time integrator $1/s$ is approximated by $1/f(\varepsilon,T)$. Suppose that a SISO continuous-time system $\bar{P}(s)$ is represented in transfer function form as

$$\bar{P}(s) = \frac{\bar{b}_n s^n + \bar{b}_{n-1} s^{n-1} + \ldots + \bar{b}_1 s + \bar{b}_0}{\bar{a}_n s^n + \bar{a}_{n-1} s^{n-1} + \ldots + \bar{a}_1 s + \bar{a}_0} \quad . \tag{2.27}$$

Substituting $s = f(\varepsilon,T)$, the discrete-time model formed using the above mapping is given as

$$P(\varepsilon,T) = \bar{P}(s)\Big|_{s=f(\varepsilon,T)}$$
$$= \frac{b_n\varepsilon^n + b_{n-1}\varepsilon^{n-1} + \ldots + b_1\varepsilon + b_0}{a_n\varepsilon^n + a_{n-1}\varepsilon^{n-1} + \ldots + a_1\varepsilon + a_0} \qquad (2.28)$$

There are many different mappings for $s \rightarrow \varepsilon$ and $s \rightarrow z$, such as the forward difference approximation, backward difference approximation, and Tustin's method. The latter is also known as bilinear transformation, and it represents the method of trapezoidal approximation in numerical integration, which exhibits better numerical accuracy and algorithm stability than the other two approximations mentioned. Several mappings of s to ε and z are shown in Table 2.2.

Name of Mapping	$s \rightarrow \varepsilon$	$s \rightarrow z$
Forward Difference	$s \rightarrow \varepsilon$	$s \rightarrow \frac{z-1}{T}$
Backward Difference	$s \rightarrow \frac{\varepsilon}{\varepsilon T+1}$	$s \rightarrow \frac{z-1}{Tz}$
Tustin's Method	$s \rightarrow \frac{2\varepsilon}{\varepsilon T+2}$	$s \rightarrow \frac{2}{T}\cdot\frac{z-1}{z+1}$

Table 2.2: Several approximations used in mapping models

These mappings are examined in detail by Åström et al. [47], Franklin et al. [55], and Middleton et al. [62]. The forward difference approximation has the disadvantage that a stable analogue system can be mapped to an unstable digital one. The backward difference approximation overcomes this stability problem, although this mapping does not make use of the entire stability region of the discrete-time domain. The Tustin's approximation compresses the entire *jw*-axis into the circumference of the circular domain of stability in Table 2.1. Thus, the smaller the domain of stability, the more compressed is the mapping, and this results in greater distortion.

In the current context of discussions, one of the benefits of using the ε operator for higher sampling rates becomes apparent. Since the domain of stability increases with the sampling rate, the frequency distortion with Tustin's mapping also becomes less significant at the same time. In fact, as T approaches 0 gradually, the ε-domain turns into the s-domain. For the opposite, as the

sampling interval increases, the stability domain of ε eventually becomes smaller than that of z, i.e. its radius becomes less than one. So below some critically slow sampling rates, the frequency distortion associated with Tustin's mapping expresses in ε becomes more significant than using z. In fact, in consideration of a discrete-time model of a continuous-time system, it is reported by Comeau in [37] that for sampling rates much higher than seven times the cut off frequency, a *very significant improvement* in numerical accuracy is obtained with the ε operator. For sampling frequency below seven times the cut off frequency, the z operator provides *marginally* better performance than the ε operator. Further details of mapping models is illustrated by Hori et al. in Chapter 4 of [30].

2.2.3 Pole-Zero Matching Models

This class of discrete-time models is obtained by mapping the finite poles and zeros of a transfer function in the continuous-time *s*-plane to the discrete-time ε-plane using the following convention: A pole or zero at $s = \bar{a}$ in the continuous-time domain is mapped to the discrete-time domain as

$$(s = \bar{a},\ |\bar{a}| < \infty) \rightarrow \left(\varepsilon = \frac{e^{\bar{a}T} - 1}{T} \quad \text{or} \quad z = e^{\bar{a}T}\right) \quad . \tag{2.29}$$

Typically, real poles and zeros, and complex conjugate poles and zeros, are grouped in first order and second order elements respectively before applying the mapping. A second order element with a pair of complex-conjugate roots (poles or zeros) is mapped from the *s*-plane to the ε-plane as

$$(s + \bar{a})^2 + \bar{b}^2 \rightarrow (\varepsilon + a)^2 + b^2 \tag{2.30}$$

where

$$\begin{aligned} a &= \frac{1 - e^{-\bar{a}T}\cos(\bar{b}T)}{T} \\ b &= \frac{e^{-\bar{a}T}\sin(\bar{b}T)}{T} \end{aligned} \quad , \tag{2.31}$$

and from the *s*-plane to the *z*-plane as

$$(s+\bar{a})^2+\bar{b}^2 \rightarrow (z+a')^2+(b')^2 \tag{2.32}$$

where

$$\begin{aligned} a' &= -e^{-\bar{a}T}\cos(\bar{b}T) \\ b' &= e^{-\bar{a}T}\sin(\bar{b}T) \end{aligned} \tag{2.33}$$

It is also possible to consider the mapping of infinite zeros. These are illustrated by Cormier in [36] and Franklin et al. in [55]. It is emphasized here that, from the definition of pole-zero matching (MPZ) model given by (2.29), a stable continuous-time system will result in a stable MPZ discrete-time model. Further, it is obvious that, since

$$a = \frac{e^{\bar{a}T}-1}{T} \rightarrow \bar{a} \quad \text{as} \quad T \rightarrow 0 \ , \tag{2.34}$$

i.e. the discrete-time poles and zeros approach the continuous-time ones as the sampling interval approaches zero. Thus, the discrete-time system formed using the MPZ method is a discrete-time model of the continuous-time system as per Definition 2.2 and Theorem 2.4.

The concept of designing a discrete-time control system is shown next.

2.3 Design Overview

There are three major approaches in the design of discrete-time control systems. The first is the hybrid approach which considers both the continuous-time and discrete-time systems in a feedback connection simultaneously. The analysis typically involves optimal control design of sampled-data systems which can take into account the continuous-time behaviour of digitally controlled systems [7] & [6]. However, the mathematical analysis involved in general is far more complex than the next two approaches.

The second approach is the direct design approach. This approach uses an appropriate discrete-time model of the plant for a direct design of a discrete-time controller in a desired discrete-time domain. The benefit of this idea is that the mathematics involved is much simpler since the

analysis is carried out entirely in the discrete-time domain. However, the drawback to this method is that the sampling period T must be selected *à priori* in order to obtain a discrete-time model of the plant. Thus, to change the sampling period of the system, the whole design procedure must be repeated. This can be a cumbersome exercise during the controller design process. Also, upper bounds for the sampling period can only be obtained after considering the closed loop bandwidth [55] and, depending on specifications, this may only be available *after* controller design is more or less completed. This creates an obvious dilemma that does not occur in continuous-time controller design. In addition, by carrying out the design analysis exclusively in the discrete-time domain, the intersample behaviour is essentially ignored, as the system operates in open loop between the sampling instances. This can be a significant problem for systems with a large intersample ripple or hidden oscillation that corresponds to the loss of observability in obtaining a discrete-time model of the open loop plant, or the presence of poorly damped zeros in the open loop plant that are cancelled by the controller [47].

The third major approach to the design of discrete-time control systems relates to the concept of performing an indirect design, which emphasizes the continuous-time design of a control system for the plant. In this approach, a desired closed loop control system is designed in the analogue domain. The continuous-time controllers are then replaced by its discrete-time approximations with additions of samplers and hold devices. This approach has the benefit that the analysis is carried out in the familiar continuous-time domain, and thus a better physical understanding of the system can be obtained. The completed analogue design yields a desired closed loop performance which is then set as a benchmark for the discrete-time approximations. Consequently, issue with ill-favoured intersample behaviour is partially solved with most workable sampling periods. Besides, the approximations obtained typically are functions of the sampling period. Thus, changing the sampling period is a simpler affair. There are different ways to approximate or discretize the continuous-time controllers. The success of the design depends on the characteristics of the method of discretization. These are considered in the next few sections.

As a summary, the above three major approaches to the design of a discrete-time control system is illustrated in Figure 2.3. This thesis will focus on the last of the three major approaches, that is,

the indirect design approximation.

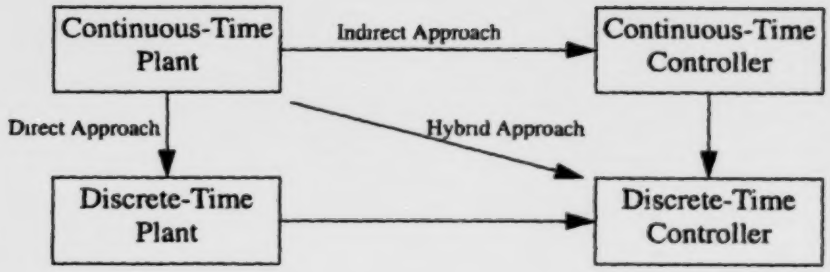

Figure 2.3: Three approaches in designing discrete-time control systems

2.4 Indirect Design of Discrete-Time Controller

The design of discrete-time control systems via the indirect design approach involves discretizing designed analogue controllers. The discretization process is composed of selecting a sampling period and finding a set of discrete-time controllers to approximate the functionality and performance of its pre-designed continuous-time complement in some sense. There are roughly two different ways to carry out the discretization. The first is the local discretization approach. This approach treats each controller (block) individually in an open loop setting, that is, discretization is applied to each controller "locally". The schemes that can be used to accomplish local discretization are typically much easier to apply than the other approach. However, the disadvantage to following this path is that the resultant discrete-time control system typically does not perform well unless a very high sampling rate is used. Furthermore, the stability of the resultant sampled-data system is also not guaranteed with lower sampling rates [58]. In actual practice, a sampling rate of at least twenty times the closed loop bandwidth is needed in order to provide some smoothness in the response and to limit the magnitude of the control steps [55]. This drawback compounds into problems in word length, sampler precision, computational resource, hardware complexity and cost.

In light of the problems associate with the local discretization methods, the second approach is to

take the closed loop performance into consideration. Many design schemes have been proposed by various researches to tackle this problem, including published literature by Rattan in [21], Kennedy et al. in [14], and Keller et al. in [12] and [13]. While they offer limited success in solving the design problem, they all have some form of disadvantages; some schemes do not guarantee closed loop stability, while others contains heuristic elements that needs to be justified, or have non-systematic and complicated design procedures.

To surmount the short-coming of the aforementioned discretization schemes, Markazi et al. in [29] and Markazi in [38] proposed a global discretization scheme called the Plant Input Mapping (PIM) method that takes into account the closed loop continuous-time system performance during the discrete-time controller design process. Consider again Figure 2.1, and denote the closed loop transfer function from the reference input $\bar{r}$ to the plant input $\bar{u}$ as the Plant Input Transfer Function (PITF). The controller synthesis procedure for the PIM method involves finding a set of discrete-time controllers that, together with the step invariant model of the plant, forms a discrete-time PITF that is identical to the pole-zero matching (MPZ) model of the PITF of the continuous-time system. From properties of the MPZ method and step invariant model of the plant, the PIM digital re-design method guarantees the closed loop stability of the resultant discrete-time control system for any non-pathological sampling interval. Moreover, the rapprochement of continuous-time and discrete-time results in the time domain as the sampling interval approaches zero is shown by Markazi [38] and Rabbath [41]. Extensive simulation studies conducted in [38], [30] and [41] indicate that this method gives superior performance to other indirect methods for the same sampling interval. Yet, this method offers a systematic approach to the indirect design of discrete-time control systems using relatively simple and well known procedures. Further details of the PIM digital re-design are given in Section 2.6 in this chapter.

The methods of local discretization is illustrated next.

2.5 Local Discretization Methods

As explained previously in Section 2.4, this method discretizes each controller block in the

feedback system separately as in the open loop setting. Consider a simple two-degrees-of-freedom (2-DOF) SISO continuous-time control system shown in Figure 2.4

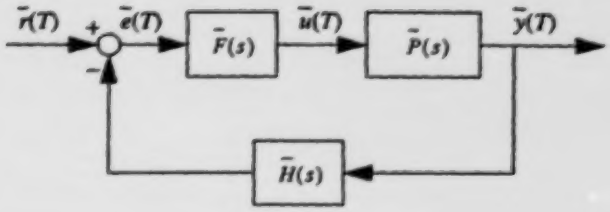

Figure 2.4: A 2-DOF SISO feedback analogue compensator design

The design procedure goes as follows: Assume that the continuous-time control system is well designed and gives satisfactory closed loop system performance, and that a sampling rate f_s is first selected based on the continuous-time closed loop system bandwidth, in accordance with Shannon's sampling theorem as stated in Theorem 2.9. Next, the controller blocks $\bar{F}(s)$ and $\bar{H}(s)$ are discretized individually. This can be done using any of the three aforementioned classes of discrete-time models, expressed in a desired discrete-time operator. Typically, a mapping model or MPZ model is used. Finally, samplers and hold devices are added in the appropriate locations, resulting in a sampled-data system which, for the case of the system depicted in Figure 2.4, may resemble the following:

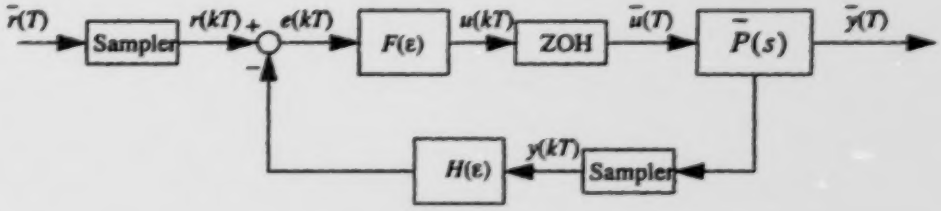

Figure 2.5: A 2-DOF feedback discrete-time feedback control system

An important feature for local discretization method is its ease of application. In practice, discrete-time control system designed using a local discretization technique typically requires a sampling rate of at least 10-20 times the closed loop bandwidth in order to achieve stability and 20-30 times to achieve acceptable performance [47].

For the case of multivariable systems, the definition of closed loop system bandwidth becomes a

little more complex. Modern control system design and synthesis for MIMO systems is usually carried out in the state space domain. However, the preceding discretization treatment can still be applied with a little more mathematical development. The reason for this is as follows: In a SISO system, the bandwidth of a feedback loop is determined by the variation of the closed loop system gain with frequency; for MIMO systems however, the norm of the closed loop system transfer function matrix does not have a unique gain in general. $\|\bar{G}(s)\bar{u}(s)\|$ depends on the direction of the input vector $\bar{u}(s)$. This leads to the definition of matrix norms.

Definition 2.10

If $\|x\|$ denotes any vector norm, then an induced matrix norm for G is defined by

$$\|G\| = \sup \frac{\|Gx\|}{\|x\|} . \tag{2.35}$$

If the Euclidean vector norm is defined on $\|x\|$ such that

$$\|x\| = (x^H x)^{1/2} , \tag{2.36}$$

where the superscript H denotes taking the complex-conjugate transpose of a x, then the induced matrix norm is the Hibert or spectral norm

$$\|G\| = \bar{\sigma} \tag{2.37}$$

where $\bar{\sigma}^2$ is the maximum eigenvalue for $G^H G$. The positive square roots of the eigenvalues are called the singular values of G. However, in this case, since G is considered to be a transfer function matrix in s such that $G \in R_p^{m \times l}(s)$ with $m \geq l$, setting $s = jw$ ($0 \leq w < \infty$), it is appreciable that the singular values of G are also functions of w. To avoid confusion, therefore, they are denoted as the *principal gains* of $G(s)$. Finally, $\bar{\sigma}(w)$ and $\underline{\sigma}(w)$ are defined as the maximum principal gain and minimum principal gain of G, respectively [60].D

In considering the ratios

$$\frac{\|G(s)u(s)\|}{\|u(s)\|} \text{ and } \frac{\|G^{-1}(s)y(s)\|}{\|y(s)\|} , \tag{2.38}$$

it is possible to show that

$$\frac{\|G^{-1}(jw)y(jw)\|}{\|y(jw)\|} \leq \frac{1}{\underline{\sigma}(w)} \tag{2.39}$$

and

$$\frac{\|G(jw)u(jw)\|}{\|u(jw)\|} \leq \bar{\sigma}(w). \tag{2.40}$$

Hence, putting $y(jw) = G(jw)u(jw)$, a bound can be obtained such that

$$\underline{\sigma}(w) \leq \frac{\|G(jw)u(jw)\|}{\|u(jw)\|} \leq \bar{\sigma}(w). \tag{2.41}$$

This illustrates that the gain of a multivariable system is sandwiched between the smallest and largest principal gains. From definition of the sampling theorem in Theorem 2.9, if the frequency w_{by} at which

$$\bar{\sigma}(T(jw_{by})) = \frac{1}{\sqrt{2}}\bar{\sigma}(T(0)) \tag{2.42}$$

is defined and used as a transmission bandwidth of the closed loop system, where $\bar{T}(s)$ is the closed loop transfer function of the system, then by choosing a sampling frequency to be twice of w_{by}, the local discretization method can be used in a similar spirit as the SISO system formulation. $\bar{T}(s)$ used in control system design is stable and has a constant gain at low frequencies such that it typically carries the low-pass characteristics of physical systems.

2.5.1 Some issues with Local Discretization

The foregoing exposition suggests that local discretization is well established and uses relatively simple methods, since the sampled-data system usually performs satisfactorily. However, in practice, there are limitations which makes the selection of the best sample rate for a digital control system a compromise. Bounded by the finite word length effect, the performance of a digital controller generally improves with increasing sample rate, but cost may also increase rapidly with faster sampling. A decrease in sample rate, if it can be tolerated, means more time is available for control calculations. Hence, slower computers are possible for a given control function, or more control capability is available for a given computer. Either result lowers the cost

per function. For systems with A/D converters, slower sampling means less conversion speed is required, which also lowers cost. Too slow of a sampling rate, however, leads to a poor system performance and even instability.

These are important considerations for systems designated for use on-board an autonomous flight vehicles[1] such as missile flight control systems. Since it is highly probable that they will only be used once, they naturally desire low production cost without sacrificing functionality and performance. This is a typical dilemma faced by many engineers in discrete-time control system design. Summing up the foregoing discussion, it is desirable to have a simple and systematic discretization method that would mimic the closed loop performance of a continuous-time system while using much lower sampling rate than it would be needed for the local discretization method. In a nutshell, the PIM digital re-design method provides a feasible solution for the above.

2.6 Plant Input Mapping (PIM) Method

The Plant Input Mapping (PIM) method is a global digital re-design method for pre-designed continuous-time closed loop control systems for proper LTI plants. Description of the characteristics of the PIM method, which include the convergence of the continuous-time performance of the digitally controlled system as the sampling interval approaches zero, the comparison of performance of locally discretized systems with PIM re-designed ones for relatively large sampling periods, and the conditions for guaranteed stability are given by Markazi et al. in [29], Markazi in [38] and Rabbath in [41]. They are recapitulated in this section.

2.6.1 General Framework

Consider a proper LTI continuous-time plant $\bar{P}(s)$ represented in the state space form as

1. The generic term "autonomous flight vehicle" can have several different meanings. For example, it can be used for Unmanned Air Vehicle (UAV) deployed in reconnaissance and surveillance mission for both military and civilian authorities.

$$\bar{P}: \quad \begin{aligned} \dot{\bar{x}}(t) &= \bar{A}\bar{x}(t) + \bar{B}\bar{u}(t) \\ \bar{y}(t) &= \bar{C}\bar{x}(t) + \bar{D}\bar{u}(t) \end{aligned} \quad . \tag{2.43}$$

The transfer function representation of the plant is given as

$$\bar{P}(s) = \bar{C}(sI - \bar{A})^{-1}\bar{B} + \bar{D} \quad . \tag{2.44}$$

Definition 2.11

Let $\Omega \subset \mathrm{C}$ be a closed subset of the complex plane that defines the stability region of a particular operator as given in Table 2.1. A real square matrix is then said to be Ω-Hurwitz if all of its eigenvalues are contained in Ω .D

Theorem 2.12

Suppose $A \in \mathrm{R}^{n\times n}$, $B \in \mathrm{R}^{n\times m}$, $C \in \mathrm{R}^{p\times n}$, $D \in \mathrm{R}^{p\times m}$ are a realization of an m-input p-output system $P(\rho) = C(\rho I - A)^{-1}B + D$, where $[A, B]$ is stabilizable and $[C, A]$ is detectable, and ρ is the operator that is either s, ε, or z, depending on the context.

Select $K \in \mathrm{R}^{m\times n}$, $L \in \mathrm{R}^{n\times p}$ such that $(A - BK)$ and $(A - LC)$ are Ω-Hurwitz. Define

$$M(\rho) = -K[\rho I - (A - BK)]^{-1}B + I \quad , \tag{2.45}$$

$$N(\rho) = (C - DK)[\rho I - (A - BK)]^{-1}B + D \quad , \tag{2.46}$$

$$X(\rho) = K[\rho I - (A - LC)]^{-1}(B - LD) + I \quad , \tag{2.47}$$

$$Y(\rho) = K[\rho I - (A - LC)]L \quad . \tag{2.48}$$

Then

1) $M(\rho) \in R_p^{p\times p}(\rho)$, $N(\rho) \in R_p^{m\times p}(\rho)$, $X(\rho) \in R_p^{p\times p}(\rho)$, $Y(\rho) \in R_p^{p\times m}(\rho)$, such that

2) the four transfer function matrices $M(\rho)$, $N(\rho)$, $X(\rho)$, $Y(\rho) \in \mathrm{RH}_\infty$,

3) M, N, X, Y satisfies the Bezout identity

$$XM + YN = I \quad , \tag{2.49}$$

and

4) $P = NM^{-1}$ represents the right coprime factorization of the system transfer function matrix P,

where RH_∞ denotes the set of real proper (transfer) functions that are analytic outside the region of stability, and $R_p(\rho)$ denotes the set of rational proper transfer function matrices.D

Proof

The proof for the case of $\rho = s$, i.e. when the system $\bar{P}(s)$ is in continuous-time, is shown in the well known paper by Nett et al. [19]. The proof for the discrete-time operators ε and z can be similarly derived algebraically, and is omitted here for brevity.B

Remark 2.12

The non-unique nature of the result for the four transfer function matrices M, N, X and Y is a characteristic of the MIMO pole placement [49]. The Bezout identity is classified as a particular type of diophantine equation by Kucera [16].c

The analysis for the digital re-design of continuous-time MIMO systems are first given, follow by the presentation of the procedure used in applying PIM method to analogue SISO systems.

2.6.2 PIM method for MIMO systems

Consider the closed loop continuous-time control system shown in Figure 2.6, where $\bar{E}(s)$, $\bar{F}(s)$ and $\bar{H}(s)$ are proper transfer function matrices, and $\bar{P}(s)$ is the plant to be controlled. It is assumed that this closed loop system is asymptotically stable, and gives satisfactory performance. The latter can usually be quantified in terms of the rise time, settling time, overshoot and damping associated with the system output, as well as other measures such as disturbance attenuation and system robustness. Following the digital re-design process, the sampled-data control system will resemble one shown in Figure 2.7. The controllers $E(\varepsilon)$, $F(\varepsilon)$, $H(\varepsilon)$ are to be calculated.

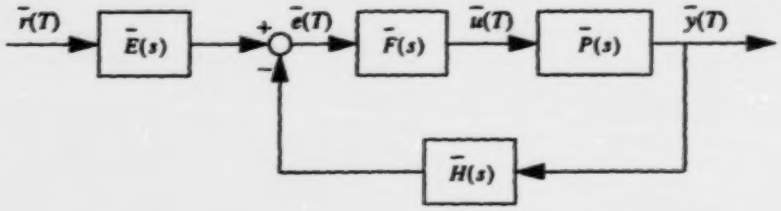

Figure 2.6: Continuous-time control system considered for applying PIM digital re-design

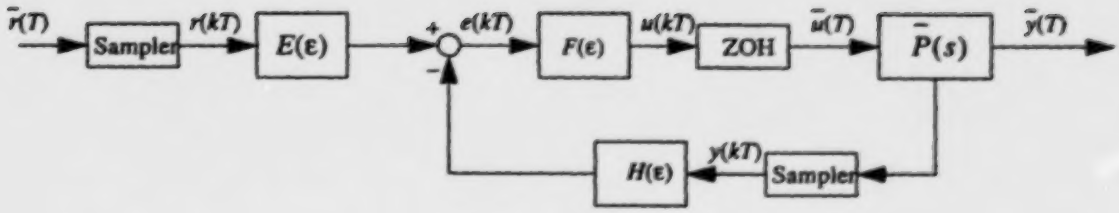

Figure 2.7: Sampled-data system results from applying the PIM digital re-design

From Figure 2.6, denote the transfer function from the reference input $\bar{r}(s)$ to the plant input signal $\bar{u}(s)$ as the plant input transfer function (PITF) $\bar{\Phi}(s)$. Similarly, denote the transfer function from the reference input $\bar{r}(s)$ to the plant output signal $\bar{y}(s)$ as closed loop system transfer function $\bar{T}(s)$. These three signals $\bar{r}(s)$, $\bar{u}(s)$ and $\bar{y}(s)$ can be multichannel signals for MIMO systems. The transfer functions $\bar{\Phi}(s)$ and $\bar{T}(s)$ can be expressed as

$$\begin{aligned} \bar{\Phi}(s) &= [I + \bar{F}(s)\bar{H}(s)\bar{P}(s)]^{-1}\bar{F}(s)\bar{E}(s) \\ \bar{T}(s) &= \bar{P}(s)\bar{\Phi}(s) \end{aligned} \tag{2.50}$$

Since $\bar{T}(s)$ is assumed to be asymptotically stable, $\bar{T}(s) \in \mathrm{RH}_\infty$, and thus (2.50) also asserts the stability of the PITF $\bar{\Phi}(s)$. The following theorem further relates the stability criteria of the closed loop system transfer function $\bar{T}(s)$ with the PITF $\bar{\Phi}(s)$.

Theorem 2.13

Consider a closed loop continuous-time control system as shown in Figure 2.6 with a stable PITF $\bar{\Phi}(s) \in \mathrm{RH}_\infty$. Then the closed loop system transfer function matrix $\bar{T}(s) \in \mathrm{RH}_\infty$ if and only if $\exists$ $\bar{W}(s) \in \mathrm{RH}_\infty$ such that

$$\bar{\Phi}(s) = \bar{M}(s)\bar{W}(s) \tag{2.51}$$

where $\bar{M}(s)$ is defined in the coprime factorization of the continuous-time plant $\bar{P}(s)$ in Theorem 2.12.D

Proof

"$\Rightarrow$" Theorem 2.12 shows the existence of non-unique transfer function matrices $\bar{M}(s)$, $\bar{N}(s)$,

$\bar{X}(s)$ and $\bar{Y}(s) \in \mathrm{RH}_\infty$ that satisfy the Bezout Identity where $\bar{M}(s)$ and $\bar{N}(s)$ are coprime such that

$$\bar{X}\bar{M} + \bar{Y}\bar{N} = I \ . \tag{2.52}$$

Multiply both sides of (2.52) by $\bar{M}^{-1}(s)\bar{\Phi}(s)$ yields

$$\begin{aligned} \bar{X}(s)\bar{\Phi}(s) + \bar{Y}(s)\bar{N}(s)\bar{M}^{-1}(s)\bar{\Phi}(s) &= \bar{M}^{-1}(s)\bar{\Phi}(s) \\ \bar{X}(s)\bar{\Phi}(s) + \bar{Y}(s)\bar{P}(s)\bar{\Phi}(s) &= \bar{M}^{-1}(s)\bar{\Phi}(s) \\ \bar{X}(s)\bar{\Phi}(s) + \bar{Y}(s)\bar{T}(s) &= \bar{M}^{-1}(s)\bar{\Phi}(s) \ . \end{aligned} \tag{2.53}$$

Define

$$\bar{W}(s) = \bar{X}(s)\bar{\Phi}(s) + \bar{Y}(s)\bar{T}(s) \ . \tag{2.54}$$

If $\bar{W}(s) \in \mathrm{RH}_\infty$, then since $\bar{X}$, Φ and $\bar{Y} \in \mathrm{RH}_\infty$, it follows that

$$\bar{T} \in \mathrm{RH}_\infty \ , \tag{2.55}$$

satisfying (2.51).

"$\Leftarrow$" From (2.54), since $\bar{X}$, $\bar{\Phi}$, $\bar{Y}$ and $\bar{T} \in \mathrm{RH}_\infty$, it follows that $\bar{W}(s) \in \mathrm{RH}_\infty$, satisfying (2.51).B

Note that, the equivalent form in continuous-time is, from equation (2.51)

$$\bar{W}(s) = \bar{M}^{-1}(s)\bar{\Phi}(s) \ . \tag{2.56}$$

Remark 2.13

Thus from the definition of $\bar{W}$, this implicitly implies that the unstable poles of the plant, which appears as zeros of $\bar{M}^{-1}(s)$ for the matrix factorization of the plant, must also be intrinsically present as transmission zeros of the PITF $\Phi(s)$ and disappears from $\bar{W}(s)$ for closed loop stability. Indeed, this is the basic principle of how a SISO and MIMO closed loop feedback connection stabilizes an unstable plant.c

The discretization of the continuous-time plant is now presented. Following discussions in Section 2.2 on discrete-time models of the continuous-time systems, consider the SIM $P(\varepsilon)$ of the

plant $\bar{P}(s)$.

Definition 2.14 Non-Pathological Sampling Period (Chen et al. [50])

A sampling period T is said to be non-pathological with respect to the continuous-time plant if none of the points $\sigma + jw_s l$ in the s-plane, where l is an interger not equal zero, $w_s = 2\pi f_s = 2\pi/T$, and σ is a non-negative real part of the continuous-time plant pole, is also a pole of the plant.D

Lemma 2.15

Given a coprime factorization of a continuous-time plant as $\bar{P}(s) = \bar{N}(s)\bar{M}^{-1}(s)$, The SIM of the plant, $P(\varepsilon)$ will have no unstable pole-zero cancellation, provided the sampling period is non-pathological.D

Proof

The stabilizability and detectability of the continuous-time plant are preserved in the SIM plant model if the sampling interval T is chosen to be non-pathological (Chen et al. [50]).B

Following Lemma 2.15, a coprime factorization for the discrete-time plant $P(\varepsilon) = N(\varepsilon)M^{-1}(\varepsilon)$ can be obtained using Theorem 2.12. From Figure 2.7, the discrete-time PITF $\Phi(\varepsilon)$ and the closed loop system transfer function $T(\varepsilon)$ for the sampled-data system are expressed as

$$\begin{aligned} \Phi(\varepsilon) &= [I + F(\varepsilon)H(\varepsilon)P(\varepsilon)]^{-1}F(\varepsilon)E(\varepsilon) \\ T(\varepsilon) &= P(\varepsilon)\Phi(\varepsilon) \end{aligned} \qquad (2.57)$$

The following theorem similarly states the closed loop stability criteria of the discrete-time control system in relation to its PITF.

Theorem 2.16

Consider the PITF $\Phi(\varepsilon)$ in (2.57) for the discrete-time system shown in Figure 2.7. The closed loop system transfer function $T(\varepsilon) \in RH_\infty$ if and only if $\exists\ W(\varepsilon) \in RH_\infty$ such that

$$\Phi(\varepsilon) = M(\varepsilon)W(\varepsilon)\,. \qquad (2.58)$$

D

Proof

This is similar algebraically to the proof of Theorem 2.13.B

The conditions for attaining closed loop stability for the continuous-time and discrete-time systems were shown above, with the connection that the discrete-time plant is the SIM of the continuous-time plant. The following presentation introduces the procedure to calculate the set of discrete-time controllers $E(\varepsilon)$, $F(\varepsilon)$, $H(\varepsilon)$ for setting up the sampled-data system. A further connection between the continuous-time and discrete-time system is established using the MPZ model of the continuous-time PITF to form the PITF of the discrete-time system.

In constructing the sampled-data system shown in Figure 2.7, Theorem 2.16 implicitly states that, for $W(\varepsilon)$ to be stable, all unstable poles of the discrete-time plant that appears as transmission zeros of $M(\varepsilon)$ must also be present as transmission zeros of the discrete-time PITF $\Phi(\varepsilon)$. Thus the mapping of poles of the continuous-time plant $\bar{P}(s)$ to the discrete-time plant $P(\varepsilon)$, particularly the unstable ones through the SIM models must also be performed on the mapping of transmission zeros of $\bar{\Phi}(s)$ to $\Phi(\varepsilon)$. This can be achieved by evaluating discrete-time PITF $\Phi(\varepsilon)$ as the MPZ model of $\bar{\Phi}(s)$. Thus a further connection between the closed loop continuous-time and discrete-time systems is established. The use of the MPZ model also preserves the closed loop stability of the continuous-time system in the discretized domain. This connection is complete if it is possible to find a set of discrete-time controllers $E(\varepsilon)$, $F(\varepsilon)$, and $H(\varepsilon)$ such that (2.57) and (2.58) are satisfied. This is established in the next theorem.

Theorem 2.17

Consider the discrete-time control system shown in Figure 2.7. Suppose there exists a discrete-time PITF $\Phi(\varepsilon)$ that satisfies Theorem 2.16. Then the following holds:

1. The particular set of controllers

$$E(\varepsilon) = W(\varepsilon), \quad F(\varepsilon) = X^{-1}(\varepsilon), \quad H(\varepsilon) = Y(\varepsilon) \tag{2.59}$$

realize the desired stable closed loop discrete-time PITF $\Phi(\varepsilon)$, where $W(\varepsilon)$ satisfies (2.58) such that

$$W(\varepsilon) = M^{-1}(\varepsilon)\Phi(\varepsilon) \tag{2.60}$$

and $X(\varepsilon)$ and $Y(\varepsilon)$ satisfy the Bezout Identity in Theorem 2.12. Further, the resultant sampled-data system is internally stable.

2. The set of controllers

$$\begin{aligned} E(\varepsilon) &= K(\varepsilon)W(\varepsilon) \\ F(\varepsilon) &= [K(\varepsilon)X(\varepsilon) + \Gamma(\varepsilon)N(\varepsilon)]^{-1} \\ H(\varepsilon) &= K(\varepsilon)Y(\varepsilon) - \Gamma(\varepsilon)M(\varepsilon) \end{aligned} \tag{2.61}$$

where $\{K(\varepsilon), K^{-1}(\varepsilon), \Gamma(\varepsilon)\} \in \mathrm{RH}_\infty$ gives a stable closed loop discrete-time system. $K(\varepsilon)$ is an artibrary parameter in RH_∞, and it can be used to alter, if desired, performances other than closed loop characteristics.D

Proof

1. From (2.57) the desired discrete-time PITF is

$$\begin{aligned} \Phi(\varepsilon) &= [I + F(\varepsilon)H(\varepsilon)P(\varepsilon)]^{-1}F(\varepsilon)E(\varepsilon) \\ &= F(\varepsilon)[I + H(\varepsilon)P(\varepsilon)F(\varepsilon)]^{-1}E(\varepsilon)\,. \end{aligned} \tag{2.62}$$

Substituting $E = W$, $F = X^{-1}$, $H = Y$ and $P = NM^{-1}$ into (2.62) yields

$$\Phi = X^{-1}[I + YNM^{-1}X^{-1}]^{-1}W \quad . \tag{2.63}$$

Applying the Bezout Identity to be above

$$\begin{aligned} \Phi &= X^{-1}[I + (I - XM)M^{-1}X^{-1}]^{-1}W \\ &= MW \end{aligned} \tag{2.64}$$

Finally, the discrete-time closed loop transfer function $T(\varepsilon)$ is given by

$$\begin{aligned} T(\varepsilon) &= P(\varepsilon)\Phi(\varepsilon) \\ &= NM^{-1}MW \\ &= NW \end{aligned} \tag{2.65}$$

which is asymptotically stable since $N(\varepsilon)$ and $W(\varepsilon) \in \mathrm{RH}_\infty$.

2. This is algebraically similar to the proof of 1. See [38].B

Theorem 2.17 gives a three controllers implementation of the discrete-time control system. For the special case of a stable plant $P(\varepsilon)$, it is possible to realize the desired discrete-time PITF using a single controller in a unity feedback connection. This is capitulated as

Corollary 2.18
Consider a discrete-time control system as illustrated in Figure 2.7. If the plant $P(\varepsilon) \in \mathrm{RH}_\infty$, the desired discrete-time PITF can be realized with

$$\begin{aligned} E(\varepsilon) &= H(\varepsilon) = I \\ F(\varepsilon) &= \Phi(\varepsilon)[I - P(\varepsilon)(\Phi(\varepsilon))]^{-1} . \end{aligned} \tag{2.66}$$

D

Proof
The resultant discrete-time PITF $\Phi(\varepsilon)$ is found to be

$$\begin{aligned} &= \{I + [\Phi(I - P\Phi)^{-1}]P\}^{-1}[\Phi(I - P\Phi)^{-1}] \\ &= \Phi(I - P\Phi)^{-1}[I + P\Phi(I - P\Phi)^{-1}]^{-1} \\ &= \Phi\{[I + P\Phi(I - P\Phi)^{-1}](I - P\Phi)\}^{-1} \\ &= \Phi\{I - P\Phi + P\Phi\}^{-1} \\ &= \Phi . \end{aligned} \tag{2.67}$$

B

Further illustration of the application of PIM method to MIMO systems is shown in Section 3.4.

2.6.3 PIM method for SISO systems

The PIM method can also be applied to SISO systems. In such a case, the mathematical procedure simplifies considerably, as multichannel signals $\bar{r}$, $\bar{u}$, $\bar{y}$ become scalar signals, and transfer function matrices become scalar transfer functions. Rabbath et al. [32] gave an excellent account of PIM based discrete-time SISO control systems. This is summarized as follows:

Re-consider the continuous-time control system illustrated in Figure 2.6 as a SISO system with the same previous assumptions. Assume that $\bar{E}(s)$, $\bar{F}(s)$ and $\bar{H}(s)$ are controller blocks that render desirable closed loop performance in continuous-time. Since $\bar{P}(s)$ is now a SISO plant, let

$$\bar{P}(s) = \frac{\bar{b}(s)}{\bar{a}(s)} = \frac{\bar{b}_n s^n + \bar{b}_{n-1} s^{n-1} + \ldots + \bar{b}_1 s + \bar{b}_0}{\bar{a}_n s^n + \bar{a}_{n-1} s^{n-1} + \ldots + \bar{a}_1 s + \bar{a}_0} \quad . \tag{2.68}$$

A PIM based discrete-time control system can be obtained in three steps. Similar to the PIM digital re-design of a MIMO system, the first is the evaluation of the step invariant model of the continuous-time plant. This is obtained using method described in Section 2.2.1, and is denoted as

$$P(\varepsilon,T) = \frac{b(\varepsilon)}{a(\varepsilon)} = \frac{b_n \varepsilon^n + b_{n-1} \varepsilon^{n-1} + \ldots + b_1 \varepsilon + b_0}{a_n \varepsilon^n + a_{n-1} \varepsilon^{n-1} + \ldots + a_1 \varepsilon + a_0} \quad . \tag{2.69}$$

The second stage is the evaluation of continuous-time and discrete-time PITF. The continuous-time PITF $\bar{\Phi}(s)$ is given by (2.50), and the degree of the numerator and denominator coprime polynomial of $\bar{\Phi}(s)$ is denoted by q and p, respectively. For the formulation of the discrete-time system, an analogous treatment for MIMO systems, highlighted by Theorem 2.13 and Theorem 2.16, is applied where the discrete-time PITF is obtained by discretizing the stable continuous-time PITF $\bar{\Phi}(s)$ to form a stable $\Phi(\varepsilon)$ using the MPZ method, such that the following conditions are met:

$$\begin{aligned} \lim_{T \to 0} \Phi(\varepsilon)\Big|_{\varepsilon = \frac{z-1}{T}} &= \bar{\Phi}(s) \quad , \quad \text{pointwise in } s \\ \Phi(\varepsilon)\big|_{\varepsilon = \varepsilon_0} &= \bar{\Phi}(s)\big|_{s = s_0} \end{aligned} \tag{2.70}$$

where

$$\varepsilon_0 = \frac{e^{s_0 T} - 1}{T} \quad , \qquad 0 \le s_0 < 1 \, . \tag{2.71}$$

The third step relates to the evaluation of discrete-time controllers such that the desired discrete-time PITF $\Phi(\varepsilon)$ can be realized as a closed loop system shown in Figure 2.7. This procedure is considerably simpler than the evaluation for MIMO systems, where a Bezout Identity is solved in

(2.52). Instead, the calculation is carried out by solving for $u(\varepsilon)$ and $v(\varepsilon)$ in a Diophantine equation given by

$$u(\varepsilon)a(\varepsilon) + v(\varepsilon)b(\varepsilon) = d(\varepsilon) \tag{2.72}$$

where

$$\begin{aligned} u(\varepsilon) &= u_l\varepsilon^l + u_{l-1}\varepsilon^{l-1} + \ldots + u_1\varepsilon + u_0 \\ v(\varepsilon) &= v_k\varepsilon^k + v_{k-1}\varepsilon^{k-1} + \ldots + v_1\varepsilon + v_0 \end{aligned} \quad , \tag{2.73}$$

and $d(\varepsilon)$ is the denominator of $\Phi(\varepsilon)$ expressed as

$$d(\varepsilon) = d_p\varepsilon^p + u_{p-1}\varepsilon^{p-1} + \ldots + u_1\varepsilon + u_0 \quad , \tag{2.74}$$

and further, l and k are set such that $l = p - n$ and $k = n - 1$.

Note that in the evaluation of the discrete-time PITF for this SISO case, $\Phi(\varepsilon)$ can be customarily written as

$$\Phi(\varepsilon) = \frac{r(\varepsilon)a(\varepsilon)}{d(\varepsilon)} \tag{2.75}$$

where $r(\varepsilon)$ is of degree $(q - n)$.

There are several different ways of solving the Diophantine equation given by (2.72), as explained below.

a) Eliminant Matrix Method

Equating the coefficients of like powers of ε on both side of (2.72) results in the following matrix algebraic equation

$$\underbrace{\begin{bmatrix} a_n & & b_n & & \\ \vdots & \ddots & \vdots & \ddots & \\ \vdots & & a_n & \vdots & b_n \\ a_0 & & \vdots & b_0 & \vdots \\ & \ddots & \vdots & & \vdots \\ & & a_0 & & b_0 \end{bmatrix}}_{A_e} \underbrace{\begin{bmatrix} u_l \\ \vdots \\ u_0 \\ v_k \\ \vdots \\ v_0 \end{bmatrix}}_{X_e} = \underbrace{\begin{bmatrix} d_p \\ d_{p-1} \\ \vdots \\ \vdots \\ d_1 \\ d_0 \end{bmatrix}}_{Y_e} \tag{2.76}$$

where $A_e \in R^{(p+1)\times(l+k+2)}$, $X_e \in R^{(l+k+2)\times 1}$, $Y_e \in R^{(p+1)\times 1}$, and $l = p-n$, $k = n-1$.

Theorem 2.19 (Middleton et al. [62])

The algebraic equation (2.76) has a unique solution for a general A_e if and only if the plant $P(\varepsilon)$ given by (2.69) is coprime.D

Remark 2.19

i) Theorem 2.19, together with Lemma 2.15, gives conditions for the existence of a unique solution to (2.76) for $p \geq (2n-1)$.

ii) When $p = (2n-1)$, A_e is the Sylvester Matrix associated with $P(\varepsilon)$.

iii) When $p < (2n-1)$, a stable system $\bar{\Sigma}(s)$ with equivalent numerator and denominator of order greater than or equal to $(2n-1-p)$ can be added to the original continuous-time plant. The PIM digital re-design method for SISO system is then re-applied to the modified plant $\bar{P}(s)\bar{\Sigma}(s)$. A modified PITF and hence Y_e is obtained. Using coefficients of the SIM of the *original* plant results in a square A_e matrix, and the system of equations given by (2.76) can be solved using standard procedure such as Gaussian elimination.c

b) State Space Method

A state space solution for $u(\varepsilon)$ and $v(\varepsilon)$ is developed using this method. The computation algorithm is described in [32].

c) Least-Squares Method

This is studied by Rabbath et al. in [32], and is used for applying the reduced order PIM method.

This will be shown in Section 2.6.5.

After solving for $u(\varepsilon)$ and $v(\varepsilon)$ in (2.73), the transfer function of the discrete-time controllers can be obtained with the following rule. Let $\mu(\varepsilon)$ be an arbitrary polynomial of degree l such that the roots of $\mu(\varepsilon)$ lie in the stability region of the ε-domain.

1. If $k \le l$ and $(q-n) \le l$, set

$$E(\varepsilon) = \frac{r(\varepsilon)}{\mu(\varepsilon)}, \quad F(\varepsilon) = \frac{\mu(\varepsilon)}{u(\varepsilon)}, \quad H(\varepsilon) = \frac{v(\varepsilon)}{\lambda(\varepsilon)} . \tag{2.77}$$

2. If $1/u(\varepsilon)$ is stable, $k \le l$ and $(q-n) \le l$, set

$$E(\varepsilon) = \frac{r(\varepsilon)}{u(\varepsilon)}, \quad F(\varepsilon) = 1, \quad H(\varepsilon) = \frac{v(\varepsilon)}{u(\varepsilon)} . \tag{2.78}$$

3. If $1/r(\varepsilon)$ is stable, and $k \le (q-n) \le l$, set

$$E(\varepsilon) = 1, \quad F(\varepsilon) = \frac{r(\varepsilon)}{u(\varepsilon)}, \quad H(\varepsilon) = \frac{v(\varepsilon)}{r(\varepsilon)} . \tag{2.79}$$

4. If $1/v(\varepsilon)$ is stable, and $(q-n) \le k \le l$, set

$$E(\varepsilon) = \frac{r(\varepsilon)}{v(\varepsilon)}, \quad F(\varepsilon) = \frac{v(\varepsilon)}{u(\varepsilon)}, \quad H(\varepsilon) = 1 . \tag{2.80}$$

Setting up the discrete-time controllers as in Figure 2.7 completes the digital re-design process.

2.6.4 PIM method for Multi-Loop systems

This extension of the PIM method is developed by Ro et al. [35]. The idea is to apply the PIM digital re-design method to the innermost loop of the continuous-time multi-loop system and then move to the outermost loop in stages.

To illustrate the concept, consider a system with two feedback loops as shown in Figure 2.8.

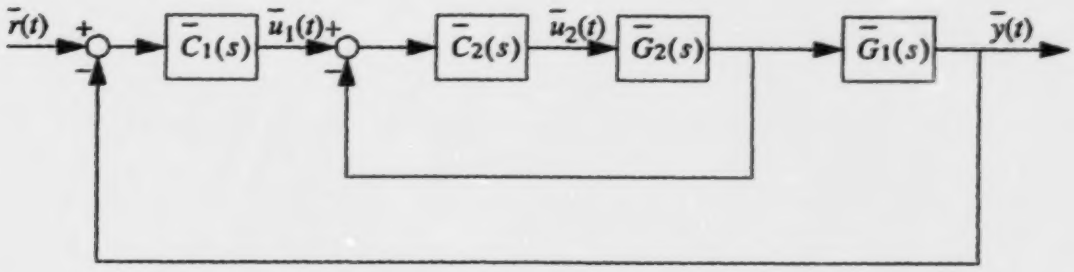

Figure 2.8: An analogue 2-loop feedback SISO system

Following the PIM digital re-design method for SISO systems established in Section 2.6.3, the innermost loop with the continuous-time plant $\bar{G}_2(s)$ and controller $\bar{C}_2(s)$ is first discretized (Refer to Figure 2.9).

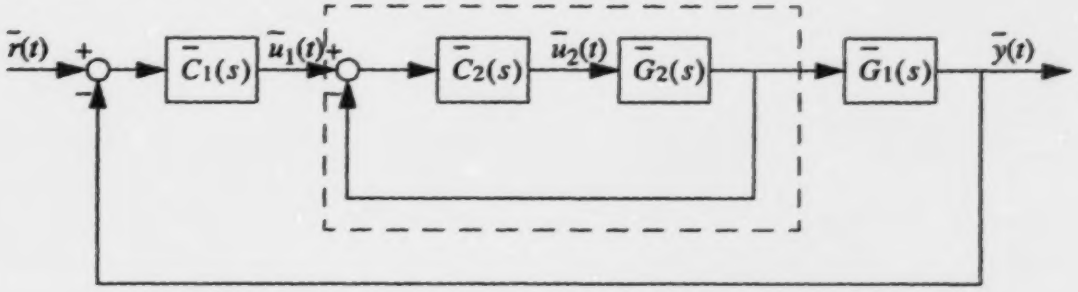

Figure 2.9: Focusing on the innermost loop

A step invariant model $P_2(\varepsilon)$ is obtained for the continuous-time plant $\bar{P}_2(s) = \bar{G}_2(s)$. The continuous-time PITF $\bar{\Phi}_2(s)$ where

$$\bar{\Phi}_2(s) = \frac{\bar{C}_2(s)}{1 + \bar{P}_2(s)\bar{C}_2(s)} \tag{2.81}$$

is mapped to $\Phi_2(\varepsilon)$ using the MPZ method. A discrete-time control system is obtained after solving the Diophantine equation and selecting the desired feedback controller configuration by following the procedure described in Section 2.6.3.

The next step is to perform the digital re-design of the outerloop. Referring to Figure 2.10, the

continuous-time plant considered now is given by

$$\bar{P}_1(s) = \bar{G}_1(s)\bar{G}_2(s)\bar{\Phi}_2(s) \tag{2.82}$$

and the discrete-time plant for the outer loop $\bar{P}_1(\varepsilon)$ is obtained by using the MPZ model of $\bar{\Phi}_2(s)$ and the SIM of $\bar{G}_2(s)$ and $\bar{G}_1(s)$ because this is how the inner loop is implemented digitally.

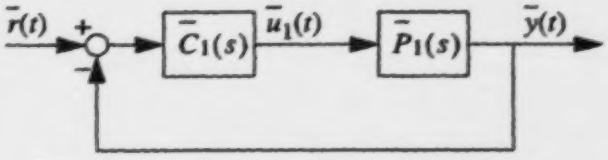

Figure 2.10: Performing a re-design of the outer loop

The continuous-time PITF for the outerloop is defined as

$$\bar{\Phi}_1(s) = \frac{\bar{u}_1(s)}{\bar{r}(s)} = \frac{\bar{C}_1(s)}{1 + \bar{P}_1(s)\bar{C}_1(s)} \tag{2.83}$$

where $\bar{P}_1(s)$ is defined by (2.82). The PITF $\Phi_1(\varepsilon)$ is then evaluated as the MPZ model of $\bar{\Phi}_1(s)$. By again following the same design steps for the PIM design for SISO systems and considering $\bar{P}_1(s)$, $P_1(\varepsilon)$, $\bar{\Phi}_1(s)$ and $\Phi_1(\varepsilon)$ defined above, a discrete-time control system for the outerloop can be obtained. The re-designed discrete-time control system resembles Figure 2.11.

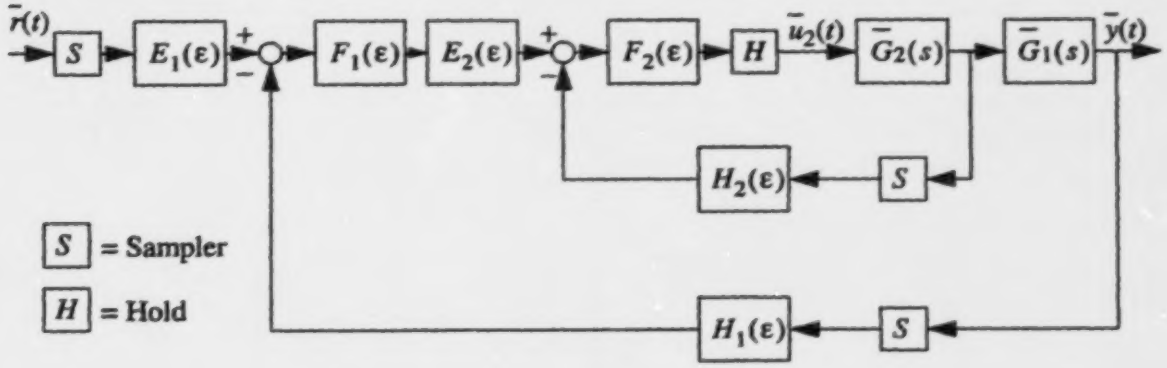

Figure 2.11: PIM digitally re-designed 2-loop sampled-data system

An actual numerical example of a two loop system is shown in [35] with comparison of other local discretization methods. For systems with more than two feedback loops, the procedure for the outerloop re-design is repeated until the outermost loop is reached.

2.6.5 Reduced Order PIM method for SISO systems

This method is originally proposed by Rabbath et al. in [32] to overcome a potential drawback for PIM re-design of SISO systems, that is the resultant digital controllers typically have the same high order as the plant. The order reduction technique revolves around the use of the least-square method in solving the system of equations resulting from the Diophantine equation.

Recall from the PIM digital re-design method for SISO systems in Section 2.6.3 that the Diophantine equation is formed by setting the degrees of $s(\varepsilon)$ and $v(\varepsilon)$ to $l = p - n$ and $r = n - 1$ respectively. For the reduced order PIM method for SISO systems, the digital controller orders are set equal to the continuous-time ones using the following procedure:

Consider Figure 2.6 again as a SISO system. The continuous-time PITF $\bar{\Phi}(s)$ can be written as

$$\bar{\Phi} = \frac{\bar{F}\bar{E}}{1 + \bar{F}\bar{H}\bar{P}} . \tag{2.84}$$

Let

$$\bar{E}(s) = \frac{\bar{n}_E(s)}{\bar{d}_E(s)}, \quad \bar{F}(s) = \frac{\bar{n}_F(s)}{\bar{d}_F(s)}, \quad \bar{H}(s) = \frac{\bar{n}_H(s)}{\bar{d}_H(s)} . \tag{2.85}$$

Then $\bar{d}(s)$, the denominator of $\bar{\Phi}(s)$, is evaluated as

$$\underbrace{\bar{d}_E(s)\bar{d}_F(s)\bar{d}_H(s)}_{= \bar{u}(s)} \bar{a}(s) + \underbrace{\bar{d}_F(s)\bar{n}_E(s)\bar{n}_H(s)}_{= \bar{v}(s)} \bar{b}(s) = \bar{d}(s) \tag{2.86}$$

where

$$\begin{aligned} \bar{d}(s) &= \bar{d}_p s^p + \bar{d}_{p-1} s^{p-1} + \ldots + \bar{d}_1 s^1 + \bar{d}_0 \\ \bar{u}(s) &= \bar{u}_i s^i + \bar{u}_{i-1} s^{i-1} + \ldots + \bar{u}_1 s^1 + \bar{u}_0 \\ \bar{v}(s) &= \bar{v}_j s^j + \bar{v}_{j-1} s^{j-1} + \ldots + \bar{v}_1 s^1 + \bar{v}_0 \end{aligned} . \tag{2.87}$$

By equating like powers of s, a system of equation $AX = Y$ can be formed in continuous-time such that

$$A \in R^{(p+1)\times(i+j+2)} \quad , \quad X \in R^{(i+j+2)\times 1} \quad \text{and} \quad Y \in R^{(p+1)\times 1} \; . \tag{2.88}$$

Comparing the Diophantine equation for discrete-time systems in (2.72) to (2.74), and for continuous-time systems in (2.86) to (2.87), the focal point of the least-squares method is to limit $l = i$ and $r = j$ for $u(\varepsilon)$ and $v(\varepsilon)$, respectively, for the discrete-time system such that $(i+j+2) < (p+1)$.

Now equating like powers of ε in both sides of (2.72), a system of equation $AX = Y$ is formed where

$$A \in R^{(p+1)\times(i+j+2)}, X \in R^{(i+j+2)\times 1}, Y \in R^{(p+1)\times 1}, \text{and } (i+j+2) < (p+1). \tag{2.89}$$

This is clearly an over-determined system, and the "best fit" solution can be obtained using the least-square method [64] such that

$$\widehat{X} = (A^T A)^{-1} A^T Y \tag{2.90}$$

where $\widehat{X}$ is the least-square solution to $AX = Y$, provided $\text{Rank}(A) = (i+j+2)$. The following theorem assures the uniqueness of the least-square solution $\widehat{X}$ in (2.90)

Theorem 2.20 (Rabbath [41])

Consider the system of equation given by $AX = Y$, where A, X and Y satisfy (2.89). If the degrees of $u(\varepsilon)$ and $v(\varepsilon)$ are set to $l = p - n$ and $r < n - 1$, respectively, and $r \leq l$. There exists a unique solution $\widehat{X}$, obtained in a least-square sense, when $b(\varepsilon)$ and $a(\varepsilon)$ that constitute A are coprime.D

Remark 2.20

In fact in this case, $[(A^T A)^{-1} A^T]$ is a non-unique left inverse of A [70]. This can be calculated numerically using the singular decomposition of A.c

Denoting the discrete-time PITF formed using the least-square solution as $\widehat{\Phi}(\varepsilon)$, the discrete-

time system $\widehat{\Phi}(\varepsilon)$ has the same set of zeros as that of $\Phi(\varepsilon)$, but different pole locations. When $\widehat{\Phi}(\varepsilon)$ has all of its poles in the stability region $|T\varepsilon + 1| < 1$, a steady state or low-frequency requirement can be met by multiplying a gain K to $\widehat{\Phi}(\varepsilon)$ such that

$$\widehat{\Phi}(\varepsilon)\Big|_{\varepsilon=\varepsilon_0} \cdot K = \Phi(\varepsilon)\Big|_{\varepsilon=\varepsilon_0}. \tag{2.91}$$

The behaviour and stability of the discrete-time system as $T \to 0$ are established with the following theorems.

Theorem 2.21 (Rabbath [41])
There exists a $T_s > 0$ such that the system $\widehat{\Phi}(\varepsilon)\Big|_{\varepsilon=\varepsilon_0} \cdot K$ has all of its poles inside the stability region $|T\varepsilon + 1| < 1$ if $0 < T < T_s$.D

Theorem 2.22 (Rabbath [41])
The discrete-time system $\widehat{\Phi}(\varepsilon)\Big|_{\varepsilon=\varepsilon_0} \cdot K$ converges to $\bar{\Phi}(s)$, pointwise in s, as $T \to 0$.D

While having a lower order digital controller have many implementation advantages, the drawback in utilizing the reduced-order PIM method is that it is not certain that the resulting closed loop system is stable. Although it is shown in [32] that $\widehat{X}$ approaches the continuous-time full order solution as T approaches zero, the denominator of the resultant PITF with coefficients in $\widehat{Y}$ defined as

$$\widehat{Y} = A\widehat{X} = A(A^TA)^{-1}A^TY \tag{2.92}$$

is not necessarily stable for finite T. Thus this creates a dilemma for designers wishing to utilize the full potentials of PIM. Further exposition of the idea of order reduction for PIM method will be shown later in sections of Chapters 3 and 4.

2.7 Implementation of Discrete-Time Systems

There are many issues that can be addressed in the implementation of digital feedback controllers.

Examples include numerical properties of different control algorithms and realization structures, selection of suitable hardware, choice of hardware and software programming languages, implication of using fixed-point and floating-point arithmetic, issues with computer simulation, etc. Many of these originally stem from application in the DSP field. Consideration of those in the context of digital filters is given in many DSP text books, such as one by Proakis et al. [65]. For digital control, a survey on many of the above is given by Hanselmann in [11]. Moreover, Moroney in [63] also gives detailed account of many concerns faced by designers in the digital control community. Amongst those topics, a description of some finite word length (FWL) effects associated with fixed-point implementation of digital controllers, as well as its realization structure are given in this section of the thesis, in order to facilitate the understanding of topics to be covered in Chapters 3 and 4.

2.7.1 Realization Structure of Digital Controllers

Once a set of digital controllers is selected for controlling an analogue plant with addition of hold devices and samplers, the first step of the implementation procedure is to choose a structure for the controllers suitable for implementation with the available arithmetic. With fixed-point calculation at least, it is in most cases crucial to transform a digital controller description into another one which has the same input-to-output relation but exhibits better numerical sensitivity. Determination of numerically efficient structure has long been a main issue in the field of digital filtering. The digital control community has been able to inherit some important research work done in this area. In the following, some basic structures are discussed without taking the closed loop feedback into account.

Consider a digital controller that belongs to the class of SISO LTI discrete-time system represented by a transfer function in ε as

$$\frac{Y(\varepsilon)}{U(\varepsilon)} = F(\varepsilon) = \frac{b_0 + b_1\varepsilon^{-1} + \ldots + b_m\varepsilon^{-m}}{1 + a_1\varepsilon^{-1} + \ldots + a_n\varepsilon^{-n}} \quad . \tag{2.93}$$

Using the definition of the ε operator and properties of the ε-transform from Section 2.1, this system can also be implemented as

$$y(n) = -\sum_{k=1}^{N} a_k' \cdot y(n-k) + \sum_{k=0}^{M} b_k' \cdot u(n-k) \tag{2.94}$$

which is a general linear constant coefficient difference equation. A SISO LTI system can also be represented in the state space form by the realization

$$\begin{aligned} \varepsilon x(k) &= Ax(k) + Bu(k) \\ y(k) &= Cx(k) + Du(k) \end{aligned} \tag{2.95}$$

It is possible to view (2.94) as a computational procedure or algorithm for determining the output sequence $y(n)$ of the system defined by (2.93) or (2.95) from the input sequence $u(n)$. It is the simplest and most straight forward algorithm. However, in different ways the computation in (2.94) can be arranged into equivalent sets of difference equations. Each set of equations defines a computational procedure or an algorithm for implementing the system. From each set of equation it is possible to construct a block diagram consisting of an interconnection of delay elements, multipliers and adders. Such a block diagram is called the realization of the system.

Thus different arrangements of (2.93) and (2.94) as well as different magnitude of the summation indices in (2.94) (and thus the order of system in (2.93)) result in different number of delay elements, multipliers and adders, and it is these differences that characterize each algorithm's computational complexity, memory requirements and FWL effects.

FWL effects refers to the quantization effects that are inherent in any digital implementation of discrete-time systems, either in hardware or in software. This effect is dependent on the choice of system realization. If the system is to be implemented in software, the set of re-arranged equations of (2.94) can be written as a program that runs on a digital computer. Alternatively, the structure in block diagram form implies a hardware configuration for implementing the system. A summary of some useful structures is given below.

2.7.2 Direct Form Structure

There are two types of these: Direct form I and II structures. They are named as such because the

polynomials appear directly as coefficients in the difference equation or block diagram which is their main feature. Unfortunately, both structures are known to be extremely sensitive to coefficient quantization, particularly when the order of the system is large.

2.7.3 Cascade Form Structure

This is a more numerically reliable SISO structure that is well accepted in digital filtering. A system is implemented in factored form as a cascade series connection of first order (with real poles and zeros) or second order blocks (with complex conjugate pairs). In addition this structure offers possibilities of optimal distribution of poles and zeros among the blocks.

2.7.4 Parallel Form Structure

This structure is also a numerically reliable structure and corresponds to implementing the partial fraction expansion of the system. The partial fraction blocks are commonly chosen to be of first and second order and can be implemented by suitable structures. A slight drawback is that there is no control over the pairing of zeros with the system poles due to the nature of partial faction expansion.

2.7.5 State Space Form Structure

A discrete-time system represented in state space form given by (2.95) can also be implemented by directly translating it into a simple computer program. There are infinitely many state space realizations of a system, and they are related to each other by a similarity transformation T as

$$\begin{aligned} \tilde{A} &= T^{-1}AT \\ \tilde{B} &= T^{-1}B \\ \tilde{C} &= CT \\ \tilde{D} &= D\,. \end{aligned} \tag{2.96}$$

Two well known state space realizations of a system are the controllable canonical form and observable canonical form. They uses coefficients of a transfer function directly and thus are very

convenient for control engineer. However they also suffer from considerable numerical problems for higher order systems for the same reason as direct form structure.

It is possible to consider the previously mentioned cascade form and parallel from realizations in the context of a state space formulation. The parallel form representation is called the *normal form* representation. In such a case the "A" matrix is block diagonal with groupings of real and complex conjugate pair poles. More detail is given by Hanselmann [11] and Moroney [63].

Some FWL effects of digital systems are now considered.

2.7.6 Representation of Numbers

The use of digital hardware and software to perform computation for a control algorithm dictates the need for some kind of representation of numbers for digital calculation. There are typically two types: fixed-point representation and floating-point representation. In general, fixed-point numbers have a much more limited dynamic range than floating-point numbers. This crucial difference accounts for many unique characteristic pertaining to the use of fixed-point computation. Those are listed in the following sections.

In practice, there are many reasons why a designer may chose to use fixed-point arithmetic over floating point arithmetic. Those could be issues related to calculation speed, cost of hardware, available selection of hardware for the particular design, etc. Furthermore, whereas general microprocessors might allow for comfortable floating-point arithmetic, there are often restrictions dictating the use of short word length fixed-point arithmetic. It is therefore pertinent to understand some of these issues in a design.

2.7.7 Quantization of Digital Controller Coefficients

In the realization of digital controller in hardware or in software on a general-purpose computer, the accuracy with which filter coefficients can be specified is limited by the word length of the computer or the length of register provided to store the coefficients. Since the coefficients used in

the actual implementation of a digital filter are not exact, the poles and zeros of the system function will, in general, be different from the desired poles and zeros. Consequently, the filter actually obtained have a *different frequency response* in comparison with the frequency response of the digital controller with unquantized coefficient. Take for example, a digital controller with the system function

$$F(\varepsilon) = \frac{\sum_{k=0}^{M} b_k \varepsilon^{-k}}{\sum_{k=0}^{N} a_k \varepsilon^{-k}}. \tag{2.97}$$

In the actual implementation of the digital controller, with quantized coefficients, the system function becomes

$$F'(\varepsilon) = \frac{\sum_{k=0}^{M} b_k' \varepsilon^{-k}}{\sum_{k=0}^{N} a_k' \varepsilon^{-k}} \tag{2.98}$$

where the quantized coefficients $\{b_k'\}$ and $\{a_k'\}$ can be related to the unquantized coefficients $\{b_k\}$ and $\{a_k\}$ by the relation

$$\begin{aligned} b_k' &= b_k + \Delta b_k \; ; \qquad k = 0, 1, \ldots, M \\ a_k' &= a_k + \Delta a_k \; ; \qquad k = 0, 1, \ldots, N \end{aligned} \tag{2.99}$$

and $\{\Delta b_k\}$, $\{\Delta a_k\}$ represent the quantization error for the digital controller coefficients.

The sensitivity of quantization of digital controller coefficients can depend on the closeness between possible pole and zero locations and the desired pole and zero locations. The former is determined by the realization chosen for the digital controller. Using the techniques described in earlier sections to reduce FWL effects, it is possible to reduce the effects of coefficient quantization by factoring the digital controller into first and second order sub-sections either in

cascade-form or parallel-form realization. By doing so, the coefficients in the sub-systems are smaller in magnitude, thus it is possible to allocate more decimal points to the fixed point arithmetic and results in finer resolution in the representation of numbers. This is an important theme to note for later discussions.

2.7.8 Quantization of Signals

Quantization of signals occur when fixed-point calculation is carried out, or when an analogue signals are quantized to form digital signals and vice versa. It takes place in the form of truncation or rounding. Signal quantization introduces three effects: bias, noise and limit cycles [11]. Bias is introduced by truncation, and therefore in general cases it is better to use rounding. A character of rounding of signals, ignoring all other FWL effects, is that if the original unquantized digital system is stable, then the resultant quantized system is also stable [22].

2.7.9 Overflow

As a result of finite-precision arithmetic operations performed in the digital controller, some registers may overflow if the input signal level becomes too large. In other words, some intermediate result becomes so large that it no longer fits into the available number-range. Overflow represents another form of undesirable non-linear distortion on the designed signal at the output of the controller. It is possible to prevent overflow or at least minimize its rate of occurrence by scaling. Note that the addition and subtraction operations produce exact results as long as there is no problem with overflow. In the Simulink simulation environment, the user can be alerted of any signal overflow by checking a specific option in the set up.

2.7.10 Limit Cycle Oscillation

Limit cycles observed in practical control systems are often due to round off errors from A/D and D/A converters, as well as finite precision arithmetic. For cascade realization of a higher order digital controller, when the first sub-section exhibits a zero-input limit cycle, the output limit cycle is filtered by the succeeding sections. If the frequency of the limit cycle falls near a

resonance frequency of the succeeding sections, the amplitude of the sequence can be enhanced by the resonance characteristic. This situation may be avoided by placing the cascade sections in the order of decreasing maximum frequency gain.

2.8 Overview of Missile Flight Control Systems

This thesis focuses on the digital *re*-design of verified analogue control law that is associated with a missile autopilot. Nonetheless, an overview of missile flight control systems is presented to illustrate its feature and design.

The design and integration of flight control system for a missile is by no mean an easy task. This is the case particularly for a modern tactical air-to-air missile in pursuit of a highly maneuverable aircraft. Not only must the missile control system steer itself towards the target, but because the target is typically moving swiftly and rapidly, the problem also consist of estimating the target motion, generating guidance command to *optimally* steer the missile towards the target intercept, and controlling the coupled, non-linear, multivariable, uncertain dynamics of the air-to-air missile. Each portion of the problem, i.e. estimation, guidance and control, is inherently non-linear and time varying, and all three combine to form a highly complex integrated system [8].

Before going into further details, some useful terms are defined. A navigation system is one that automatically determines the position of the missile with respect to some reference frame. This can be done, for example, via the use of a global positioning system (GPS). The guidance system, on the other hand, automatically calculates the necessary correction to keep the missile on course and sends a proper signal to the control system or autopilot. The control system controls the direction of motion of the missile by sending signals to the control actuators to alter the position of control surfaces of the missile, such as its fins.

A simplified block diagram typical of an advanced air-to-air missile system is given in Figure 2.12. What happens is that the target information obtained from a seeker is processed by an estimation filter, such as an extended Kalman filter, to obtain estimates of relative missile-to-

target position, velocity, and acceleration. Note that these filter estimates are heavily dependent on the assumed target acceleration model. A guidance law based on some modern control theory uses the estimates of states and time-to-go-until-intercept to produce a *commanded acceleration*. The autopilot receives this command signal and sends an input to the fin actuator based on the airframe aerodynamics characteristic and sensed angular rates and linear accelerations of the missile body. The action alters the dynamics of the missile, and the process repeats via the feedback loops.

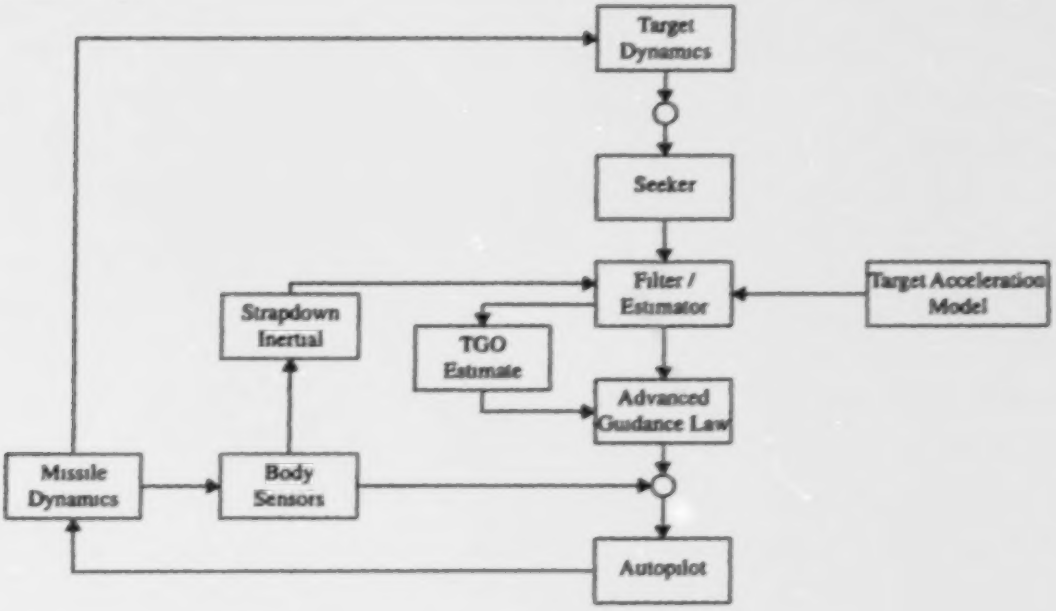

Figure 2.12: A typical air-to-air missile block diagram

The study of target state estimation and advanced guidance law design is summarized by Cloutier et al. in [8] and Blakelock in [46]. In many ways the guidance of a missile is intricately connected to the autopilot of the missile. The guidance law design needs to take into account the acceleration limits of the airframe, as well as the autopilot's finite response time. It is also possible to derive guidance laws to deal with a specific type of control employed by a missile.

Some brief information on missile autopilot design is given next.

There are many different physical ways to control the action of a missile. Some of these are

illustrated by Garnell in Chapter 3 of [45]. Depending on the missile configuration, it can be done using aerodynamic control surfaces located in the rear (elevators and rudders) or front (canard) of the missile. In addition, the motion of the missile can also be altered using an external nozzle or by varying the angle of thrust direction such as thrust vectoring control (TVC). Using aerodynamic control, there are mainly two ways to steer a missile; either by using skid-to-turn design (STT) or bank-to-turn (BTT) design.

An autopilot is a closed system that is typically embedded inside the main guidance loop. The design of autopilot for STT missile has been around for a long time and is a relatively mature area. More recent interest in asymmetrical missile spurs activity in the design of BTT autopilots [4]. In general, an airframe with a non-circular cross-section improves the aerodynamic efficiency of both the missile and the host aircraft. However, this complicates the control of the missile in roughly three different ways. First, the missile's asymmetrical cross section gives a large acceleration capability in its pitch plane but only limited capability in the yaw plane. Hence, it is necessary to roll or bank the missile to maximize its maneuverability. Second, other constraints, such as engine performance, often require that the angle of attack remain positive and the side-slip-angle be kept small. Third, the asymmetrical shape of the missile produces significant non-linear dynamic coupling among the roll, pitch and yaw axes.

BTT and STT missile autopilot systems can be designed using many techniques, such as classical control, LQG regulator control, generalized singular LQ control, eigenstructure assignment. For classical control, an initial design is typically performed by ignoring the dynamic interaction among the roll, pitch and yaw axes. This allows individual SISO controllers to be designed for each axis. BTT control, for example, is then achieved by directing pitch and roll axis acceleration commands from the guidance system to the corresponding controller channel and by operating the yaw channel in a regulatory mode to minimize sideslip angle. Final gain settings are determined during a 6 DOF non-linear computer simulation analysis.

There are many published literature on the design of analogue autopilots using other modern multivariable analysis techniques as mentioned above. A summery of these accounts are contained in [8]. In contrast, the digital control of missile has not been receiving much attention.

This is perhaps due to the unavoidable difficulty of analyzing the performance of a multivariable or multichannel digital controller embedded in the inner loop of the combined missile flight control system that includes, among many, the estimation and guidance system in outer loops that is a mixture of analogue and digital systems. It is certainly true that as long as an adequate method of controller discretization is available, one can always perform the design in the analogue domain and then later obtain a set of digital controllers for actual implementation via the suitable discretization. This is the subject of this thesis.

As a reference, a diagram showing the different dynamics of a missile is shown in Figure 2.13.

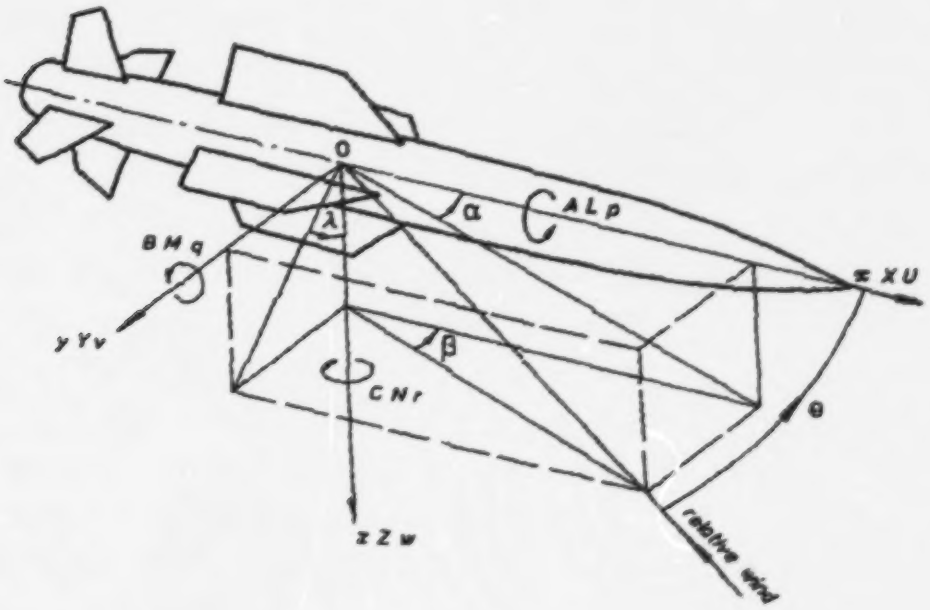

Figure 2.13: A schematic diagram of missile dynamics

Chapter 3

PIM Digitally Re-designed Missile Control System

This chapter examines the application of PIM digital re-design methods to a continuous-time control system for an air-to-air missile concept. An investigation of some digital implementation effects on the missile contol system is carried out by DERA in [42]. However, much analysis performed in that report seems in fact invalid, since the closed loop continuous-time system is unstable. Although the reason for the oversight is not known, the problem is rectified in this thesis by raising the natural frequency of the second order actuator from $w_n = 100$ rad/s to $w_n = 250$ rad/s. This action pushes the actuator system poles further away from the analogue plant poles, doubling the approximate original distance which has a factor of less than 10 in comparing their real parts. The ensuing analogue closed loop control system is illustrated in Section 3.1, and its performance and stability property is examined in Section 3.2.

Section 3.3 displays some interesting properties for the class of Single-Input Multi-Output (SIMO) systems. It shows that under certain conditions, a SIMO system can be re-formulated as a multi-loop system for the purpose of control system design. This includes the closed loop missile control system. Section 3.3 also compares the treatment of the missile control system as a MIMO system and as a multi-loop system for the purpose of PIM digital re-design. Section 3.4 then illustrates the necessary design steps in applying the PIM methods, using the missile control system as an example, and Section 3.5 presents the numerical result which is obtained from simulation studies using MATLAB 5.2 with Simulink 2.2 and Fixed-Point Blockset 1.0.

The missile dynamic model and its designed continuous-time control system are first given.

3.1 Analogue Missile Control System

The analogue missile dynamic model studied in this thesis is the yaw-plane dynamics of a tail-controlled air-to-air missile concept originally developed by British Aerospace, Filton. This is the same missile model studied by DERA in [42] and King in [43]. The model is an average model aimed at capturing the variation of the flight conditions and to be a representative for the region of flight envelop of interest. This in [43] is taken from models that were varied in incidence ($0^\circ \leq \alpha \leq 20^\circ$) and roll angle ($0^\circ \leq \phi \leq 20^\circ$). The speed and altitude of the missile model are assumed to be Mach 3.0 and 40m, respectively. The accelerometer is assumed to be located at 0.8m ahead of the Centre of Gravity (CG) position.

3.1.1 Missile Dynamic Model

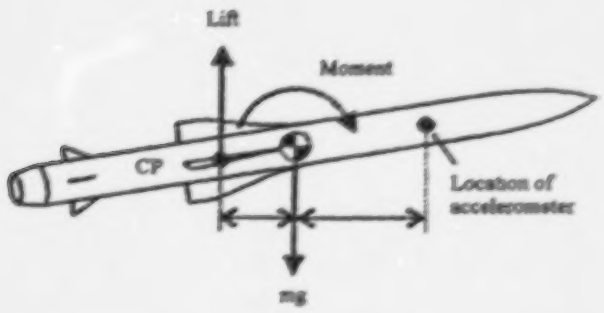

Figure 3.1: Configuration of a statically stable, tail-controlled air-to-air missile

The missile dynamic model in state space form is given by

$$\bar{P}_m : \quad \begin{aligned} \dot{\bar{x}} &= \bar{A}\bar{x} + \bar{B}\bar{u} \\ \bar{y} &= \bar{C}\bar{x} + \bar{D}\bar{u} \end{aligned} \tag{3.1}$$

where

$$\bar{A} = \begin{bmatrix} -3.18 & -996.37 \\ 0.49 & 1.23 \end{bmatrix}, \qquad \bar{B} = \begin{bmatrix} 12.11 \\ -17.96 \end{bmatrix},$$
$$\bar{C} = \begin{bmatrix} -3.18 & 0 \\ -2.79 & -0.99 \\ 0 & 1 \end{bmatrix}, \qquad \bar{D} = \begin{bmatrix} 12.11 \\ -2.24 \\ 0 \end{bmatrix}. \tag{3.2}$$

The state vector is $\bar{x} = \begin{bmatrix} \bar{v} & \bar{r} \end{bmatrix}^T$, where $\bar{v}$ = lateral velocity (m/sec) and $\bar{r}$ = yaw rate (rad/sec). The single input $\bar{u} = \xi$ is the rudder deflection in rad. The output vector is $\bar{y} = \begin{bmatrix} \bar{a}_y & \hat{\bar{a}}_y & \bar{r} \end{bmatrix}^T$, where $\bar{a}_y$ = acceleration (m/sec) at CG, $\hat{\bar{a}}_y$ = acceleration (m/sec) at accelerometer, and $\bar{r}$ = yaw rate (rad/sec). All quantities are given in SI units.

Equation (3.1) indicates that the missile yaw plane dynamics are modelled as a second order system. In transfer function form, the missile model is represented as

$$\bar{P}_m: \qquad \bar{y} = \underbrace{\begin{bmatrix} \dfrac{12.11s^2 - 14.9s - 5.093 \times 10^4}{s^2 + 1.95s + 484.3} \\ \dfrac{-2.24s^2 - 20.39s - 5.086 \times 10^4}{s^2 + 1.95s + 484.3} \\ \dfrac{-17.94s - 51.12}{s^2 + 1.95s + 484.3} \end{bmatrix}}_{\bar{P}_m(s)} \bar{u} \,. \tag{3.3}$$

The poles of the open loop system are located at $-0.9750 \pm j21.9852$, and thus, $\bar{P}_m(s) \in \mathrm{RH}_\infty$. The denominator polynomial of $\bar{P}_m(s)$ is

$$\bar{d}_{P_m}(s) = s^2 + 1.95s + 484.3. \tag{3.4}$$

It is clear from (3.1) and (3.3) that the open loop system $\bar{P}_m(s)$ is a single-input multi-output system. One property of a SIMO system is clearly apparent: since the output of the (open loop) system is not coupled to multiple inputs, conventional definition of classical system performance specification such as damping, natural frequency and overshoot can be applied to each output

channel individually. Examining $\bar{P}_m(s)$ given by (3.3), it can be observed that the open loop SIMO system has the common denominator polynomial whose pole locations determine the system's stability, i.e. steady state behaviour, if exist, whereas it typically has different zero locations that indicate a different transient motion for each system output.

Equation (3.4) suggests that the system has the natural frequency w_n = 22.0068 rad s^{-1} and damping ratio ζ = 0.0443. Figure 3.2 shows the response of the open loop system when it is subjected to an unit step rudder deflection of 1 radian. This time response illustrates that the missile described by (3.3) is naturally stable but has an under-damped short period (weathercock) mode [45].

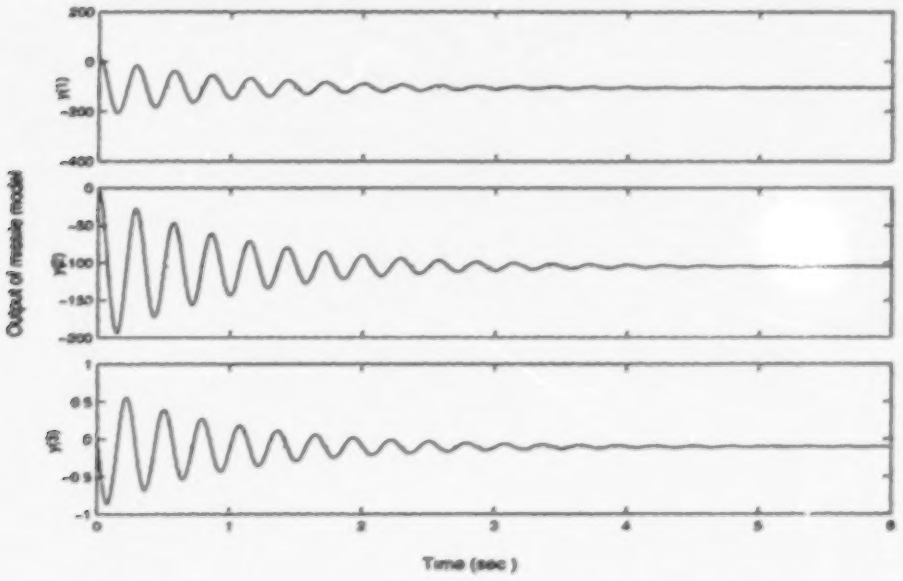

Figure 3.2: Step response of the open loop system $\bar{P}_m(s)$

3.1.2 Missile Control System

The analogue missile flight control system utilized in this thesis is designed in [42]. The analogue control law adopted is a Raytheon 3-loop design, which uses negative feedback of yaw rate to damp short period oscillation, and negative feedback of lateral acceleration to obtain the desired

acceleration response. The control design uses an accelerometer placed as far forward of the CG as possible - it senses an additional component due to yaw acceleration, and thus allows the control law an useful element of anticipation. This is defined by the following relation

$$\tilde{\hat{a}}_y = \tilde{a}_y + \tilde{x}_a \dot{\tilde{r}} \tag{3.5}$$

where $\tilde{x}_a = 0.8\text{m}$ is the apriori distance of the accelerometer in relation to the CG position.

Figure 3.3 illustrates the architecture of the analogue flight control system of the yaw plane dynamics model. The gains K_r and K_a correspond to the rate and acceleration feedback loops respectively. An integrator is placed for the acceleration loop to reduce its steady state error. In addition, the designed control law uses a second rate-feedback loop that attributes to an extra gain K_ψ. This is called the "synthetic stability loop" and has an effect similar to extending the accelerometer moment arm ($\tilde{x}_a$) and improves stability [42].

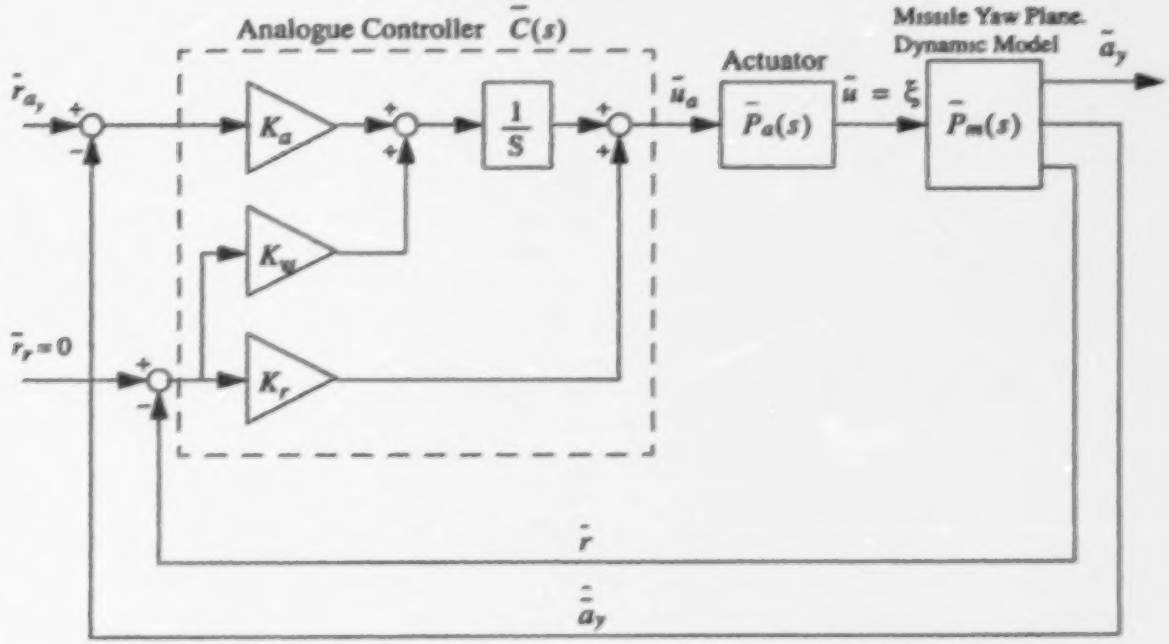

Figure 3.3: Architecture of the analogue missile flight control system

Figure 3.3 shows that the control of yaw plane dynamics of the missile is done by controlling its lateral acceleration while keeping the yaw rate close to zero. As described in Chapter 2.8, typically the missile's guidance system performs a series of calculation to determine the desired missile-states according to some pre-determined flight path or target tracking algorithm. A missile acceleration signal $\bar{a}_y$ is then sent to the missile's autopilot. The reference or command yaw rate $\bar{r}_r$ is always set to zero in Figure 3.3. It indicates that the control system desires to minimize the yawing motion and thereby damping out the short period mode oscillation [42] [45]. Hence, the reference or command acceleration $\bar{r}_{a_y}$ is the only non-zero input signal to the closed system. The control law derived from Figure 3.3 is given by

$$\bar{C}(s) = \begin{bmatrix} \dfrac{K_a}{s} & \dfrac{K_\psi + K_r s}{s} \end{bmatrix}. \tag{3.6}$$

Consistent with Figure 3.3, (3.6) indicates that, with $\bar{C}(s)$ as a 1×2 transfer function matrix, the control law takes the error signals $(\bar{r}_{a_y} - \bar{\bar{a}}_y)$ and $(\bar{r}_r - \bar{r})$ as its input and issues a signal to the control actuator $\bar{P}_a(s)$. This signal is referred to as the actuator input signal $\bar{u}_a(s)$. The parameters chosen in [42] for the analogue control law are summarized as

$$K_a = -1.38\,, \quad K_\psi = -208.6\,, \quad K_r = -5.32\,. \tag{3.7}$$

The control actuator servo is modelled by a simple second order transfer function $\bar{P}_a(s)$, where

$$\bar{P}_a(s) = \frac{w_n^2}{s^2 + 2\zeta w_n s + w_n^2}. \tag{3.8}$$

As discussed at the beginning of this chapter, the natural frequency and damping ratio used in the second order actuator model are

$$\begin{aligned} w_n &= 250 \text{ rad/s}, \\ \zeta &= 0.7\ . \end{aligned} \tag{3.9}$$

Substituting these values into (3.8) yields

$$\bar{P}_a(s) = \frac{62500}{s^2 + 350s + 62500}. \tag{3.10}$$

For the purposes of control system design and analysis, the open loop missile model is combined with the control actuator servo model to form an open loop *plant*, $\bar{P}(s)$, i.e.

$$\bar{P}(s) = \bar{P}_m(s)\bar{P}_a(s)$$

$$= \frac{62500}{s^2 + 350s + 62500} \begin{bmatrix} \dfrac{-2.24s^2 - 20.39s - 5.086 \times 10^4}{s^2 + 1.95s + 484.3} \\ \dfrac{-17.94s - 51.12}{s^2 + 1.95s + 484.3} \\ \dfrac{12.11s^2 - 14.9s - 5.093 \times 10^4}{s^2 + 1.95s + 484.3} \end{bmatrix}. \qquad (3.11)$$

The characteristics of the closed loop continuous-time system is analysed next.

3.2 Characteristics of the continuous-time closed loop system

A brief account of the performance of the analogue closed loop system is given here for convenience of comparison with discretized systems given later in this chapter. Consider the closed loop analogue missile control system shown in Figure 3.3. When a unit step input of 1 m/s^2 is supplied to $\bar{r}_{a_y}$, the controlled plant produces the output in time shown in Figure 3.4.

Comparing Figures 3.2 and 3.4, the closed loop controlled plant exhibits much better damping, considerably less overshoot and much shorter settling time in its step response, particularly for $\bar{a}_y$ and $\bar{r}$. This represents a much more desirable response in time. To review the frequency response characteristics of the closed loop system, the Bode diagram for the transfer function from $\bar{r}_{a_y}$ to $\bar{a}_y$ is illustrated in Figure 3.5.

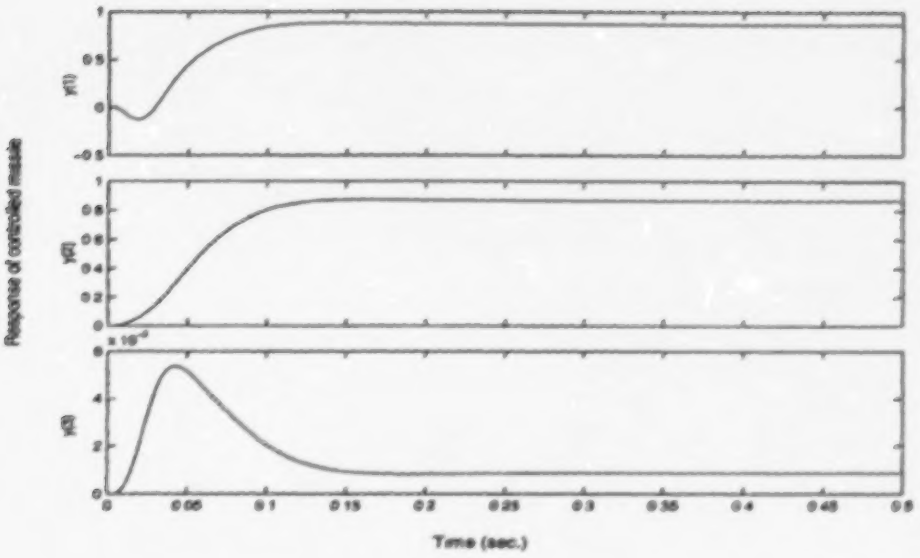

Figure 3.4: Step input response of the closed loop system (with $\bar{r}_r = 0$)

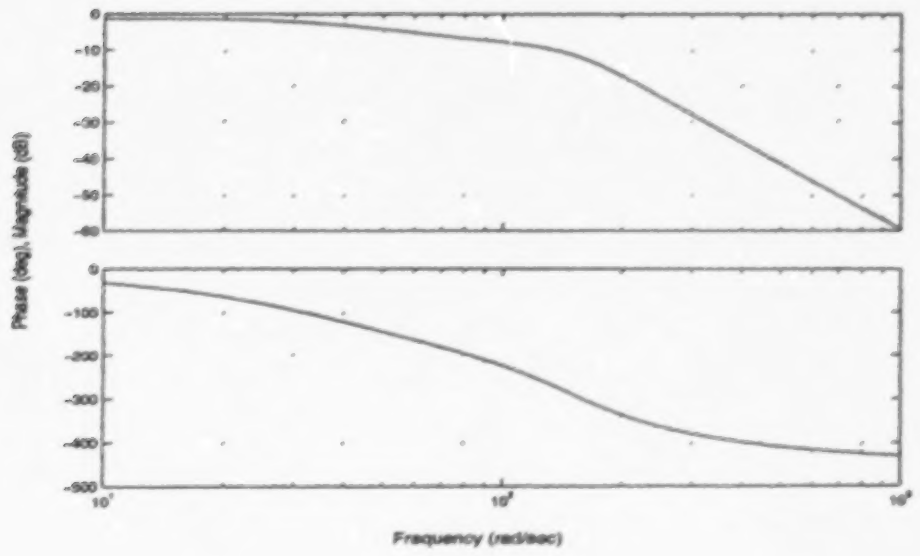

Figure 3.5: Bode diagram of transfer function from reference input to the actual output of the analogue closed loop system.

Since the analogue closed loop system is not a simple SISO system, for reasons described in Chapter 2.5, it is necessary to contemplate the analogue closed loop system as a MIMO system and use the concept of principal gains to assess the system performance. Define

$$\bar{S} = [I + \bar{P}\bar{C}]^{-1} \tag{3.12}$$

which is the sensitivity, and

$$\bar{T} = \bar{S}\bar{P}\bar{C}. \tag{3.13}$$

In general, there are four closed loop requirements to achieving desirable system performance [60]:

1) Sensitivity: keep $\bar{\sigma}(\bar{S})$ as small as possible.
2) Measurement noise propagation: keep $\bar{\sigma}(I - \bar{S})$ as small as possible. (This conflicts with 1.)
3) Tracking of reference signal (for 1 DOF design): keep $\underline{\sigma}[I - \bar{S}] \approx 1$ and $\bar{\sigma}[I - \bar{S}] \approx 1$. (This conflicts with 2, but not 1.)
4) Minimization of control energy: keep $\bar{\sigma}(\bar{C})$ as small as possible. (Expect to conflict with 1, 3.)

As is the case with SISO systems, there are conflicts within these different requirements for satisfactory closed loop performance. It is therefore expected that there will be some tradeoffs during the design process. Expressing the closed loop requirements in terms of open loop principal gains, typically the designer will seek to make $\underline{\sigma}(\bar{P}\bar{C})$ large at low frequencies, and minimze $\bar{\sigma}(\bar{P}\bar{C})$ at high frequencies.

From the definition of $\bar{S}$ in (3.12), the multiplication of transfer function matrices $\bar{P}$ and $\bar{C}$ given by (3.11) and (3.6) results in a non-square matrix. Thus, some extra precaution and understanding is needed in the computation of $\bar{S}$ and indeed analysis of the closed loop system. Figure 3.3 shows that the feedback loop does not include the missile's lateral acceleration signal $\bar{a}_y$, because the control system designed in [42] opted for the use of an accelerometer placed at an off-CG position as described in Section 3.1. Therefore when considering the calculation of $[I + \bar{P}\bar{C}]^{-1}$, it is necessary to only consider the last 2 enteries of $\bar{P}(s)$ in (3.11) that constitute the feedback of the closed loop system. This convention is understood hereafter in this thesis.

Following the above digression, the plot of principal gains for the sensitivity of the system is

displayed in Figure 3.6 for inspection of system performance.

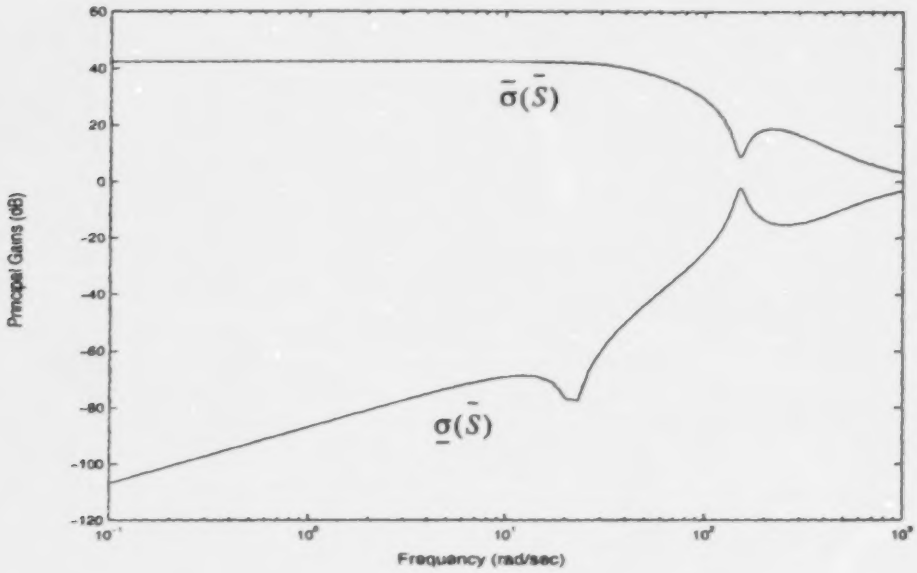

Figure 3.6: Plot of principal gains for the sensitivity $\bar{S}$ of the analogue system

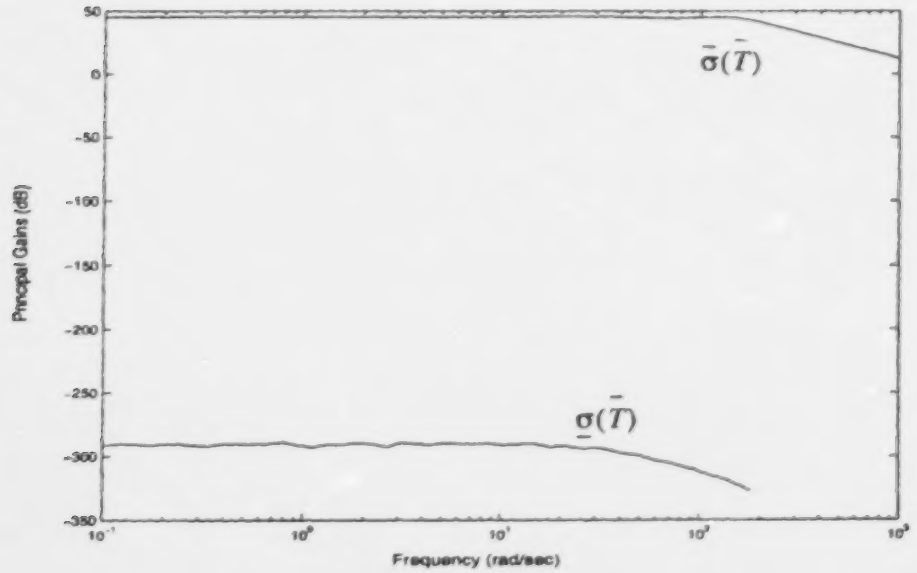

Figure 3.7: Plot of principal gains for the analogue system transfer function $\bar{T}$

The plot of the principal gains for the system transfer function $\bar{T}$ is given in Figure 3.7 for consideration of command input tracking.

In light of the above discussion, Figures 3.6 and 3.7 show that the overall closed loop performance of the designed continuous-time system in fact is non-impressive. In Section 3.3, some simplification in frequency response analysis of this type of system is shown. This simplification is possible since the missile control system is SIMO and not MIMO.

3.3 Comparison of MIMO and Multi-Loop PIM methods

Later in Sections 3.4.2 and 3.4.3, the analogue closed loop missile control system is formulated as a MIMO system and a multi-loop system which are then digitally re-designed using their associated PIM method. Results from computer simulation for the two discrete-time systems are shown in Section 3.5. Before this is done, it is useful to see briefly how the two PIM methods compare in their digital re-design procedure, resultant sampled-data system structures, and performances. For this purpose, some properties of SIMO systems are first given.

3.3.1 A Glimpse of SIMO Systems

Characteristics of SIMO systems are usually omitted from common control literature, since their properties are "in between" those derived from SISO and MIMO systems. However, SIMO systems do possess interesting features that warrants some investigation. For instance, the following holds for such a closed loop feedback system:

Lemma 3.1

If an analogue closed loop LTI system and its associated proper LTI open loop plant are both SIMO systems in view of their respective inputs and outputs, and further, if the compensators in the feedback system are also proper and LTI, then the closed loop system can alternatively be represented as a multi-loop system.D

Proof

Without loss of generality, assume that the closed loop system is a 2-loop feedback system. The proof uses block diagram algebra, and can be easily extended to a general m-loop feedback system where $m \geq 2$. Consider a continuous-time SIMO closed loop system shown in Figure 3.8 with a SIMO open loop plant $\bar{G}(s)$ given as

$$\bar{G}(s) = \begin{bmatrix} \bar{G}_1(s) \\ \bar{G}_2(s) \end{bmatrix} = \begin{bmatrix} \dfrac{\bar{b}_1(s)}{\bar{a}(s)} \\ \dfrac{\bar{b}_2(s)}{\bar{a}(s)} \end{bmatrix}. \tag{3.14}$$

In Figure 3.8, $\bar{r}$ is the reference input to the closed loop SIMO system, $\bar{e}$ is the error signal, $\bar{u}(s)$ is the plant input, and $\bar{y}_1$, $\bar{y}_2$ are the outputs of the system. The closed loop compensator must have the following form

$$\bar{C}(s) = \begin{bmatrix} \bar{C}_1(s) & \bar{C}_2(s) \end{bmatrix}, \tag{3.15}$$

i.e., $\bar{G}(s)$ is a 2×1 transfer function matrix and $\bar{C}(s)$ is a 1×2 transfer function matrix. The closed loop system resembles

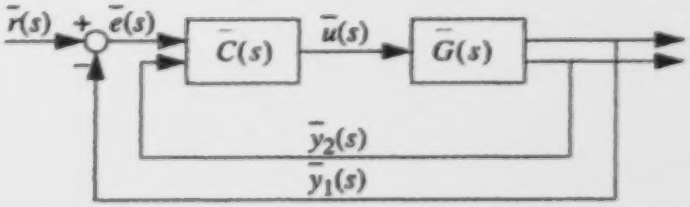

Figure 3.8: A simple SIMO system with two feedback loops

The next step uses block diagram algebra to re-structure the open loop plant $\bar{G}(s)$ as in Figure 3.9

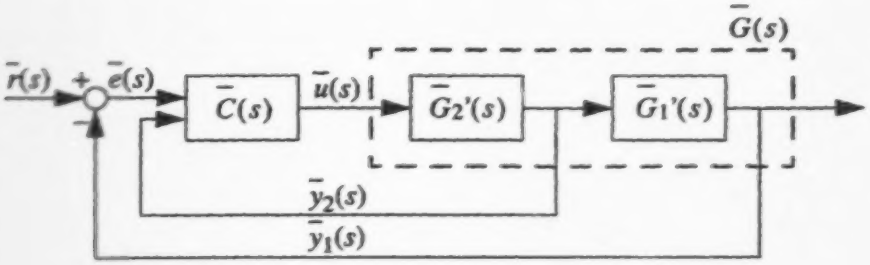

Figure 3.9: First step in re-structuring the two-loop SIMO system

where

$$\bar{G}_2'(s) = \frac{\bar{b}_2(s)}{\bar{a}(s)}, \qquad \bar{G}_1'(s) = \frac{\bar{b}_1(s)}{\bar{b}_2(s)}. \tag{3.16}$$

Note that this re-structuring is only a conceptual manipulation and the actual system is not to be realized this way.

If the controller $\bar{C}(s)$ supplies any particular input $\bar{u}(s)$ to the plant in the original and modified system depicted in Figure 3.8 and Figure 3.9 respectively. Then, the outputs of the two systems are equivalent since

$$\bar{y}_2'(s) = \bar{G}_2'(s)\bar{u}(s) = \frac{\bar{b}_2(s)}{\bar{a}(s)} \cdot \bar{u}(s) = \bar{y}_2(s), \quad \text{and}$$
$$\bar{y}_1'(s) = \bar{G}_1'(s)\bar{G}_2'(s)\bar{u}(s) = \frac{\bar{b}_1(s)}{\bar{b}_2(s)} \cdot \frac{\bar{b}_2(s)}{\bar{a}(s)} \cdot \bar{u}(s) = \frac{\bar{b}_1(s)}{\bar{a}(s)} \cdot \bar{u}(s) = \bar{y}_1(s). \tag{3.17}$$

Further, (3.14) and (3.16) together with (3.17) show that

$$\bar{y}_1(s) = \bar{G}_1'(s)\bar{y}_2(s). \tag{3.18}$$

Using this information, the next step involves applying the similar technique as above to the

controller $\bar{C}(s)$ that results in the following:

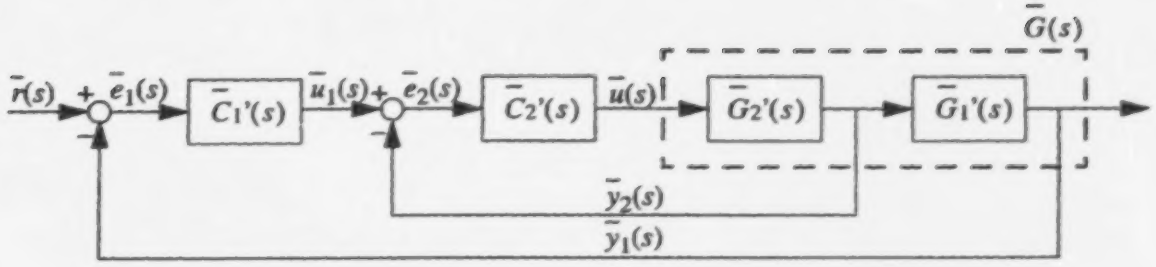

Figure 3.10: The final modified SIMO system

To find the expressions for the controllers of the modified system that gives equivalent output signals $\bar{y}_1(s)$ and $\bar{y}_2(s)$, consider the following: From the original system in Figure 3.8, the plant input $\bar{u}(s)$ can be expressed as

$$\begin{aligned} \bar{u} &= \bar{C}_1\bar{e} + \bar{C}_2\bar{y}_2 \\ &= \bar{C}_1[\bar{r} - \bar{y}_1] + \bar{C}_2\bar{y}_2 \\ &= \bar{C}_1\bar{r} - \bar{C}_1\bar{y}_1 + \bar{C}_2\bar{y}_2 . \end{aligned} \tag{3.19}$$

From the modified system, assume that (3.16) and (3.17) holds, then

$$\begin{aligned} \bar{u} &= \bar{C}_2'\bar{e}_2 \\ &= \bar{C}_2'[\bar{C}_1'\bar{e}_1 - \bar{y}_2] \\ &= \bar{C}_2'[\bar{C}_1'(\bar{r} - \bar{y}_1) - \bar{y}_2] \\ &= \bar{C}_2'\bar{C}_1'\bar{r} - \bar{C}_2'\bar{C}_1'\bar{y}_1 - \bar{C}_2'\bar{y}_2 . \end{aligned} \tag{3.20}$$

A comparison of (3.19) and (3.20) reveals that the two systems give identical output signals if

$$\begin{aligned} \bar{C}_2' &= -\bar{C}_2 \text{ , and} \\ \bar{C}_1' &= -\frac{\bar{C}_1}{\bar{C}_2} . \end{aligned} \tag{3.21}$$

Finally, it can be shown that the transfer functions $\frac{\bar{u}(s)}{\bar{r}(s)}$, $\frac{\bar{y}_1(s)}{\bar{r}(s)}$ and $\frac{\bar{y}_2(s)}{\bar{r}(s)}$ are the same in both the SIMO closed loop system and the multi-loop system:

For the SIMO system shown in Figure 3.8, refering to (3.14) and (3.15), then (3.19) gives

$$\begin{aligned} \bar{u} &= \bar{C}_1[\bar{r} - \bar{G}_1\bar{u}] + \bar{C}_2\bar{G}_2\bar{u} \\ &= \bar{C}_1\bar{r} - \bar{C}_1\bar{G}_1\bar{u} + \bar{C}_2\bar{G}_2\bar{u} \,. \end{aligned} \tag{3.22}$$

Therefore,

$$\frac{\bar{u}}{\bar{r}} = \frac{\bar{C}_1}{1 + \bar{C}_1\bar{G}_1 - \bar{C}_2\bar{G}_2}. \tag{3.23}$$

Since $\bar{y}_1$ can be written as

$$\bar{y}_1 = \left(\frac{\bar{y}_1}{\bar{u}}\right)\left(\frac{\bar{u}}{\bar{r}}\right)\bar{r} = \bar{G}_1\left(\frac{\bar{C}_1}{1 + \bar{C}_1\bar{G}_1 - \bar{C}_2\bar{G}_2}\right)\bar{r}, \tag{3.24}$$

this implies

$$\frac{\bar{y}_1}{\bar{r}} = \frac{\bar{G}_1\bar{C}_1}{1 + \bar{C}_1\bar{G}_1 - \bar{C}_2\bar{G}_2}. \tag{3.25}$$

From a similar derivation,

$$\bar{y}_2 = \left(\frac{\bar{y}_2}{\bar{u}}\right)\left(\frac{\bar{u}}{\bar{r}}\right)\bar{r} = \bar{G}_2\left(\frac{\bar{C}_1}{1 + \bar{C}_1\bar{G}_1 - \bar{C}_2\bar{G}_2}\right)\bar{r}, \tag{3.26}$$

thus,

$$\frac{\bar{y}_2}{\bar{r}} = \frac{\bar{G}_2\bar{C}_1}{1 + \bar{C}_1\bar{G}_1 - \bar{C}_2\bar{G}_2}. \tag{3.27}$$

At the same time, consider Figure 3.10 as well as (3.15) and (3.19) for the multi-loop system. For the inner loop shown in Figure 3.10,

$$\frac{\bar{u}}{\bar{u}_1} = \frac{\bar{C}_2'}{1 + \bar{C}_2'\bar{G}_2'}. \tag{3.28}$$

Shifting the focus to the outer loop, it can be seen that

$$\tilde{u}_1 = \bar{C}_1'(\tilde{r} - \tilde{y}_1). \tag{3.29}$$

But since $\tilde{y}_1 = \bar{G}_1'\bar{G}_2'\tilde{u}$, this implies

$$\tilde{u}_1 = \bar{C}_1'\tilde{r} - \bar{C}_1'\bar{G}_1'\bar{G}_2'\tilde{u}. \tag{3.30}$$

Using (3.29), it is apparent that

$$\frac{\tilde{u}}{\tilde{r}} = \frac{\bar{C}_1'\bar{C}_2'}{1 + \bar{C}_2'\bar{G}_2' + \bar{C}_1'\bar{C}_2'(\bar{G}_1'\bar{G}_2')}. \tag{3.31}$$

Refering to (3.16) and (3.21), then

$$\frac{\tilde{u}}{\tilde{r}} = \frac{\bar{C}_1}{1 - \bar{C}_2\bar{G}_2 + \bar{C}_1\bar{G}_1}. \tag{3.32}$$

Therefore, since $\tilde{y}_2 = \bar{G}_2'\tilde{u} = \bar{G}_2\tilde{u}$,

$$\frac{\tilde{y}_2}{\tilde{r}} = \frac{\bar{G}_2\bar{C}_1}{1 + \bar{C}_1\bar{G}_1 - \bar{C}_2\bar{G}_2} \tag{3.33}$$

Using the similar procedure,

$$\frac{\tilde{y}_1}{\tilde{r}} = \frac{\bar{G}_1\bar{C}_1}{1 + \bar{C}_1\bar{G}_1 - \bar{C}_2\bar{G}_2} \tag{3.34}$$

Thus compare (3.22), (3.25) and (3.27) with (3.32), (3.33) and (3.34) respectively, and note that the above procedure can easily be generalized to systems with m feedback loops, the lemma holds.B

Remark 3.1

a) Note that by simultaneously satisfying the two relations given by (3.16) and (3.21), the signals $\tilde{u}$, $\tilde{y}$ and $\tilde{r}$ are equivalent in either system. Furthermore, the error signals can be related as

$$\tilde{e} = \tilde{e}_1 . \tag{3.35}$$

b) In consideration of continuous-time design, by re-structuring a SIMO system as a multi-loop

system, it may facilitate the design process by using a loop-by-loop approach. Desired properties of the controlled plant output signals $\bar{y}_1(s)$ and $\bar{y}_2(s)$ are usually known in advance, and once the controllers in the multi-loop setting is designed (i.e. $\bar{C}_1'$ and $\bar{C}_2'$), they can easily be translated back to their SIMO equivalents ($\bar{C}_1$ and $\bar{C}_2$) using (3.21). The design process can also be repeated if it turns out that the controller design for the previous loop(s) results in some undesirable dynamics that hinders the performance of the current loop.

Direct SIMO controller design is also possible, although closing all loops at the same time necessitates consideration of the performance of all channels concurrently. This is a cumbersome step if there are many feedback loops to consider at the same time [60]. Of course if it can be done efficiently and systematically, it could be a favoured design method.

c) From Remark 3.1(b) in view of Remark 3.1(a), by using (3.16) and (3.21), the performance of SIMO and multi-loop systems in the classical sense can easily be related to each other in the controller design process.

d) By examining the given design steps in a little more detail, the outer loop of the re-structured multi-loop system is the same as the SIMO system. It corresponds to tracking of the reference signal by a system output.

e) Note that no assumptions have been made about the stability or minimum phase property of $\bar{G}(s)$. If, say, for example, $\bar{G}(s)$ is stable but $\bar{G}_2(s)$ is a non-minimum phase transfer function. Then from (3.14), roots of $\bar{b}_2(s)$ belongs to the open right-half-plane (ORHP), and thus from (3.16), $\bar{G}_1'(s)$ is unstable for the outer loop design. However, it is easy to see that, in Figure 3.10,

$$\frac{\bar{y}_2}{\bar{u}_1} = \frac{\bar{G}_2'\bar{C}_2'}{1+\bar{G}_2'\bar{C}_2'}, \tag{3.36}$$

and therefore, for the outer loop design, the "plant" transfer function $\bar{P}_1'$ is

$$\bar{P}_1' = \bar{G}_1'\begin{pmatrix}\bar{y}_2\\ \bar{u}_1\end{pmatrix} = \bar{G}_1' \cdot \frac{\bar{G}_2'\bar{C}_2'}{1+\bar{G}_2'\bar{C}_2'} \tag{3.37}$$

Now from definitions of $\bar{G}_1'(s)$ and $\bar{G}_2'(s)$ in (3.16), $\bar{b}_2(s)$ in numerator of $\bar{G}_2'(s)$ will cancell with $\bar{b}_2(s)$ in denominator of $\bar{G}_1'(s)$ and therefore the controller design of the outer loop concerns a stable plant also, which it should. It is pertinent to understand that there is no issue of pole-zero cancellation in this case: $\bar{G}_1'(s)$ and $\bar{G}_2'(s)$ are just "fictitous plants" system set-up so that a control system can be designed in an alternate way. Both $\bar{G}_1'(s)$ and $\bar{G}_2'(s)$ will contain the same $\bar{b}_2(s)$. The same principle also apply if $\bar{G}_i'(s)$ are improper. So long as the original system $\bar{G}(s)$ is a proper system, the problem will not arise when it comes to designing that particular loop.

It terms of stability of the system. If $\bar{G}(s)$ is unstable, then following a similar idea as the previous, the controller design for each loop will also involve stabilizing an unstable "plant" with $\bar{a}(s)$ constituting part of its denominator.

f) It may seem, in accordance with the traditional knowledge of multi-loop systems, that it is necessary to arrange $\bar{G}_i'(s)$ such that the plant dynamics goes from the fastest to the slowest in moving from the innermost loop to the outermost loop. However, from Remark 3.1(c), since the performance of the system in terms of its outputs $\bar{y}_i$'s can be translated directly from the multi-loop re-structured system to the original SIMO system, the above concern does not apply. The simple reason to this is that the multi-loop controller design accounts for the dynamics of $\bar{G}_i'(s)$ and not $\bar{G}_i(s)$, which forms the *actual* transfer function of the plant.

g) Following comments from Remark 3.1(a), (b), (c), suppose a set of controllers $\bar{C}_1'$ and $\bar{C}_2'$ are designed using the multi-loop formulation. They can either be translated back to their SIMO

equivalent as Remark 3.1(b) suggests, or they can be used in the following feedback setting:

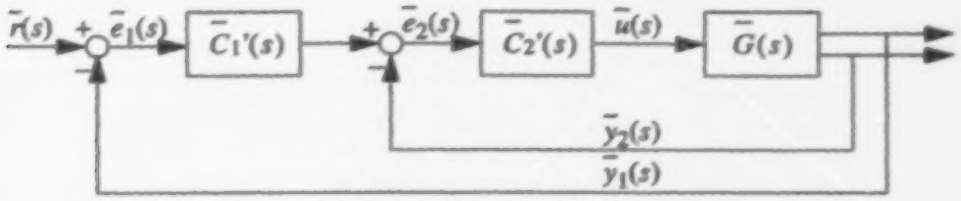

Figure 3.11: A re-configured SIMO feedback control system

This represents an alternative structure to control a SIMO system.

h) Note that only one non-zero reference input to the closed loop SIMO system is allowed. However, it is possible to apply other reference inputs $\bar{r}_i$ to the corresponding outputs $\bar{y}_i$, $i = 2, 3, \ldots, m$, so long as they are all zero-inputs. This may seem trivial, but it slightly widens the class of systems that Lemma 3.1 accounts for. This is re-stated as Lemma 3.2.

g) It can be shown that Lemma 3.1 and the above Remarks also apply to the design of digital systems.c

Lemma 3.2

An analogue LTI MIMO closed loop feedback system can be re-structured as a SIMO system if

1) the associated plant is a single-input multi-output system. and
2) all but one reference input to the MIMO *closed loop* system are zero.D

Proof

The *i*th non-zero reference input to the closed loop system is used to command the *i*th output of the plant. Assuming the negative feedback convention, the crucial step is to swap the *i*th entry of the controller *and* plant transfer function with their first one, such that the non-zero reference input now corresponds to the first entry of the output. This is illustrated as follows: First, Figure 3.12 shows a MIMO feedback system with a SIMO plant and a non-zero *i*th reference input.

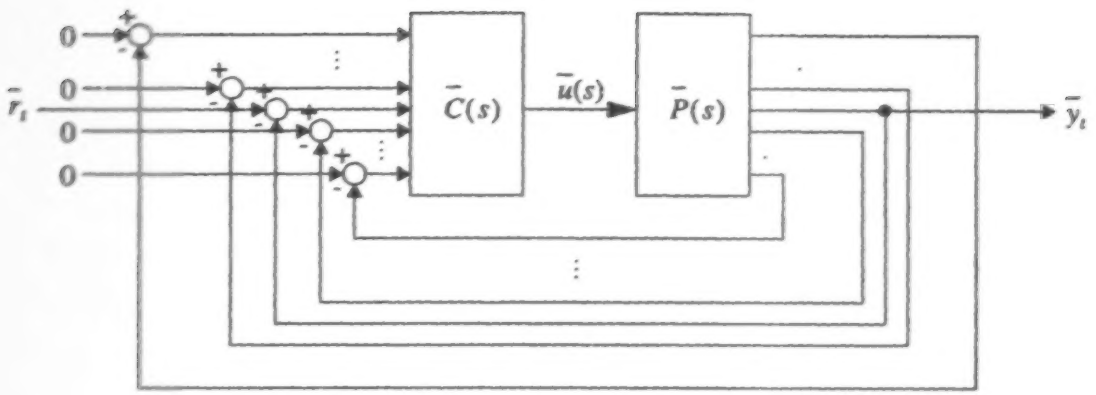

Figure 3.12: A MIMO feedback system with one non-zero reference input

The reference input $\bar{r}_i$ is now swapped with $\bar{r}_1$. The same is also exercised on components of the controller and plant transfer function. This results in the following:

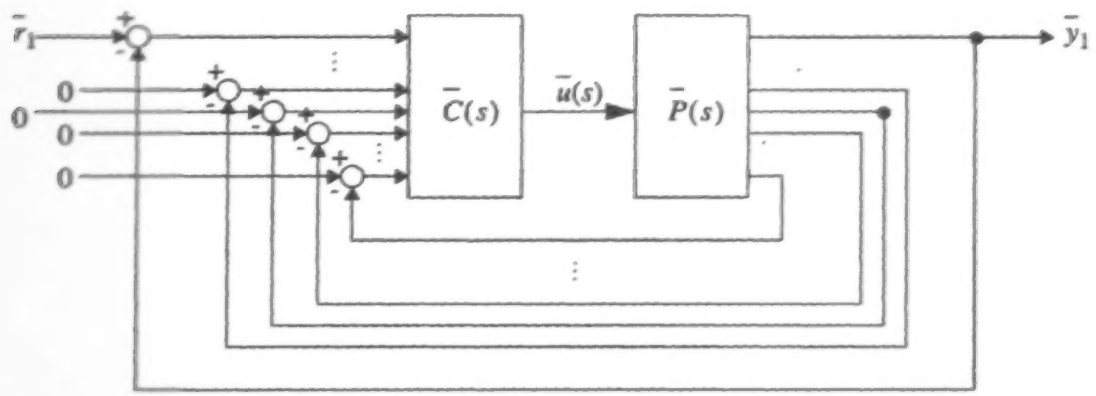

Figure 3.13: A re-organized feedback system with the non-zero reference input now corresponds to the first system output

For the re-structured system, since

$$\bar{r}_i(s) = 0\,; \quad 2 \le i \le m, \tag{3.38}$$

The control law can be written as

$$\begin{aligned}\bar{u}(s) &= \bar{C}_1(s)\bar{e}_1(s) + \bar{C}_2(s)\bar{e}_2(s) + \ldots + \bar{C}_m(s)\bar{e}_m(s) \\ &= \bar{C}_1(s)[\bar{r}_1(s) - \bar{y}_1(s)] + \bar{C}_2(s)[0 - \bar{y}_2(s)] + \ldots + \bar{C}_m(s)[0 - \bar{y}_m(s)] \\ &= \bar{C}_1(s)[\bar{r}_1(s) - \bar{y}_1(s)] + [-\bar{C}_2(s)]\bar{y}_2(s) + \ldots + [-\bar{C}_m(s)]\bar{y}_m(s)\,.\end{aligned} \tag{3.39}$$

Thus, re-defining the *i*th entry of the controller transfer function $\bar{C}_i''(s)$ for $2 \le i \le m$ as

$$\bar{C}_i''(s) = -\bar{C}_i(s), \tag{3.40}$$

the resultant system further becomes as given in Figure 3.14.

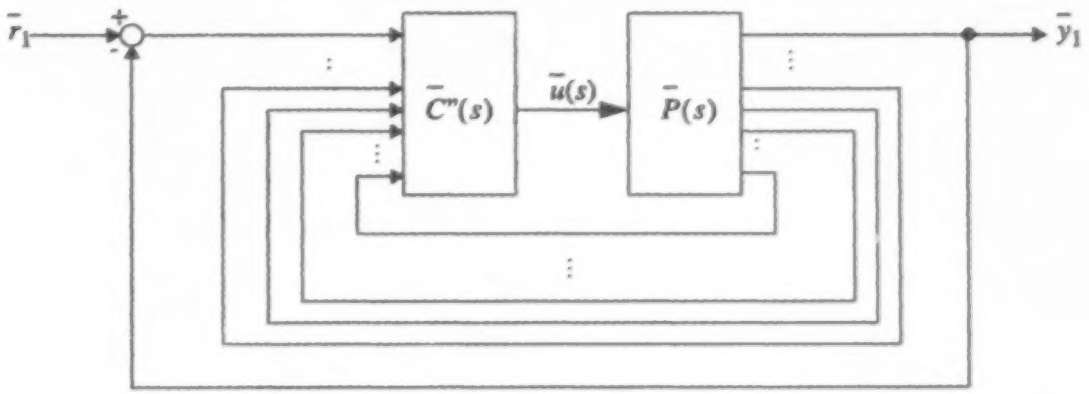

Figure 3.14: The final re-organized MIMO system

The proof is completed by applying Lemma 3.1.B

Remark 3.2

a) It is clear that the MIMO analogue missile control system depicted in Figure 3.3 can be re-structured as described above.

b) It can be shown that Lemma 3.2 also applies to the design of digital systems.c

Lemma 3.2 is important for design and analysis of the said class of systems. In the presentation of local discretization in Chapter 2.5, the concept of principal gains is introduced along with the determination of the closed loop system bandwidth for choosing a suitable sampling rate. In the analysis of the closed loop continuous-time missile control system in Chapter 3.2, the relationship

between the principal gains and the performance of a system was stated. Suppose a continuous-time m-loop feedback system falls into the class of system described in Lemma 3.2. Since the proper plant and closed loop system both obviously have m outputs, from the definition of sensitivity, $\bar{S}(s)$ will be a $m \times m$ transfer function matrix, i.e.,

$$\bar{S}(s) \in R_p^{m \times m}(s) . \tag{3.41}$$

On the other hand, since Lemma 3.2 suggests that the considered missile control system can be transformed into a SIMO system, the re-formulated closed loop system will consist of 1 input and m outputs. The closed loop system transfer function $\bar{T}(s)$ is then,

$$\bar{T}(s) \in R_p^{m \times 1}(s) . \tag{3.42}$$

Thus, for example, for the purpose of determining the command input tracking performance of the system or a sampling period T for local discretization, a much simpler plot of the norm of $\bar{T}(s)$ suffices. Consider $\bar{u}(s)$ as the scalar input to the closed loop system, the output $\bar{y}(s)$ is given as

$$\bar{y}(s) = \bar{T}(s)\bar{u}(s) , \tag{3.43}$$

which implies

$$\|\bar{y}(s)\| = \|\bar{T}(s)\bar{u}(s)\| \le \|\bar{T}(s)\| \|\bar{u}(s)\| . \tag{3.44}$$

Therefore, the ∞-norm can be taken on $\bar{T}(s)$ to determine its maximum gain. If

$$\bar{T}(s) = \begin{bmatrix} \bar{T}_1(s) \\ \vdots \\ \bar{T}_m(s) \end{bmatrix} , \tag{3.45}$$

then

$$\|\bar{T}(s)\|_\infty = \max |\bar{T}_i(s)| \tag{3.46}$$

for a certain i. Thus, setting $s = jw$ gives

$$\|\bar{T}(jw)\|_\infty = \max |\bar{T}_i(jw)| .$$

Compared to the Bode diagram of a scalar transfer function, the plot for $\bar{T}(s)$ involves an extra

step of finding the maximum magnitude of $|T_i|$ for $i = 1, 2, \ldots, m$. The important point is that $\|\bar{y}(s)\|$ no longer depends on the direction of $\bar{u}(s)$ since it is a scalar. This is a subtle but definite departure from the case for MIMO systems where $\bar{T}(s)$ is a transfer function matrix, as well as $\bar{S}(s)$.

There are other possible interesting features of SIMO systems in which this thesis will not embark on. Those are described in Chapter 5.2.

In the next section, some implication for digital re-design of the class of systems stated in Lemma 3.2 is given in the context of PIM methods. This allows a comparison to be made between the multi-loop PIM method and the MIMO PIM method.

3.3.2 General Comparison of Multi-Loop PIM method with MIMO PIM method

In this section the application of the MIMO PIM method and multi-loop PIM method to the class of MIMO systems considered by Lemma 3.2 is examined. This compliments the discussions made in the previous section by examining the correspondence between their discretized systems obtained using the methods of PIM. Specifically, a comparison of the two methods is made on its design procedure and implementation structure. Using the analogue missile control system as an example, result from computer simulation will then be shown in Section 3.5 and the applicable interpretation of them can then be related back to the discussion in this section. This comparison is conceptually shown in Figure 3.15.

The motivation of carrying out a comparison between the aforementioned methods of PIM arose when it became clear in Lemma 3.2 that the MIMO analogue missile feedback control system can be re-structured as a multi-loop system. Such comparison gives more insight and knowledge to the proper selection of a PIM digital re-design method when the analogue closed loop system belongs to the class of systems set forth in Lemma 3.2.

One of the important steps in PIM digital re-design is the discretization of the continuous-time

PITF using the MPZ method. This produces a discrete-time model of the continuous-time PITF. Recall in Section 2.2.3 that the mapping utilized in the MPZ method is one-to-one if the sampling period T satisfies

$$T < \frac{2\pi}{w} \tag{3.47}$$

where w is a folding frequency.

To pursue a rigorous theoretical analysis for the comparison involves, at a minimum level, the construction of a lifted model [50] of the continuous-time plant. This in turn requires significant mathematical development which this thesis shall not embark on. Instead, this section will point out an important fact that answers the question mark "?" in Figure 3.15. This is given as Lemma 3.3. Following descriptions of the MIMO PIM and multi-loop PIM methods in Chapters 2.6.2 and 2.6.4 respectively, many observations can be made of their design procedure and formulation. These are described in Remark 3.3.

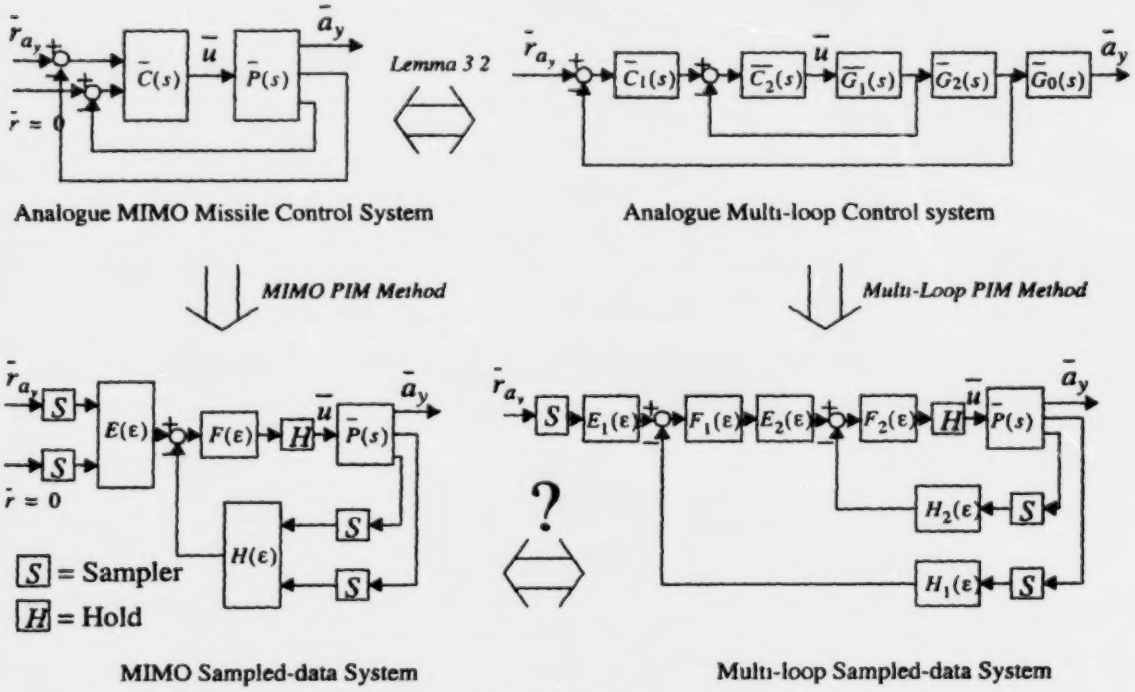

Figure 3.15: Comparison of the Multi-Loop with the MIMO PIM method

Lemma 3.3

The discrete-time PITFs that result from digitally re-designing the class of MIMO systems considered in Lemma 3.2 and its re-structured multi-loop counterpart using the MIMO PIM and multi-loop PIM methods are in general different. Moreover, the application of the MIMO PIM method in general provide at least a marginally better phase-characteristic than the multi-loop PIM method, when the number of system outputs is two or above.D

Proof

First it is possible to establish using Lemmas 3.1 and 3.2 a correspondence between the continuous-time PITF for the MIMO and re-structured multi-loop system as illustrated in Figure 3.15. In fact, the PITFs are equal.

When the number of loops is greater than one, the digital re-design of the outer loops of multi-loop system considers the "plant" as being the inner loop system cascaded with the system currently considered as plant, and the continuous-time PITF is defined accordingly. However, this continuous-time "PITF" does *not* correspond to the PITF of the MIMO system in the same way as indicated above, nor does the "plant" likewise. Thus, from the properties of the PIM methods which take the SIM of the plant and the MPZ model of the PITF, the digital re-design of the outer loops will result in sampled-data systems that cannot be connected with its MIMO counterpart in the same simple way as the continuous-time case.

It is well known that the sampling of a system in general leads to a deterioration of phase character of the frequency response of the system. While the MIMO PIM method involves only one discretization for the plant and the PITF, the multi-loop PIM method involves many stages of discretization. Each time a set of outer loop discrete-time controllers is designed to realize a "desired PITF", more phase distortion will result. It can be easily infer that

i) as T increases, and

ii) as the number of loop increases,

this difference in performance of the two sampled-data system becomes more prominent.B

Remark 3.3

a) From the block diagram algebra used in Section 3.3.1, it may seem possible to obtain a relationship for the two resultant discrete-time systems, such as one for the structure of their closed loop digital controllers. However, in this case, a "standard structure" is missing for the comparison as the purpose is to seek the difference between the two resultant structures, and more importantly, to find out which one gives better performance. Therefore, one should instead examine the resultant PITFs for the two different cases, and it is precisely here that the difference between the two different implementations begin to appear as shown above in the proof.

b) Another way to explain the difference between the two sampled-data systems is to see that, for the multi-loop system, the calculation involves the discretization of *one* PITF - this is a characteristics of a SIMO closed loop system; in the MIMO PIM setup however, the digital re-design involves taking the MPZ model of a *2×1 Plant Input Transfer Function matrix*, since the (fictitous) zero reference input of the yaw rate loop is also accounted for. This difference sets apart all subsequent calculations carried out for the two different digital re-designs that give different responses.

c) It can also be pointed out that, consistent with the general effect of sampling, the MPZ mapping of the PITF typically results in a degradation of system performance. The difference between the continuous-time and discrete-time result is less significant when the sampling interval is small. It becomes more dominant when frequency folding begins to take place for pole-zero mapping (MPZ) at larger sampling period (refer to (3.47)). MPZ mapping of different PITF fares differently.

d) An examination of the controller structures that result from the two PIM methods as in Lemma 3.3 reveals that the number of controller transfer functions (including entries in a transfer function matrix) in general is less with the MIMO PIM method than with the multi-loop PIM method. Specifically, suppose that the continuous-time system considered by Lemma 3.2 has m feedback loops. Then, in general, the MIMO PIM scheme yields $(2m + 1)$ transfer function components, whereas the multi-loop PIM yields $(3m)$ transfer functions. This could be a practical advantage for the MIMO PIM method in the implementation of a sampled-data system, and it holds even in

cases when simplification can be applied to one or both methods.

e) The expectation of better performance for the MIMO PIM digital re-design method in terms of obtaining closer sampled-data system behaviour to the continuous-time result assumes, ideally, the minimal presence of FWL effects in the actual discrete-time system implementation. as well as the absence of noise and other disturbance signals. In practice, this is seldom the case, and thus, actual system behaviour will also be influenced by the addition of these undesirable effects.c

3.4 Digital Re-Design: A Case Study

Many techniques and issues relating to the discretization of continuous-time control systems have been reported in Chapter 2. They include the description of properties of discrete-time operators, illustration of discrete-time models of continuous-time systems, and introduction to local and PIM discretization methods.

In this section, the methods of discretization for continuous-time control systems described in Sections 2.5 and 2.6 are applied to the analogue missile control system. First, three methods of local discretization are exercised on $\bar{C}(s)$. Then, the closed loop analogue missile control system is globally discretized in the MIMO and multi-loop settings using the appropriate PIM methods. The comparison of computer simulation results is shown in Section 3.5.

3.4.1 Local discretization of missile flight controller

Recall from Sections 2.5 that local discretization schemes involve replacing a continuous-time controller with one of its valid discrete-time models. This is carried out in the present section using two mapping models of $\bar{C}(s)$; namely, the backward difference approximation and Tustin's method. The MPZ model of the analogue controller is also considered. The formulated discrete-time systems are expressed using the ε operator, as well as the z operator for comparison.

Since one of the major factors for the success of local discretization is to use sufficiently high

sampling rates, the resultant discrete-time models are expressed as an explicit function of the sampling interval T.

Using (3.6) and (3.7), the continuous-time controller is given numerically as

$$\bar{C}(s) = \left[\frac{-1\,38}{s} \quad \frac{-208\,6 - 5\,32s}{s}\right]. \tag{3.48}$$

The discretization process begins with the selection of a non-pathological sampling period T with respect to the plant $\bar{P}(s)$, as defined in Definition 2.14. The choice of T must also satisfy the Shannon's sampling theorem in consideration of the closed loop system bandwidth as well as the frequency spectrum of the reference input signal. This has been discussed earlier in Section 2.5. The continuous-time controller is then replaced by the three different aforementioned discrete-time models of $\bar{C}(s)$. The resultant digital controllers are given as follows in Tables 3.1 and 3.2.

Discrete-time Model		$C(\varepsilon)$
Mapping Models	Backward Difference	$\left[\frac{-1\,38(\varepsilon T+1)}{\varepsilon} \quad \frac{-208\,6(\varepsilon T+1)-5\,32\varepsilon}{\varepsilon}\right]$
	Tustin's Method	$\left[\frac{-1.38(\varepsilon T+2)}{2\varepsilon} \quad \frac{-(104\,3T+5\,32)\varepsilon-208\,6}{\varepsilon}\right]$
MPZ Model		$\left[\frac{-1\,38}{\varepsilon} \quad \frac{-5.32(\varepsilon+a)}{\varepsilon}\right]$ where $a = \frac{1-e^{-\frac{208\,6}{5\,32}T}}{T}$

Table 3.1: Discrete-time Models of $\bar{C}(s)$ expressed in ε

Discrete-time Model		$C(\varepsilon)$
Mapping Models	Backward Difference	$\begin{bmatrix} \frac{-1.38Tz}{z-1} & \frac{-(208.6T+5.32)z+5.32}{z-1} \end{bmatrix}$
	Tustin's Method	$\begin{bmatrix} \frac{-0.69T(z+1)}{z-1} & \frac{-(104.3T+5.32)z+(5.32-104.3T)}{z-1} \end{bmatrix}$
MPZ Model		$\begin{bmatrix} \frac{-1.38}{z-1} & \frac{-5.32(z+a)}{z-1} \end{bmatrix}$ where $a = -e^{-\frac{208.6}{5.32}T}$

Table 3.2: Discrete-time Models of $\bar{C}(s)$ expressed in z

For the selection of the sampling period T, it is imperative to first determine the approximate closed loop system bandwidth. In light of the discussions in Section 3.3, the plot of principal gains for the analogue closed loop system transfer function $\bar{T}$ shown in Figure 3.7 is re-examined. The plot of the norm of $\bar{T}$ as a function of frequency is shown in Figure 3.16.

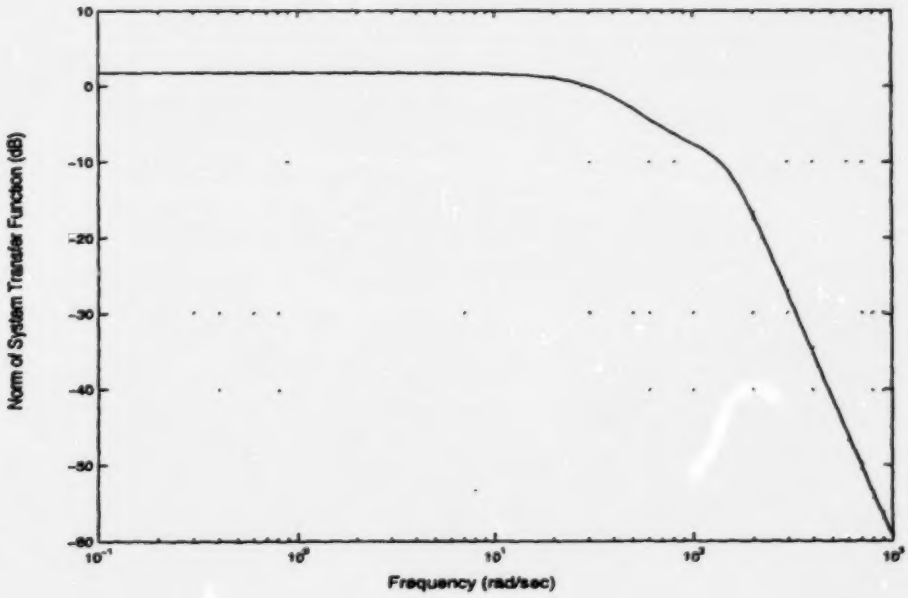

Figure 3.16: Plot of $\|\bar{T}(jw)\|_\infty$ as a function of frequency

Figure 3.16 indicates that $\bar{T}(s)$ has a closed loop system bandwidth of approximately 30 rad/sec. The sampling period can then be decided based on the above information as well as the type of command input tracking signal sent to the closed loop system. Finally, the samplers and hold devices are added to the appropriate positions in the set up. The simulation results obtained from the resultant sampled-data systems are shown in Section 3.5.

3.4.2 Application of MIMO PIM method

Considering the closed loop analogue missile flight control system as a MIMO system, the MIMO PIM method described in Section 2.6.2 is used here to perform a global digital re-design. For reasons described in Section 3.2, the plant $\bar{P}(s)$ is considered as follows for the purpose of closed loop control system analysis and design:

$$\bar{P}(s) = \frac{62500}{s^2 + 350s + 62500}\begin{bmatrix} \dfrac{-2.24s^2 - 20.39s - 5.086\times 10^4}{s^2 + 1.95s + 484.3} \\ \dfrac{-17.94s - 51.12}{s^2 + 1.95s + 484.3} \end{bmatrix}$$

$$= \begin{bmatrix} \dfrac{-1.4\times 10^3 s^2 - 1.275\times 10^6 s - 3.179\times 10^9}{s^4 + 351.9s^3 + 6.367\times 10^4 s^2 + 2.914\times 10^5 s + 3.027\times 10^7} \\ \dfrac{-1.121\times 10^6 s - 3.195\times 10^6}{s^4 + 351.9s^3 + 6.367\times 10^4 s^2 + 2.914\times 10^5 s + 3.027\times 10^7} \end{bmatrix}. \qquad (3.49)$$

From (3.11), this is a cascade combination of the control actuator servo model and part of the missile model giving the two outputs $\hat{\bar{a}}_y$ and $\bar{r}$ that form the feedback loop. The design steps of the MIMO PIM method are now outlined and applied to the analogue missile control system. The sampling rate is chosen to be $f_s = 100$ Hz and the ε operator is used.

Step 1: Select a sampling period T which is non-pathological with respect to the eigenvalues of the open loop plant as prescribed by Definition 2.14.

Since f_s is selected to be 100 Hz, this implies $T = 0.01$ sec and $w_n = 2\pi f_s = 200\pi$ rad/sec.
The open loop plant $\bar{P}(s)$ is a SIMO system whose eigenvalues are

$$\{-1.75 \times 10^2 \pm j1.7854 \times 10^2, -0.9750 \pm j21\ 9854\}. \tag{3.50}$$

Hence $f_s = 100$ Hz is a non-pathological sampling period.

Comments: It is often practically impossible to select a pathological sampling period T for real, analogue plants since the imaginary part of the plant's poles usually represent some "odd" fraction as in (3.50).

Step 2: Obtain a right coprime factorization of $\bar{P}(s)$ as defined in Theorem 2.12. Select a set of stable continuous-time poles for the controller pole placement.

A state space realization for $\bar{P}(s)$ is first obtained using MATLAB, such that $\bar{P}$ is represented by

$$\bar{P}: \quad \begin{aligned} \dot{\bar{x}} &= \bar{A}\bar{x} + \bar{B}\bar{u} \\ \bar{y} &= \bar{C}\bar{x} + \bar{D}\bar{u} \end{aligned} \tag{3.51}$$

where

$$\begin{aligned} \bar{u} &= \text{controller input signal, and} \\ \bar{y} &= \begin{bmatrix} \hat{\bar{a}}_y \\ \bar{r} \end{bmatrix}. \end{aligned} \tag{3.52}$$

Next, select a set of continuous-time poles as

$$\{\bar{\sigma}_i;\ i = 1, 2, 3, 4\} = \{-2, -15, -35, -100\} \tag{3.53}$$

and carry out the controller pole placement for (3.51) in MATLAB using the *place.m* function. A feedback gain $\bar{K}$ is obtained such that $\{\text{eig}\ [\bar{A} - \bar{B}\bar{K}]\}$ equals the desired pole locations specified in (3.53). Finally, following (2.45) and (2.46), the transfer function matrices $\bar{M}(s)$ and $\bar{N}(s)$ are evaluated as

$$\bar{M}(s) = \frac{s^4 + 351.9s^3 + 6.367\times10^4 s^2 + 2\,914\times10^5 s + 3.027\times10^7}{s^4 + 152s^3 + 5825s^2 + 6.335\times10^4 s + 1.05\times10^5}$$

$$\bar{N}(s) = \begin{bmatrix} \dfrac{-1\,4\times10^5 s^2 - 1.275\times10^6 s - 3.179\times10^9}{s^4 + 152s^3 + 5825s^2 + 6\,335\times10^4 s + 1.05\times10^5} \\ \dfrac{-1\,121\times10^6 s - 3.195\times10^6}{s^4 + 152s^3 + 5825s^2 + 6.335\times10^4 s + 1.05\times10^5} \end{bmatrix} \tag{3.54}$$

such that

$$\bar{P}(s) = \bar{N}(s)\bar{M}^{-1}(s). \tag{3.55}$$

Comments: The modal canonical form (also called normal form) where the system eigenvalues appear on the diagonal of the "*A*" matrix should be used as it carries better numerical property than the companion form [56].

Step 3: Construct a SIM of the continuous-time plant $\bar{P}(s)$ as defined by (2.25).

Using the delta toolbox for MATLAB provided by [62], a simple MATLAB function *c2del.m* can be used to carry this out directly by operating on the state space realization of $\bar{P}$ given by (3.51). The result gives a state space description of the SIM of $\bar{P}$. Put in transfer function form, the discrete-time plant $P(\varepsilon)$ for the discrete-time control system design is given, for $T = 0.01$ sec., by

$$P(\varepsilon) = \begin{bmatrix} \dfrac{-264.4\varepsilon^3 - 7\,98\times10^4\varepsilon^2 - 1.03\times10^7\varepsilon - 5\,54\times10^8}{\varepsilon^4 + 214.1\varepsilon^3 + 1.291\times10^4\varepsilon^2 + 1\,731\times10^5\varepsilon + 5\,275\times10^6} \\ \dfrac{-7.483\varepsilon^3 - 2633\varepsilon^2 - 2\,056\times10^5\varepsilon - 5\,567\times10^5}{\varepsilon^4 + 214.1\varepsilon^3 + 1\,291\times10^4\varepsilon^2 + 1.731\times10^5\varepsilon + 5\,275\times10^6} \end{bmatrix} \tag{3.56}$$

Step 4: Repeat the factorization of Step 2 for the discrete-time plant $P(\varepsilon)$.

A similar procedure is applied here. The set of discrete-time poles $\{\sigma_i\,;\, i = 1, 2, 3, 4\}$ is related to the continuous-time ones by

$$\left\{\sigma_i = \frac{e^{\bar{\sigma}_i T} - 1}{T},\quad i = 1, 2, 3, 4\right\} = \{-1.9801, -13\,9292, -29\,5312, -63\,2121\}. \tag{3.57}$$

The right coprime factorization of $P(\varepsilon)$ is then given by the transfer function matrices $M(\varepsilon)$ and $N(\varepsilon)$, for $T = 0.01$ sec., as

$$M(\varepsilon) = \frac{\varepsilon^4 + 214.1\varepsilon^3 + 1.291\times 10^4\varepsilon^2 + 1.731\times 10^5\varepsilon + 5\,275\times 10^6}{\varepsilon^4 + 108\,7\varepsilon^3 + 3370\varepsilon^2 + 3\,226\times 10^4\varepsilon + 5\,149\times 10^4}$$

$$N(\varepsilon) = \begin{bmatrix} \dfrac{-264.4\varepsilon^3 - 7\,98\times 10^4\varepsilon^2 - 1\,03\times 10^7\varepsilon - 5.54\times 10^8}{\varepsilon^4 + 108\,7\varepsilon^3 + 3370\varepsilon^2 + 3.226\times 10^4\varepsilon + 5.149\times 10^4} \\ \dfrac{-7.483\varepsilon^3 - 2633\varepsilon^2 - 2.056\times 10^5\varepsilon - 5\,567\times 10^5}{\varepsilon^4 + 108.7\varepsilon^3 + 3370\varepsilon^2 + 3.226\times 10^4\varepsilon + 5.149\times 10^4} \end{bmatrix} \tag{3.58}$$

so that

$$P(\varepsilon) = N(\varepsilon)M^{-1}(\varepsilon). \tag{3.59}$$

Comments: The MATLAB function *place.m* has the restriction that the multiplicity of poles at a particular location cannot be greater than the number of inputs. While this does not appear to be a major issue for continuous-time plants, it may be so for its discrete-time SIMs in Step 4. For some larger sampling periods T, some of the discrete-time poles given by (3.57) may become numerically similar when the continuous-time values appear sufficiently distinct and far apart. This is illustrated by the following example:

Suppose $\{\bar{\sigma}_i\,;\ \ i = 1, 2, 3, 4\} = \{-10, -20, -30, -40\}$. Then the set of discrete-time poles for the coprime factorization of the discrete-time plant are calculated, as a function of T, as follows:

$$\begin{aligned} \{\sigma_i\,,\ i = 1, 2, 3, 4\} &= \left\{\frac{e^{\bar{\sigma}_i T} - 1}{T}\,;\ \ i = 1, 2, 3, 4\right\} \\ &= \{-7\,8694, -12\,6424, -15\,5374, -17.2933\,,\ \ T = 0\,05\ \text{secs}\} \\ &= \{-6.3212, -8\,6466, -9.5021, -9\,8168\,,\ \ T = 0\,1\ \text{secs}\} \\ &= \{-1\,9865, -1\,9999, -2.0000, -2\,0000\,,\ \ T = 0\,5\ \text{secs}\}. \end{aligned} \tag{3.60}$$

It is clear that when T becomes sufficiently large, the discrete-time poles get closer and closer together. Thus, a proper selection of continuous-time poles in Step 2 is essential for the calculation involved in Step 4.

Step 5: Find the continuous-time PITF $\bar{\Phi}(s)$ from (2.50).

From numerical expressions of $\bar{C}(s)$ and $\bar{P}(s)$ given in (3.48) and (3.49), respectively, $\bar{\Phi}(s)$ is calculated using (2.50) as:

$$\bar{\Phi}(s) = \begin{bmatrix} \dfrac{-1.38s^4 - 485.7s^3 - 8.786\times10^4 s^2 - 4\,021\times10^5 s - 4\,177\times10^7}{s^5 + 351\,9s^4 + 6.367\times10^4 s^3 + 6.64\times10^6 s^2 + 2.835\times10^8 s + 5.053\times10^9} \\ \dfrac{-5.49s^5 - 2141s^4 - 4\,229\times10^5 s^3 - 1\,488\times10^7 s^2 - 2.27\times10^8 s - 6.314\times10^9}{s^5 + 351.9s^4 + 6.367\times10^4 s^3 + 6\,64\times10^6 s^2 + 2\,835\times10^8 s + 5\,053\times10^9} \end{bmatrix}. \tag{3.61}$$

Note that (3.61) addresses $\bar{\Phi}(s)$ as a 2×1 transfer function matrix. This is consistent with the MIMO system under consideration, since there are two reference inputs (albeit $\bar{r}_r = 0$) for the closed loop system, and one controller output that goes to the plant.

Step 6: Evaluate $\bar{W}(s)$ from (2.56).

From expressions of $\bar{M}(s)$ and $\bar{\Phi}(s)$ in (3.54) and (3.61), respectively, $\bar{W}(s)$ is calculated as

$$\bar{W}(s) = \begin{bmatrix} \dfrac{-1\,38s^4 - 209.8s^3 - 8039s^2 - 8.77\times10^4 s - 1\,449\times10^5}{s^5 + 351\,9s^4 + 6\,367\times10^4 s^3 + 6.64\times10^6 s^2 + 2.835\times10^8 s + 5\,053\times10^9} \\ \dfrac{-5\,49s^5 - 1043s^4 - 6.369\times10^4 s^3 - 1\,564\times10^6 s^2 - 1.383\times10^7 s - 2\,19\times10^7}{s^5 + 351.9s^4 + 6\,367\times10^4 s^3 + 6\,64\times10^6 s^2 + 2\,835\times10^8 s + 5\,053\times10^9} \end{bmatrix}. \tag{3.62}$$

Step 7: Discretize $\bar{W}(s)$ into $W(\varepsilon)$ using the pole-zero matching (MPZ) method.

First, re-organize the transfer function elements in $\bar{W}(s)$ into first and second order pairs of poles and zeros. These are then mapped using the MPZ method according to procedures described in Section 2.2.3. Alternatively, $W(\varepsilon)$ can be calculated directly by mapping the set of poles and zeros of $\bar{W}(s)$ using the *s2del.m* function from the delta toolbox [62]. The result is, for $T = 0.01$ sec.,

$$W(\varepsilon) = \begin{bmatrix} \dfrac{-1\,343\varepsilon^4 - 145\,9\varepsilon^3 - 4526\varepsilon^2 - 4\,332\times10^4\varepsilon - 6\,915\times10^4}{\varepsilon^5 + 313\,3\varepsilon^4 + 3\,993\times10^4\varepsilon^3 + 2\,465\times10^6\varepsilon^2 + 7\,206\times10^7\varepsilon + 8\,57\times10^8} \\ \dfrac{-6.422\varepsilon^5 - 900\,8\varepsilon^4 - 4\,37\times10^4\varepsilon^3 - 8.912\times10^5\varepsilon^2 - 6\,879\times10^6\varepsilon - 1\,045\times10^7}{\varepsilon^5 + 313\,3\varepsilon^4 + 3\,993\times10^4\varepsilon^3 + 2.465\times10^6\varepsilon^2 + 7\,206\times10^7\varepsilon + 8\,57\times10^8} \end{bmatrix} \tag{3.63}$$

Step 8: Calculate the discrete-time PITF $\Phi(\varepsilon)$ using (2.58).

Using (3.58) and (3.63) for $M(\varepsilon)$ and $W(\varepsilon)$, respectively, $\Phi(\varepsilon)$ is calculated, for $T = 0.01$ sec., as:

$$\Phi(\varepsilon) = \begin{bmatrix} \dfrac{-1.343\varepsilon^4 - 287.5\varepsilon^3 - 1.734\times10^4\varepsilon^2 - 2.325\times10^5\varepsilon - 7.084\times10^6}{\varepsilon^5 + 313.3\varepsilon^4 + 3.993\times10^4\varepsilon^3 + 2.465\times10^6\varepsilon^2 + 7.206\times10^7\varepsilon + 8.57\times10^8} \\ \dfrac{-6.422\varepsilon^5 - 1578\varepsilon^4 - 1.264\times10^5\varepsilon^3 - 3.733\times10^6\varepsilon^2 - 6.902\times10^7\varepsilon - 1.071\times10^9}{\varepsilon^5 + 313.3\varepsilon^4 + 3.993\times10^4\varepsilon^3 + 2.465\times10^6\varepsilon^2 + 7.206\times10^7\varepsilon + 8.57\times10^8} \end{bmatrix} \tag{3.64}$$

Step 9: Find the controller(s) required to realize the desired discrete-time PITF $\Phi(\varepsilon)$. Apply Corollary 2.18 if the plant is stable; otherwise follow the general 3-controllers set up as detailed in Theorem 2.17.

a) Since the plant $\bar{P}(s)$ is stable, the simpler case of an one-controller design is first considered. From Corollary 2.18, the desired discrete-time PITF can be realized using a single controller given by

$$F(\varepsilon) = \Phi(\varepsilon)[I - P(\varepsilon)\Phi(\varepsilon)]^{-1} \tag{3.65}$$

where, in this case,

$$E(\varepsilon) = H(\varepsilon) = I. \tag{3.66}$$

Substituting equations (3.56) and (3.64) into (3.65), $F(\varepsilon)$ is calculated, for $T = 0.01$ sec., as:

$$F(\varepsilon) = \begin{bmatrix} \dfrac{-1.343\varepsilon^4 - 287.5\varepsilon^3 - 1.734\times10^4\varepsilon^2 - 2.325\times10^5\varepsilon - 7.084\times10^6}{\varepsilon^5 + 313.3\varepsilon^4 + 3.993\times10^4\varepsilon^3 + 2.465\times10^6\varepsilon^2 + 7.206\times10^7\varepsilon + 8.57\times10^8} \\ \dfrac{-6.422\varepsilon^5 - 1578\varepsilon^4 - 1.264\times10^5\varepsilon^3 - 3.733\times10^6\varepsilon^2 - 6.902\times10^7\varepsilon - 1.071\times10^9}{\varepsilon^5 + 313.3\varepsilon^4 + 3.993\times10^4\varepsilon^3 + 2.465\times10^6\varepsilon^2 + 7.206\times10^7\varepsilon + 8.57\times10^8} \end{bmatrix} \tag{3.67}$$

The PIM digital re-design of the analogue closed loop control system is completed with the suitable addition of samplers and hold devices.

b) For the general case of a 3-controller set-up, Theorems 2.12 and 2.17 indicate that it is necessary to find a solution for the Bezout Identity given by (2.52) in order to obtain a set of digital controllers required to realize the desired discrete-time PITF $\Phi(\varepsilon)$.

From (2.47) and (2.48) in Theorem 2.12, $X(\varepsilon)$ and $Y(\varepsilon)$ can be obtained by solving an observer pole placement problem [60]. First select a set of stable observer poles $\{\bar{\gamma}_i ; i = 1, 2, 3, 4\}$ in the s-domain as

$$\{\tilde{\gamma}_i ;\ i = 1, 2, 3, 4\} = \{-20, -25, -30, -35\}. \tag{3.68}$$

Secondly, the set of stable observer poles $\{\gamma_i ;\ i = 1, 2, 3, 4\}$ in the ε-domain is calculated as

$$\begin{aligned}\{\gamma_i ,\ \ i = 1, 2, 3, 4\} &= \left\{\frac{e^{\tilde{\gamma}_i T} - 1}{T},\ \ i = 1, 2, 3, 4\right\} \\ &= \{-1.9801, -13.9292, -29.5312, -63.2121.\}\end{aligned} \tag{3.69}$$

Thirdly, employing the state space realization of the SIM $P(\varepsilon)$ of the plant obtained in Step 3, calculate an observer gain L using MATLAB such that $[A_P - LC_P]$ has a set of desired eigenvalues given by (3.69). This is the observer pole placement problem, and $X(\varepsilon)$ and $Y(\varepsilon)$ can be easily obtained from (2.47) and (2.48), for $T = 0.01$ sec., as

$$\begin{aligned}X(\varepsilon) &= \frac{\varepsilon^4 + 3\,197\varepsilon^3 + 1.42\times 10^4\varepsilon^2 + 3\,903\times 10^3\varepsilon - 4\,862\times 10^5}{\varepsilon^4 + 108.7\varepsilon^3 + 3370\varepsilon^2 + 3.226\times 10^4\varepsilon + 5\,149\times 10^5} \\ Y(\varepsilon) &= \begin{bmatrix} \dfrac{22\,19\varepsilon^3 + 1012\varepsilon^2 + 9257\varepsilon + 4839}{\varepsilon^4 + 108.7\varepsilon^3 + 3370\varepsilon^2 + 3\,226\times 10^4\varepsilon + 5.149\times 10^5} \\ \dfrac{452.4\varepsilon^3 - 5\,085\times 10^4\varepsilon^2 - 2\,279\times 10^6\varepsilon - 9\,427\times 10^6}{\varepsilon^4 + 108\,7\varepsilon^3 + 3370\varepsilon^2 + 3\,226\times 10^4\varepsilon + 5.149\times 10^5} \end{bmatrix}\end{aligned} \tag{3.70}$$

Finally, from Theorem 2.17, the PIM digital re-design of the continuous-time system results in the following set of digital controllers

$$E(\varepsilon) = W(\varepsilon) = \begin{bmatrix} \dfrac{-1\,343\varepsilon^4 - 145\,9\varepsilon^3 - 4526\varepsilon^2 - 4.332\times 10^4\varepsilon - 6\,915\times 10^4}{\varepsilon^5 + 313.3\varepsilon^4 + 3\,993\times 10^4\varepsilon^3 + 2\,465\times 10^6\varepsilon^2 + 7\,206\times 10^7\varepsilon + 8.57\times 10^8} \\ \dfrac{-6\,422\varepsilon^5 - 900.8\varepsilon^4 - 4.37\times 10^4\varepsilon^3 - 8.912\times 10^5\varepsilon^2 - 6\,879\times 10^6\varepsilon - 1\,045\times 10^7}{\varepsilon^5 + 313.3\varepsilon^4 + 3\,993\times 10^4\varepsilon^3 + 2\,465\times 10^6\varepsilon^2 + 7\,206\times 10^7\varepsilon + 8.57\times 10^8} \end{bmatrix}, \tag{3.71}$$

$$F(\varepsilon) = X^{-1}(\varepsilon) = \frac{\varepsilon^4 + 108\,6526\varepsilon^3 + 3.3698\times 10^3\varepsilon^2 + 3.2256\times 10^4\varepsilon + 5.1487\times 10^4}{\varepsilon^4 + 3\,197\varepsilon^3 + 1\,4202\times 10^4\varepsilon^2 + 3.9029\times 10^5\varepsilon - 4.8621\times 10^5}, \text{ and} \tag{3.72}$$

$$H(\varepsilon) = Y(\varepsilon) = \begin{bmatrix} \dfrac{22\,1859\varepsilon^3 + 1\,0121\times 10^3\varepsilon^2 + 9\,2568\times 10^3\varepsilon + 4\,8393\times 10^3}{\varepsilon^4 + 108.6526\varepsilon^3 + 3\,3698\times 10^3\varepsilon^2 + 3\,2256\times 10^4\varepsilon + 5\,1487\times 10^4} \\ \dfrac{452\,4351\varepsilon^3 - 5\,0853\times 10^4\varepsilon^2 - 2\,2787\times 10^6\varepsilon - 9.4270\times 10^6}{\varepsilon^4 + 108.6526\varepsilon^3 + 3.3698\times 10^3\varepsilon^2 + 3.2256\times 10^4\varepsilon + 5\,1487\times 10^4} \end{bmatrix}. \tag{3.73}$$

which give closed loop stability to the resultant discrete-time control system. Figure 3.17 shows

the schematic of this controller.

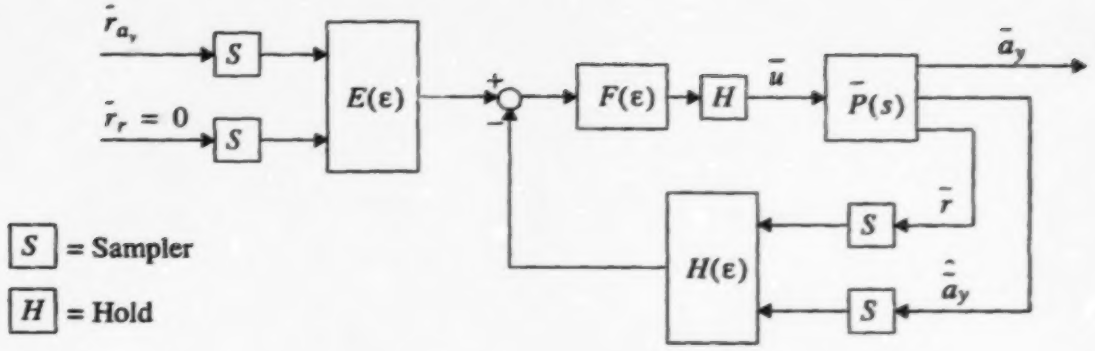

Figure 3.17: Digitally re-designed missile control system using MIMO PIM method

Comments: From the implementation point of view described in Section 2.7, it is usually desirable to have a fewer number of controllers to achieve a certain closed loop system performance. The 1-controller set up would therefore be more preferable. However, if the plant is open loop unstable, then the 3-controllers solution is required to realize the desired discrete-time PITF.

Theorems 2.12 and 2.19 indicate that the 1- and 3-controller set up have the same order as the PITF, pointing out that the order of individual controller in the 3-controller set-up is not necessarily lower than that in the 1-controller setup. In light of the discussion on the FWL effects for discrete-time systems in Section 2.7, the use of the 1-controller set up for stable plants in the implementation of the sampled-data systems that result from applying the PIM digital re-design method is preferred.

A subtle footnote should be added to compliment the above discussion. In *continuous-time* control system design, analogue signals within a closed loop system may have certain maximum loading limits, such as the pressure limit inside a hydraulic cable. A proper design should also consider the output of controller blocks so as not to exceed certain signal magnitudes; although limited to within a small voltage range, digital signals in contrast can represent analogue signals with large amplitudes. This illustrates an advantage of sampled-data control systems.

3.4.3 Application of Multi-Loop PIM method

As illustrated earlier in Section 3.3.1, it is possible to re-structure the analogue missile control system under consideration as a multi-loop system, as shown in Figure 3.18,

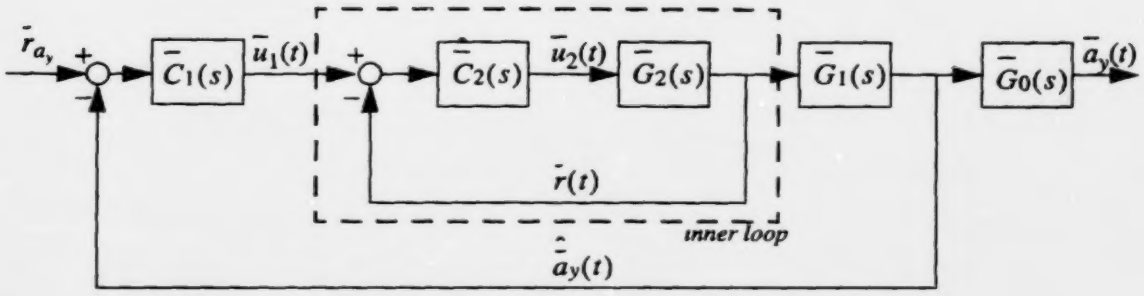

Figure 3.18: The re-structured multi-loop analogue missile control system

where

$$\bar{\bar{C}}_1(s) = \frac{K_a}{K_r s + K_\psi} = \frac{1.38}{5.49s + 208.6}, \tag{3.74}$$

$$\bar{\bar{C}}_2(s) = \frac{K_r s + K_\psi}{s} = \frac{-5.49s - 208.6}{s}, \tag{3.75}$$

$$\bar{G}_2(s) = \frac{-1.121 \times 10^6 s - 3.195 \times 10^6}{s^4 + 351.9s + 6\,367 \times 10^4 s + 2\,914 \times 10^5 s + 3\,027 \times 10^7}, \tag{3.76}$$

$$\bar{G}_1(s) = \frac{-1.121 \times 10^6 s - 3.195 \times 10^6}{17.94s^3 + 6330s^2 + 1.139 \times 10^6 s + 3.195 \times 10^6}, \tag{3.77}$$

$$\bar{G}_0(s) = \frac{-756875s^2 + 9.31 \times 10^5 s + 3.183 \times 10^9}{2.24s^4 + 804.4s^3 + 1.98 \times 10^5 s^2 + 1.908 \times 10^7 s + 3.179 \times 10^9}. \tag{3.78}$$

Following the description in Section 2.6.4, the PIM method for multi-loop systems can be applied to the 2-loop feedback system.

Step 1: Select a non-pathological sampling period T. Consider the innermost loop and obtain a SIM for the plant $\bar{P}_2(s) = \bar{G}_2(s)$.

Considering $T = 0.01$ sec. as in Section 3.4.2 and following the description of SIM of a

continuous-time system in Section 2.2.1, the discrete-time plant $P_2(\varepsilon)$ can be easily obtained, for $T = 0.01$ sec., as:

$$P_2(\varepsilon) = \frac{-7\,483\varepsilon^3 - 2633\varepsilon^2 - 2\,056\times 10^5\varepsilon - 5\,567\times 10^5}{\varepsilon^4 + 214.1\varepsilon^3 + 1.291\times 10^4\varepsilon^2 + 1\,731\times 10^5\varepsilon + 5\,275\times 10^6}. \tag{3.79}$$

Comments: Note that the number of finite zeros has increased as a result of the sampling. These extra zeros are called sampling zeros [5].

Step 2: Calculate the continuous-time PITF $\bar{\Phi}_2(s)$ for the innermost loop (from $\bar{u}_1$ to $\bar{u}_2$ in Figure 3.18), and evaluate its discrete-time model $\Phi_2(\varepsilon)$ using the MPZ method.

From (2.81), the continuous-time PITF is calculated to be

$$\bar{\Phi}_2(s) = \frac{-5\,49s^5 - 2141s^4 - 4\,229\times 10^5 s^3 - 1.488\times 10^7 s^2 - 2.27\times 10^8 s - 6.314\times 10^9}{s^5 + 351.9s^4 + 6.367\times 10^4 s^3 + 6.447\times 10^6 s^2 + 2\,817\times 10^8 s + 6\,664\times 10^8}. \tag{3.80}$$

Following the procedures outlined in Section 2.2.3, the MPZ model of $\bar{\Phi}_2(s)$ can be evaluated, for $T = 0.01$ sec., such that (2.70) is satisfied, as:

$$\Phi_2(\varepsilon) = \frac{-6\,427\varepsilon^5 - 1579\varepsilon^4 - 1.265\times 10^5\varepsilon^3 - 3\,736\times 10^6\varepsilon^2 - 6.908\times 10^7\varepsilon - 1.072\times 10^9}{\varepsilon^5 + 310\varepsilon^4 + 3\,856\times 10^4\varepsilon^3 + 2\,225\times 10^6\varepsilon^2 + 5.098\times 10^7\varepsilon + 1\,131\times 10^8}. \tag{3.81}$$

Step 3: Perform a digital re-design of the inner loop system using the PIM method.

From (3.79), (3.81) and Remark 2.19, it is clear that

$$p = 5,\ n = 4. \tag{3.82}$$

Since $p < 2n - 1$, it is necessary to add a stable system $\bar{\Sigma}_2(s)$ of order equal to two (or greater) to the plant $\bar{P}_2(s)$ and repeat the calculation done in Steps 1 and 2. This is choosen to be

$$\bar{\Sigma}_2(s) = \frac{s^2 + 525s + 68750}{s^2 + 525s + 68750}. \tag{3.83}$$

Thus $\bar{P}_2(s)$ is re-considered as

$$\bar{P}_2(s) = \bar{G}_2(s)\ \bar{\Sigma}(s)$$
$$= \frac{-1.121\times10^6 s^3 - 5\,919\times10^8 s^2 - 7\,876\times10^{10} s - 2\,196\times10^{11}}{s^6 + 877 s^5 + 3.172\times10^5 s^4 + 5\,791\times10^7 s^3 + 4\,56\times10^9 s^2 + 3\,592\times10^{10} s + 2.081\times10^{12}}. \tag{3.84}$$

The continuous-time PITF thus becomes

$$\bar{\Phi}_2(s) = \frac{-5.49 s^7 - 5023 s^6 - 1\,924\times10^6 s^5 - 3\,841\times10^8 s^4 - 3.712\times10^{10} s^3 - 1\,149\times10^{12} s^2 - 1\,892\times10^{13} s - 4\,341\times10^{14}}{s^7 + 877 s^6 + 3\,172\times10^5 s^5 + 6\,407\times10^7 s^4 + 8\,043\times10^9 s^3 + 5\,918\times10^{11} s^2 + 1\,972\times10^{13} s + 4.582\times10^{13}}. \tag{3.85}$$

Using the MPZ model of $\bar{\Phi}_2(s)$ with $T = 0.01$ sec., the denominator of $\Phi_2(\varepsilon)$ is found to be

$$d_{\Phi_2(\varepsilon)} = \varepsilon^7 + 495\,4\varepsilon^6 + 1.046\times10^5\varepsilon^5 + 1.204\times10^7\varepsilon^4 + 7.947\times10^8\varepsilon^3 + 2\,868\times10^{10}\varepsilon^2 + 4.59\times10^{11}\varepsilon + 9.719\times10^{11} \tag{3.86}$$

From the numerator and denominator coefficients of the plant $P_2(\varepsilon)$ and the PITF $\Phi_2(\varepsilon)$, the Diophantine equation given by (2.72) to (2.74) is constructed. The solution to (2.72) results in

$$u_2(\varepsilon) = \varepsilon^3 + 233\,6154\varepsilon^2 + 1\,4272\times10^4\varepsilon + 1.6202\times10^4$$
$$v_2(\varepsilon) = -6.3737\varepsilon^3 - 1.4225\times10^3\varepsilon^2 - 9.6223\times10^4\varepsilon - 1.5923\times10^6. \tag{3.87}$$

Considering (2.75) and examining the expressions for discrete-time plant $P_2(\varepsilon)$ and PITF $\Phi_2(\varepsilon)$ yield

$$r_2(\varepsilon) = -6\,4274\varepsilon^3 - 1\,3948\times10^3\varepsilon^2 - 9\,2895\times10^4\varepsilon - 1\,7458\times10^6. \tag{3.88}$$

To follow the general 3-controllers set up of (2.77), let

$$\lambda_2(\varepsilon) = \varepsilon^3 + 150\varepsilon^2 + 7400\varepsilon + 120000. \tag{3.89}$$

The controllers obtained by applying the PIM method to the innermost loop are

$$E_2(\varepsilon) = \frac{r_2(\varepsilon)}{\lambda_2(\varepsilon)} = \frac{-6.4274\varepsilon^3 - 1\,3948\times10^3\varepsilon^2 - 9\,2895\times10^4\varepsilon - 1.7458\times10^6}{\varepsilon^3 + 150\varepsilon^2 + 7400\varepsilon + 1\,2\times10^5}, \tag{3.90}$$

$$F_2(\varepsilon) = \frac{\lambda_2(\varepsilon)}{u_2(\varepsilon)} = \frac{\varepsilon^3 + 150\varepsilon^2 + 7400\varepsilon + 1\,2\times10^5}{\varepsilon^3 + 233.6154\varepsilon^2 + 1\,4272\times10^4\varepsilon + 1\,6202\times10^4}, \quad \text{and} \tag{3.91}$$

$$H_2(\varepsilon) = \frac{v_2(\varepsilon)}{\lambda_2(\varepsilon)} = \frac{-6\,3737\varepsilon^3 - 1\,4225\times10^3\varepsilon^2 - 9\,6223\times10^4\varepsilon - 1\,5923\times10^6}{\varepsilon^3 + 150\varepsilon^2 + 7400\varepsilon + 1\,2\times10^5}, \tag{3.92}$$

for the sampling period $T = 0.01$ sec.

Step 4: Consider the outer loop of Figure 3.18 and calculate its discrete-time plant $P_1(\varepsilon)$.

As explained in Section 2.6.4, $P_1(\varepsilon)$ is obtained by multiplying the MPZ model of the inner loop PITF (without $\bar{\Sigma}_2(s)$) with the SIM of $\bar{G}_2(s)$ and $\bar{G}_1(s)$ combined. Thus, for $T = 0.01$ sec.,

$$P_1(\varepsilon) = \frac{14.4\varepsilon^5 + 5222\varepsilon^4 + 1.001\times10^6\varepsilon^3 + 1.134\times10^8\varepsilon^2 + 6.296\times10^9\varepsilon + 1.126\times10^{11}}{\varepsilon^5 + 310\varepsilon^4 + 3.856\times10^4\varepsilon^3 + 2.225\times10^6\varepsilon^2 + 5.098\times10^7\varepsilon + 1.131\times10^8}. \tag{3.93}$$

Comments: The conbination of $\bar{G}_2(s)$ and $\bar{G}_1(s)$ is simply the second entry of the plant in (3.49) that gives the output $\hat{\bar{a}}_y$.

Step 5: Find the continuous-time PITF $\bar{\Phi}_1(s)$ for the outer loop and evaluate its discrete-time model $\Phi_1(\varepsilon)$ using the MPZ method.

Obtain the expression for continuous-time plant $\bar{P}_1(s)$ for the outer loop using (2.82). From (3.76), (3.77) and (3.80), $\bar{P}_1(s)$ is evaluated as

$$\bar{P}_1(s) = \frac{12.3s^5 + 4883s^4 + 1.255\times10^6s^3 + 1.48\times10^8s^2 + 2.143\times10^{10}s + 6.631\times10^{11}}{s^5 + 351.9s^4 + 6.367\times10^4s^3 + 6.447\times10^6s^2 + 2.817\times10^8s + 6.664\times10^8}. \tag{3.94}$$

To find the continuous-time PITF $\bar{\Phi}_1(s)$ for the outer loop, equation (2.83) can be used. From (3.75) and (3.94), $\bar{\Phi}_1(s)$ is calculated to be

$$\bar{\Phi}_1(s) = \frac{1.38s^5 + 485.7s^4 + 8.786\times10^4s^3 + 8.897\times10^6s^2 + 3.887\times10^8s + 9.197\times10^8}{5.49s^6 + 2158s^5 + 4.297\times10^5s^4 + 5.041\times10^7s^3 + 3.093\times10^9s^2 + 9.2\times10^{10}s + 1.054\times10^{12}}. \tag{3.95}$$

It is clear from (3.94) and (3.95) that digital re-design of the outer loop suffers the same problem with the degree condition as in Step 3. In this case, a third-order transfer function $\bar{\Sigma}_1(s)$ with equal numerator and denominator is added to the forward loop, such that

$$\bar{\Sigma}_1(s) = \frac{s^3 + 675s^2 + 151250s + 11250000}{s^3 + 675s^2 + 151250s + 11250000}. \tag{3.96}$$

The above calculation is repeated, after which $\bar{\Phi}_1(s)$ is obtained, and its the discrete-time PITF $\Phi_1(\varepsilon)$ evalutated using the MPZ method for $T = 0.01$ sec. This gives the following

denominator polynomial:

$$d_{\Phi_1(\varepsilon)} = \varepsilon^9 + 614.4\varepsilon^8 + 1\,672\times 10^5\varepsilon^7 + 2.632\times 10^7\varepsilon^6 + 2.629\times 10^9\varepsilon^5 + 1.718\times 10^{11}\varepsilon^4 + 7.31\times 10^{12}\varepsilon^3 + 1.943\times 10^{14}\varepsilon^2 + 2.923\times 10^{15}\varepsilon + 1\,895\times 10^{16} \tag{3.97}$$

Step 6: Perform a digital re-design of the outer loop using PIM method.

Following a similar procedure to Step 3, the polynomial $r_1(\varepsilon)$ is found to be

$$r_1(\varepsilon) = 0\,2058\varepsilon^3 + 55\,1076\varepsilon^2 + 4.9163\times 10^3\varepsilon + 1\,4615\times 10^5. \tag{3.98}$$

Then set

$$\lambda_1(\varepsilon) = \varepsilon^4 + 220\varepsilon^3 + 17900\varepsilon^2 + 6.38\times 10^5\varepsilon + 8.4\times 10^6. \tag{3.99}$$

The digital controllers obtained by applying the PIM digital re-design to the outer loop are

$$E_1(\varepsilon) = \frac{r_1(\varepsilon)}{\lambda_1(\varepsilon)} = \frac{0.2058\varepsilon^3 + 55\,1076\varepsilon^2 + 4.9163\times 10^3\varepsilon + 1.4615\times 10^5}{\varepsilon^4 + 220\varepsilon^3 + 17900\varepsilon^2 + 638000\varepsilon + 8400000}, \tag{3.100}$$

$$F_1(\varepsilon) = \frac{\lambda_1(\varepsilon)}{u_1(\varepsilon)} = \frac{\varepsilon^4 + 220\varepsilon^3 + 17900\varepsilon^2 + 638000\varepsilon + 8400000}{0\,9720\varepsilon^4 + 292\,7494\varepsilon^3 + 3.1878\times 10^4\varepsilon^2 + 1.4566\times 10^6\varepsilon + 2.2466\times 10^7}, \tag{3.101}$$

$$H_1(\varepsilon) = \frac{v_1(\varepsilon)}{\lambda_1(\varepsilon)} = \frac{0.0019\varepsilon^4 + 0\,7050\varepsilon^3 + 98.3905\varepsilon^2 + 6\,1738\times 10^3\varepsilon + 1\,4578\times 10^5}{\varepsilon^4 + 220\varepsilon^3 + 17900\varepsilon^2 + 638000\varepsilon + 8400000}, \tag{3.102}$$

for a sampling period $T = 0.01$ sec.

Together with the set of digital controllers obtained for the inner loop, the resultant sampled-data system resembles one shown in Figure 2.11. In this case, however, $\bar{G}_1(s)$ and $\bar{G}_2(s)$ are not the actual physical systems. As explained in Section 3.3.1, they are transfer function blocks constructed simply for design and evaluation of a discrete-time control system using the multi-

loop PIM method. The actual sampled-data system is depicted in Figure 3.19.

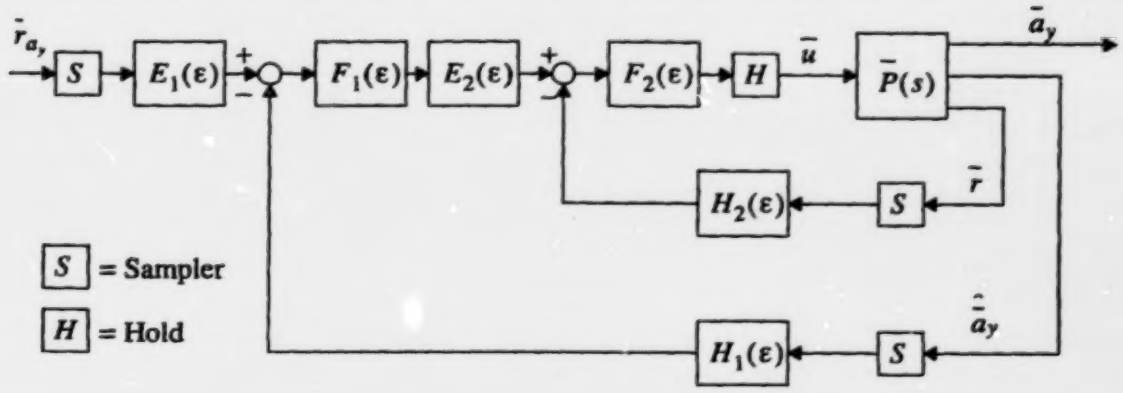

Figure 3.19: Multi-loop sampled-data system digitally re-designed using PIM method

Comments: A closer examination of Figure 3.18 reveals another possible procedure for digitally re-designing the multi-loop system using the PIM method. It may be tempting for the designer to include $\bar{C}_1(s)$ to the original innermost loop during the first stage of re-design. Doing so necessitates only one stage of digital re-design for the 2-loop system. However, this process holds the risk of resulting in an unstable system when the outer loop is closed, as there is no control over the selection of the outer loop poles. This observation also applies to systems with higher number of loops. Thus, to ensure satisfactory stability and indeed performance, it is necessary to diligently apply the PIM digital re-design method to each loop, stage by stage.

3.4.4 Reduced Order Multi-Loop PIM method

This is a variant of the PIM method that combines the multi-loop PIM and the reduced order PIM methods together into a single design framework.

The design procedure is similar to the multi-loop PIM method, except that the controller synthesis procedure at each loop uses the reduced order PIM method instead, and thus, lower order controllers can be obtained. In doing so, however, it is obvious that since the reduced order PIM method does not guarantee closed loop stability for all sampling periods, it becomes necessary to verify that for each loop during the discretization process.

The complete design procedure will not be described here as the content is highly repetitive of Sections 2.6.4 and 2.6.5. Instead, the general design steps involved are given in reference to Section 3.4.3.

Similar to the digital re-design of the re-structured multi-loop missile control system, first, the innermost loop is considered. Following design procedure for the reduced order PIM method described in Section 2.6.5, a set of lower order digital controllers are then obtained. At this point, check the stability of the ensuing discrete-time PITF. If the discretized innermost loop is found to be stable, adjusting the DC or low frequency gain as in (2.91), the inner loop re-design is then complete. Note that the rapprochement properties given by Theorem 2.21 and Theorem 2.22 apply. If the discretized inner loop is found to be unstable, then the reduced order PIM method can be re-applied by increasing the order of the digital controllers. At the worst case, the controller order would be the same as the multi-loop PIM design.

Next, the outer loop is considered. The determination of the outer loop "plant" and PITF is comparable to the multi-loop PIM method. The controller synthesis procedure then follows the reduced order PIM method again. Similar to the procedure for the innermost loop, it is necessary to check the stability of the resultant PITF following the controller design, as well as calculate the required gain adjustment. If the PITF is unstable, then follow the equivalent procedure as described for the innermost loop.

After successfully applying the above steps to the re-structured multi-loop missile control system, the following set of inner and outer loop digital controllers are obtained in reference to Figure 2.11 for a sampling period $T = 0.01$ sec.

$$E_1 = \frac{0.2058}{s+80},\quad F_1 = \frac{1.0193s + 81.5443}{s+31.3223},\quad H_1 = \frac{0.0022s + 0.2062}{s+80},\quad \text{and} \tag{3.103}$$

$$E_2 = \frac{-6.4274s - 203.1780}{s+50},\quad F_2 = \frac{0.7112s + 35.5592}{s+0.8672},\quad H_2 = \frac{-7.1057s - 191.6252}{s+50}. \tag{3.104}$$

Computer simulation result is shown in Section 3.5.

3.5 Analysis of Digitally Re-Designed Missile Control Systems

As detailed in Section 3.4, the application of the various methods of discretization to the analogue missile control system results in many discrete-time closed loop control systems with different structures as well as controller transfer functions. The results from computer simulation of these sampled-data systems are presented in this section. They will be compared qualitatively and quantitatively, particularly for those sampled-data systems synthesized using the multi-loop PIM and MIMO PIM methods. Recall that the local discretization and PIM methods fall into the class of indirectly designed discrete-time control systems, that is, it is assumed that a continuous-time controller has been formulated to bring satisfactory closed loop performance to the continuous-time plant according to its design specification, prior to the application of discretization. Therefore, performance evaluation of the aforementioned sampled-data systems is done in reference to the continuous-time missile control system. An overview of comparison criterias are given in Section 3.5.1. Specific issues relating to the set up of computer simulation to ensure diligent comparison of results are addressed in Section 3.5.2. Finally, the computer simulation results are presented in Section 3.5.3.

3.5.1 Overview of Criterias of Comparison

In this section, the following means of comparing the performance of the discrete-time missile control systems with their original continuous-time counterpart are employed:

a) A qualtitative comparison of the plant input and the output of the closed loop system, subjected to the unit step input.

b) Norms of the plant input errors and closed loop system output errors.

The step input response is an important component in control system design and analysis. It allows the user to have a first-hand visual inspection of the damping, rise time, overshoot and settling time properties of a system, which give rise to an intricate relation with classical design of SISO and SIMO systems. Sometimes a step test input supplied to a system may look like an unnecessarily and unrealistically large input for the system considered. For example, a step input in radian applied to the elevator deflection of a civilian aircraft pitch angle closed loop control

system model may look grossly exaggerated since it represents a reference input of 57.30 degrees. However, for LTI systems, the time domain response is simply an amplification of what the response is supposed to be for much smaller inputs [34] (e.g. 1.5 degrees), and in no way will this hinder the designer from infering properties of the modelled system. Thus, for the investigation in this thesis, comparison of step input responses in time give qualitative account of the change of those properties as a consequence of commissioning a digital re-design for the analogue system.

In control system design, it is often useful to have a good knowledge of the norms of certain signals within a closed loop system. The norms of a signal give information on some of its properties, such as its energy level and maximum magnitude. Two specific norms are considered as follows:

Definition 3.4

Suppose $\bar{u}(t) : R \rightarrow R^n$, i.e. for each time $t \in R$, $\bar{u}(t)$ is a vector in R^n. The L_2-norm of a continuous-time signal $\bar{u}(t)$ is defined to be

$$\|u\|_{L_2} = \left(\int_{-\infty}^{\infty} \|u(t)\|^2 dt \right)^{1/2} . \tag{3.105}$$

The L_2 space consists of all signals for which this norm is finite.D

Definition 3.5

Suppose $\bar{u}(t)$ is a continuous-time signal such that, $\bar{u}(t) : R \rightarrow R^n$. The L_∞-norm of $\bar{u}(t)$ is defined to be

$$\|u\|_{L_\infty} = \sup |u(t)| . \tag{3.106}$$

The L_∞ space consists of all signals for which this norm is finite.D

The comparison of plant input and output of the sampled-data system with those of the continuous-time missile control system provides a measure of the change and deterioration of system performance as a result of sampling. Here, deterioration is measured in the sense of deviation from the continuous-time design. It does not necessarily mean the sampled-data system

becomes unstable or exhibits large overshoot. In view of the PIM methods, which emphasize the discretization of a system's PITF using the MPZ method, the comparison of the plant input signals informs the designer on the effect of this mapping as the sampling period changes, and their ensuing system output shows the effect of this deviation of plant inputs. If the difference of these two signals are denoted as "error", then, calculation of signal norms of these errors give a quantified interpretation. It is by no mean an "once and for all" type of measure, as there are different norms which reveal different properties of a signal. The use of the 2-norm on the error signal is aimed at capturing its energy content, while the supremum norm at its absolute bound.

3.5.2 Fairness of Comparison

The Simulink interface in MATLAB provides a convenient environment to simulate and analyse the time response of closed loop control systems subjected to different reference inputs. The addition of the Fixed-Point Blockset optional package in Simulink allows engineers and research scientists to see effects of FWL on discrete-time systems as described in Section 2.7. In reality, a digital controller is implemented taking the techniques described in Section 2.7 into account to reduce FWL effects, leading to non-unique representation and realization, and thus different system performance. Therefore, a prudent comparison of simulation results of various discrete-time control systems in the time domain should only consider the *intended* floating point system performance. However, one can certainly emphasize the performance superiority of some particular systems by comparing them with others, *in addition*, using fixed point simulation. A comparison of simulation results in the time domain in this thesis will follow the above guideline.

3.5.3 Digital Control of Missile Yaw Plane Dynamics

The results of using three different local discretization methods on the analogue controller $\bar{C}(s)$ are shown in Tables 3.1 and 3.2 for the missile yaw plane dynamics. They are expressed using the ε and z operators, respectively. Three different methods of PIM are applied to the missile control system in this thesis. First, treating the analogue missile controller as a MIMO system, the MIMO PIM digital re-design method is applied to the closed loop system. This results in a sampled-data system which resembles one shown in Figure 3.17. Secondly, Lemma 3.2 is used to re-formulate

the missile control system as a multi-loop system, and then closed loop discretization is carried out using the multi-loop PIM method as in Figure 3.18. Lastly, the reduced-order multi-loop PIM method is applied to the re-formulated multi-loop system which gives a multi-loop system similar to the one shown in Figure 3.18 but with lower-order controllers.

A qualitative comparison is first made for results obtained using the MIMO PIM and multi-loop PIM methods for three sampling frequencies considered: i) $f_s = 100$ Hz, ii) $f_s = 50$ Hz, and iii) $f_s = 10$ Hz. The missile acceleration response $\bar{a}_y$ and the plant input signal $\bar{u}$ of the aforementioned sampled-data systems subjected to a unit step input is illustrated in Figure 3.20, Figure 3.21 and Figure 3.22 respectively. As a reference, the response obtained from carrying out a local discretization on the analogue controller using Tustin's approximation is also included with the first two sampling frequencies; this response becomes unstable at around $T = t_r/5$, where t_r (= 0.9 second) is the rise time of the step response of continuous-time control system.

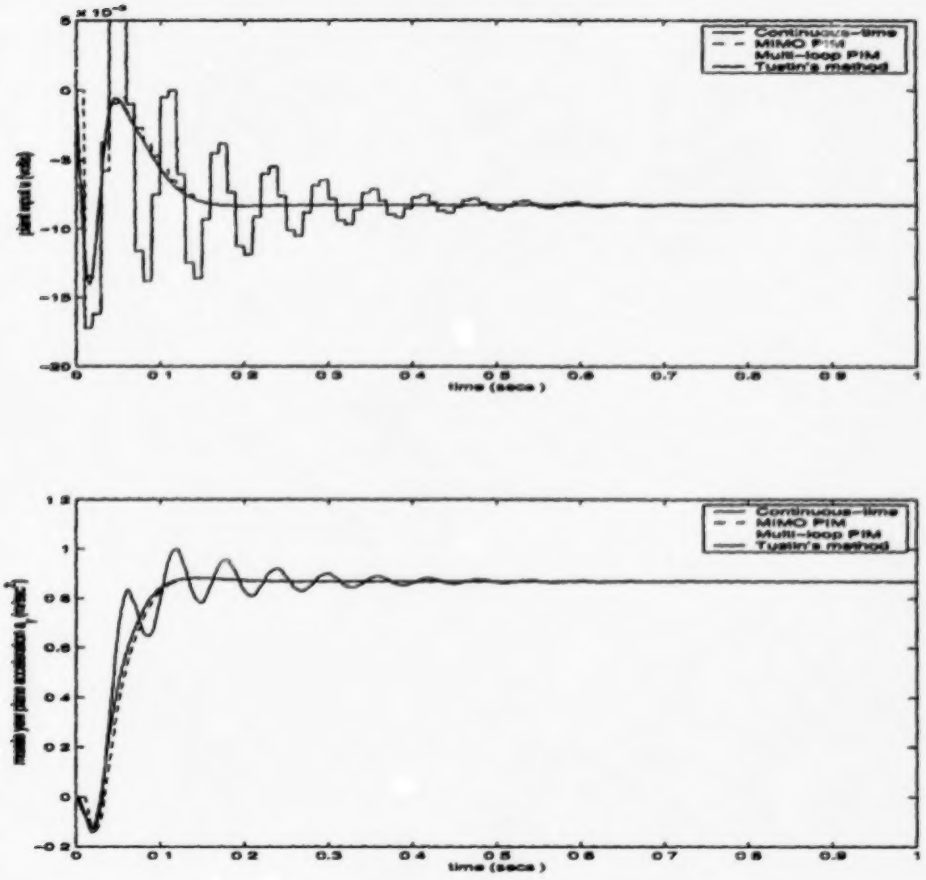

Figure 3.20: Step response of the sampled-data system obtained for $T = 0.01$ sec. (a) plant input signal $\bar{u}$, (b) lateral acceleration of missile $\bar{a}_y$.

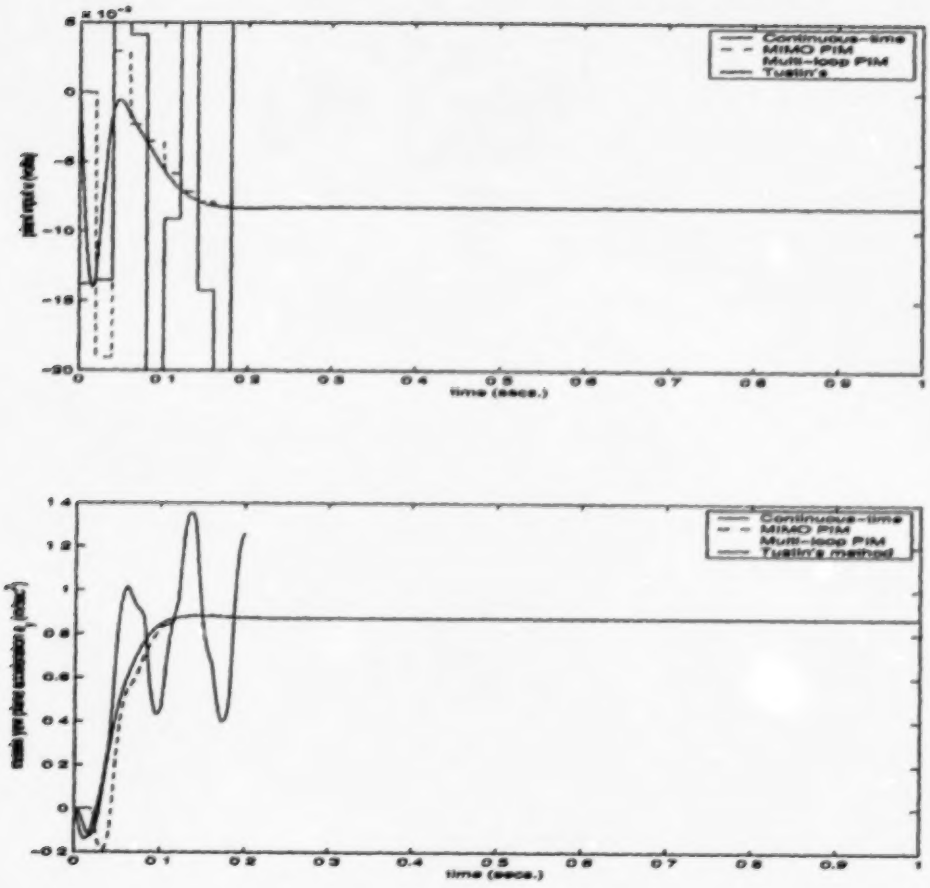

Figure 3.21: Step response of the sampled-data system obtained for $T = 0.02$ sec. (a) plant input signal $\bar{u}$, (b) lateral acceleration of missile $\bar{a}_y$.

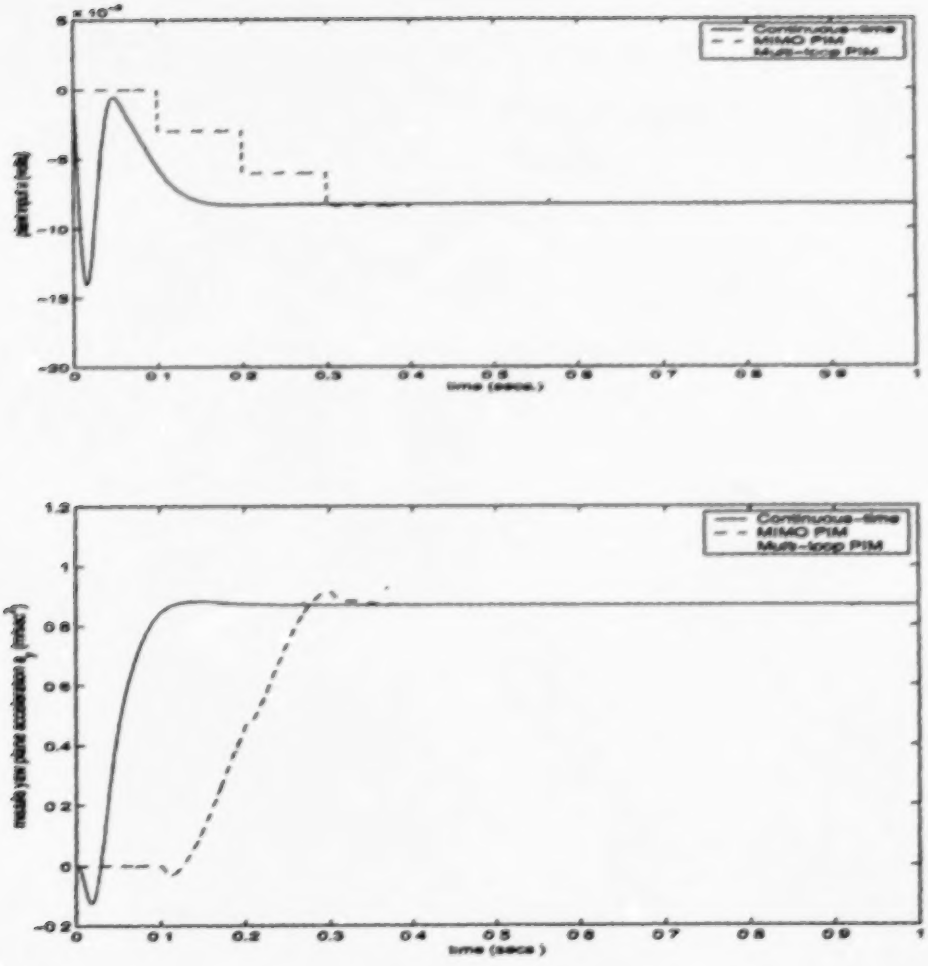

Figure 3.22: Step response of the sampled-data system obtained for $T = 0.1$ sec. (a) plant input signal $\bar{u}$, (b) lateral acceleration of missile $\bar{a}_y$.

The results showed that while the difference in response is insignificant at higher sampling rate, it becomes noticeable at the lowest sampling frequency tested: for $T = 0.1$ sec., the result indicates the MIMO PIM method gives better sampled-data system performance than the multi-loop PIM method with less overshoot and a faster settling time in the response. This observation is consistent with Lemma 3.3; the difference in performance is expected to increase as the sampling frequency is further lowered.

The L_2 and L_∞ norms of the lateral acceleration error defined as $\Delta a_y = a_y - \bar{a}_y$ for the two sampled-data systems are next considered. For the range of sampling periods where the discrete-time control systems are stable, the facts that they have the same DC gain and are subjected to the unit step input assure that the two norms will be finite. Figure 3.23 shows the L_2 and L_∞ norms of Δa_y for $T \in \left[\frac{t_r}{90}, \frac{t_r}{4}\right]$. It can be deduced from the diagram that the norms of Δa_y approaches zero with the sampling period T. For smaller sampling intervals in relation to t_r, the performance of the two sampled-data systems as illustrated by Figure 3.23 are comparable; however, at larger sampling intervals, it can be seen that the MIMO PIM method begins to have a marginal advantage in performance over the multi-loop PIM method. This trend is expected to continue for larger sampling intervals.

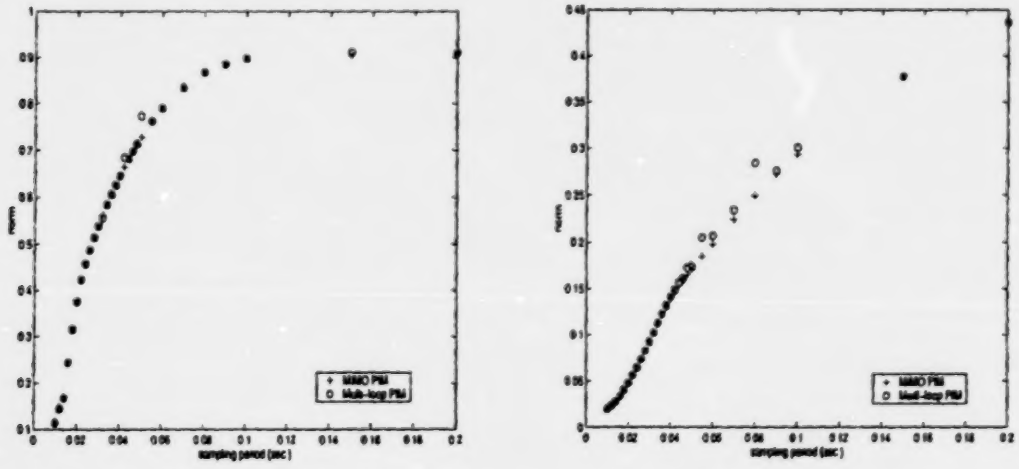

Figure 3.23: (a) $\|\Delta a_y\|_{L_\infty}$ and (b) $\|\Delta a_y\|_{L_2}$

The behaviour of sampled-data systems obtained using the reduced-order multi-loop PIM method

is next illustrated in comparison with the response of the MIMO discrete-time missile control system. The step input response and the resultant plant input signal of these two systems are demonstrated in Figure 3.24, Figure 3.25 and Figure 3.26 in which three different sampling frequencies, f_s = 100, 50 and 10 Hz, are used respectively.

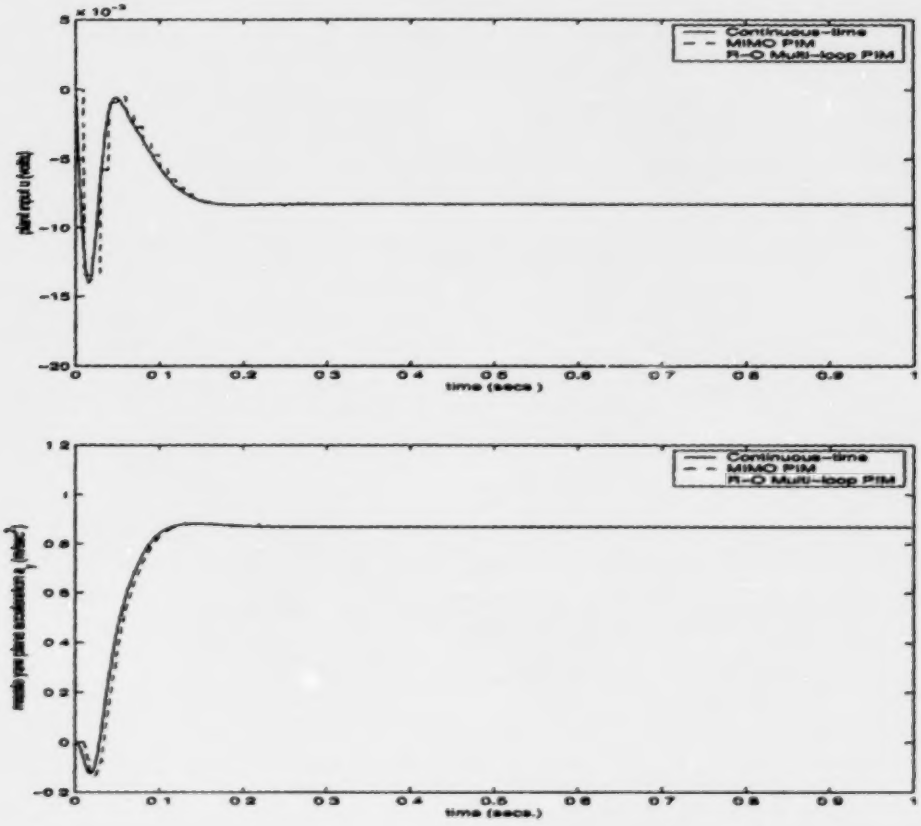

Figure 3.24: Step response of the sampled-data system obtained for $T = 0.01$ sec. (a) plant input signal $\bar{u}$, (b) lateral acceleration of missile $\bar{a}_y$.

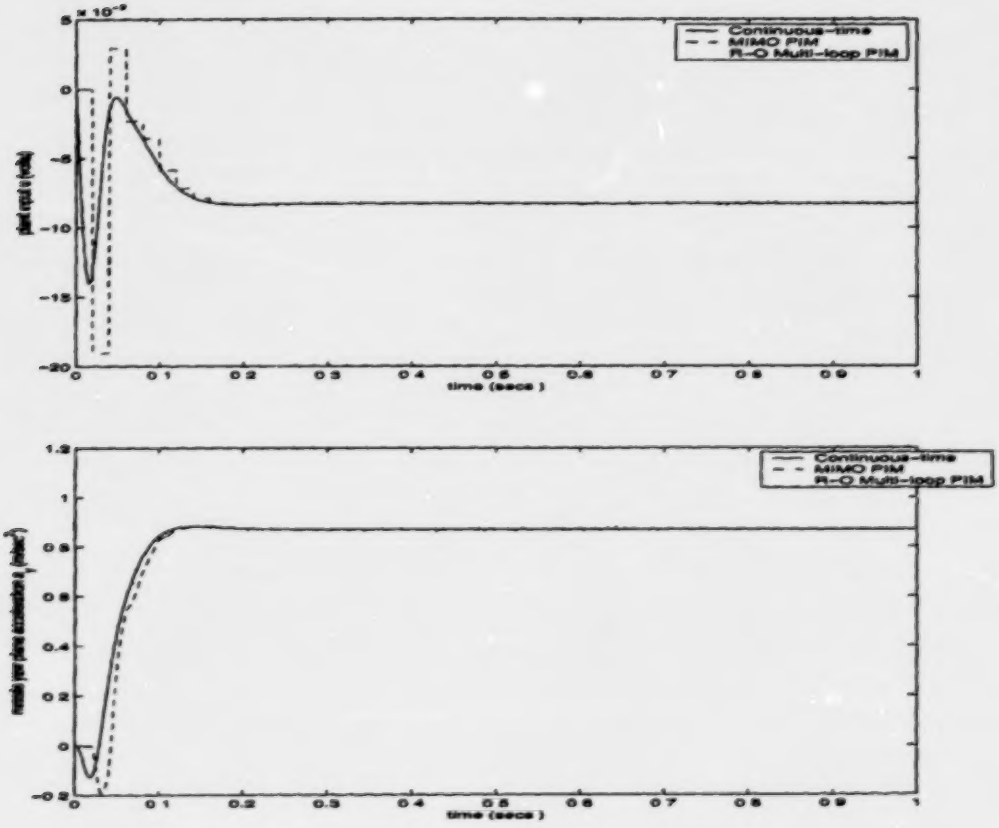

Figure 3.25: Step response of the sampled-data system obtained for $T = 0.02$ sec. (a) plant input signal $\bar{u}$, (b) lateral acceleration of missile $\bar{a}_y$.

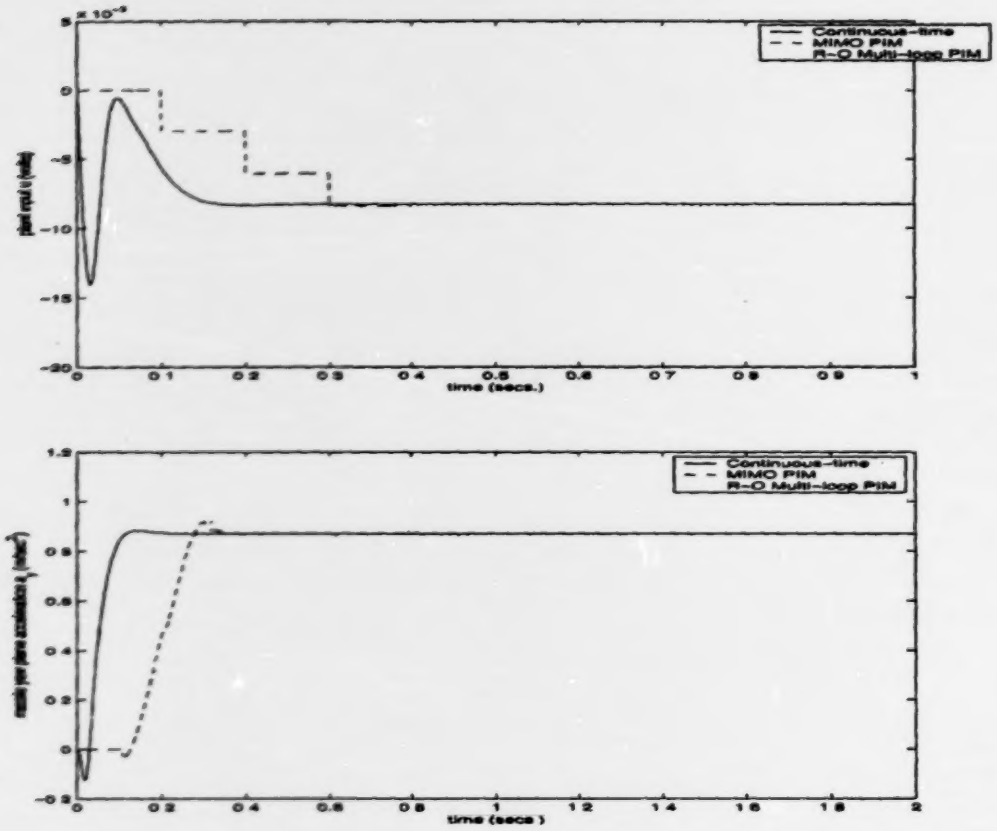

Figure 3.26: Step response of the sampled-data system obtained for $T = 0.1$ sec. (a) plant input signal $\bar{u}$, (b) lateral acceleration of missile $\bar{a}_y$.

Figures 3.24, 3.25 and 3.26 consistently illustrates that the reduced-order multi-loop PIM method give more oscillatory motion with longer settling time in comparison with the MIMO PIM method, particularly when the sampling frequency is low. This deterioration in performance is somewhat expected since the use of lower-order controllers typically represents a trade-off in control system design. The issue of controller order reduction is examined in closer detail from the PIM prospective in Chapter 4.

As a summary, relating back to developments made in Section 3.3, the results presented in this section showed definite agreement with Lemma 3.3, in that for the class of MIMO systems that can be re-strutured as multi-loop systems, the MIMO PIM mehod provides better sampled-data system preformance than the multi-loop PIM method in the time domain, ignoring the presence of FWL effects.

Chapter 4

Controller Order Reduction For PIM Methods: Further Exposition

From the practical implementation point of view, it is desired that digital controllers have as low an order as possible to minimize the FWL effect which adversely impacts the closed loop performance expected in a discrete-time control system analysis. While the PIM digital re-design methods offer stable sampled-data closed loop systems for virtually any sampling period with many advantages, a *potential* drawback exist: the resultant digital controllers in general have the same order as the plant model less one, irrespective of the order of designed analogue controllers for the continuous-time closed loop system. For the missile yaw plane dynamic model analysed in Chapter 3, this translates into fifth order controllers which may be fine. However, one can imagine a more severe *potential* problem if the task at hand involves the digital re-design of, say, a MIMO airframe model with more than fifty states as well as unstable poles using PIM. It is worth pointing out that the same problem also exists for the LQG and H_∞ controller designs.

There are a few standing issues: "are controller order reduction always necessary?" "what issues are involved as far as PIM methods are concerned?" and "what are the available options that applies to PIM re-designed systems?" An equally dumbfounding question is: "why is there such a big fuzz, given that the DSP community is known to be able to implement a digital filter of hundreds of order [65]?" This chapter addresses some of the above concerns. It particularly connects with discussions given in Sections 2.7 and 3.5.2, as well as Sections 2.6.5 and 3.4.4.

4.1 Principles of Low Order Controller Design: A PIM Prospective

Analogous to the idea of methods of PIM digital re-design, the controller order reduction is best carried out when closed loop performance, in particular stability, is taken into consideration. Many different concepts of practical controller design and controller order reduction for general LTI discrete-time systems are given by Anderson et al. in [2], Liu et al. in [18] and Anderson in [3]. There are in general three different approaches to obtaining low order controllers. Consider Figure 4.1. On the left hand side of the diagram, a model reduction of the plant is first carried out, followed by controller design for the reduced plant model. The direct design approach represents methods that take a high order plant and produce controllers that give desirable system behaviour. The third possibility uses the high order plant to design high order controllers which is then simplified.

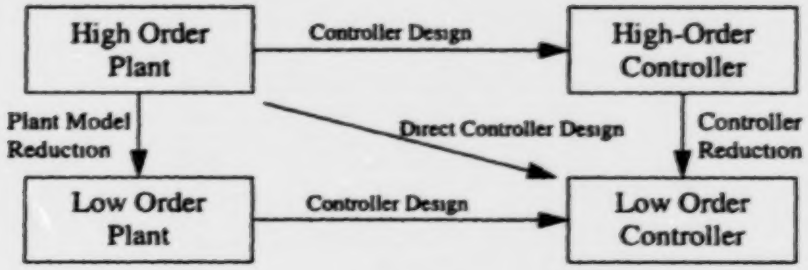

Figure 4.1: Basic approaches in low order controller design

The first approach involving plant model reduction in general does not bring the best desirable performance. Much information about the plant is lost *during the initial model reduction step*, leaving little knowledge of the plant for the controller design process. Invoking the principles behind the PIM methods, the controllers designed will at best bring stability to the closed loop system, assuming the unstable poles of the plant remains in its not-too-crude reduced model.

From the PIM prospective concerning the direct design category, the reduced-order PIM method for SISO systems by Rabbath et al. [32] described in Sections 2.6.5 and 3.4.4 in fact belongs to this class of design. Several other recently modified PIM methods proposed by Rabbath [41],

including the Truncated PIM, and the reduced-order Truncated PIM methods also correspond to this category. The major benefit of this approach is that it takes a high order plant and *directly* designs a set of lower-order controllers requirnng almost no additional efforts. For the reduced-order PIM method however, because the denominator polynomial of the resultant discrete-time PITF differs from the desired one for the first and last cases above, it becomes necessary to perform an extra calculation to verify the stability of the designed sampled-data system. This issue will be examined in the next section.

As far as the third option for lower-order controller design goes, the regular PIM methods can be used to obtain a set of high order digital controllers for SISO and MIMO systems. From there on, a few methods can be used to reduce the order of designed controllers. Some of them takes account of the closed loop system performance and stability much as in the spirit of PIM. Several ideas follow closely on the use of H_∞ design techniques, such as those by Lui et al. [18] and Anderson [3]. The reduced-order PIM method is the main focus of this chapter.

4.2 Reduced-Order PIM method for SISO systems: A re-visit

This direct design method for SISO systems by Rabbath et al. [32] was shown in Sections 2.6.5 and 3.4.4. Some further implication and development of this method is illustrated here. Recall that the coefficients of the digital controllers are partly obtained by solving the algebraic equation

$$AX = Y \tag{4.1}$$

where $A \in R^{(p+1)\times(i+j+2)}$ contains coefficients of the plant, $X \in R^{(i+j+2)\times 1}$ represents the coefficients of the controllers, and $Y \in R^{(p+1)\times 1}$ represents the coefficients of the denominator of the desired PITF. The least-square solution $\widehat{X}$ for (4.1) is given by

$$\widehat{X} = (A^T A)^{-1} A^T Y \tag{4.2}$$

which Rabbath et al. [32] employs. Now, using $\widehat{X}$ in (4.2) to obtain the required digital controllers for the sampled-data system, the coefficients of the discrete-time PITF denominator is then given by $\widehat{Y}$ as

$$\widehat{Y} = A\widehat{X} = A(A^TA)^{-1}A^TY. \tag{4.3}$$

Due to the nature of least-square problems, in general $\widehat{Y} \neq Y$ for non-square, rank deficient "A" matrices, and, therefore, it is not certain whether all roots of the denominator polynomial formed using coefficients in $\widehat{Y}$ belong to the domain of stability given in Table 2.1 for finite T. To investigate this issue, define an error $\widehat{e}$ as

$$\widehat{e} \equiv \widehat{Y} - Y = A(A^TA)^{-1}A^TY - Y = [A(A^TA)^{-1}A^T - I]Y = \Psi Y \tag{4.4}$$

where

$$\Psi \equiv [A(A^TA)^{-1}A^T - I]. \tag{4.5}$$

Then this implies

$$\|\widehat{e}\| = \|\Psi Y\| \leq \|\Psi\|\|Y\|. \tag{4.6}$$

where $\|\widehat{e}\|$ represents an error bound for $\left(\widehat{Y} - Y\right)$. It was shown in Chapters 2 and Chapter 3 that the PIM method gives desirable sampled-data system response. As a result of this error, the ensuing discrete-time control system will exhibit responses different from those obtained by carrying out the PIM method. It is therefore important for the designer to justify this need, apart from checking the resultant closed loop stability. This is an important consideration, and will be the subject of discussion in Section 4.3.

4.2.1 A Modified Reduced-Order PIM Method

Following the preceding exposition on direct design of low order controllers using the reduced-order PIM digital re-design method, a modification is proposed here. This involves adding a diagonal weighting matrix to place emphasis on the relative importance of coefficients in the least-square problem formulation given by (4.1). The design technique is first given, followed by its rationale and use.

The design procedure is identical to the reduced-order PIM method up to the point where a set of

algebraic equations is set up as (2.89) from the diophantine equation in (2.86) and (2.87). Knowing that the resultant $\widehat{Y}$ will not equal the actual Y vector, a square diagonal weighting matrix W is then attached from the left to both sides of (4.1) so as to weigh the relative importance of the Y-values, i.e. the coefficients of the desired denominator polynomial. Thus, the set of algebraic equations becomes

$$(WA)X = WY \tag{4.7}$$

where $A \in R^{(p+1)\times(i+j+2)}$, $X \in R^{(i+j+2)\times 1}$, $Y \in R^{(p+1)\times 1}$, and $W \in R^{(p+1)\times(p+1)}$ such that $w_{ij} = 0$ for $i \neq j$, $w_{ij} \neq 0$ for $i = j$.

Assuming that Rank(A) = ($i + j + 2$), the solution to the weighted least-square problem [59] is uniquely given by

$$\widehat{X}_w = [(WA)^T(WA)]^{-1}(WA)^T WY. \tag{4.8}$$

The error $\widehat{e}_w$ in this case is

$$\begin{aligned} \widehat{e}_w \equiv (\widehat{Y}_w - Y) &= (WA)[(WA)^T(WA)]^{-1}(WA)^T WY - Y \\ &= \{(WA)[(WA)^T(WA)]^{-1}(WA)^T W - I\}Y. \end{aligned} \tag{4.9}$$

Once a solution $\widehat{X}_w$ in (4.8) is obtained for the weighted least-square problem, the sampled-data system controllers are then selected by following the same procedure as the reduced-order PIM method. In particular, it is essential to similarly calculate a gain K_w to satisfy the steady-state or low frequency requirement, such that

$$\widehat{\Phi}_w(\varepsilon)\big|_{\varepsilon=\varepsilon_0} \cdot K_w = \Phi(\varepsilon)\big|_{\varepsilon=\varepsilon_0}. \tag{4.10}$$

The following Lemmas validate the use of the weighted least-square solution in the modified reduced-order PIM formulation as well as the behaviour of the resultant sampled-data system as $T \to 0$.

Lemma 4.1

A unique solution to (4.7) exist if $b(\varepsilon)$ and $a(\varepsilon)$ that constitute A are coprime, and W satisfies the

condition as stated in (4.7).D

Proof

This follows directly from Theorem 2.20 for the set of algebraic equations involved with the reduced-order PIM method given by (2.76), provided W has non-zero diagonal entries such that it has full rank and thus W^{-1} is uniquely defined.B

Lemma 4.2

Supposed that $\bar{A}$ for the continuous-time system has linearly independent columns. Suppose also that, for each non-pathological sampling period T selected, A for the discrete-time system has linearly independent columns. Further assume that W is a function of T such that

$$\lim_{T \to 0} W = I. \tag{4.11}$$

Then, the modified least-square solution $\widehat{X_w}$ approaches the continuous-time solution $\bar{X}$ as T approaches zero.D

Proof

Since the discrete-time system associated with the "A" matrix is a SIM of the continuous-time system, and the desired discrete-time PITF is a MPZ model of the continuous-time PITF, one can write

$$\begin{aligned} A &= \bar{A} + \Delta\bar{A}, \text{ and} \\ Y &= \bar{Y} + \Delta\bar{Y} \end{aligned} \tag{4.12}$$

where

$$\lim_{T \to 0} \Delta\bar{A} = 0 \text{ and } \lim_{T \to 0} \Delta\bar{Y} = 0. \tag{4.13}$$

Furthermore, from (4.11), one can express W as

$$W = I + \Delta W \tag{4.14}$$

where,

$$\lim_{T \to 0} \Delta W = 0. \tag{4.15}$$

Knowing that the solution $\bar{X}$ exists, if the columns of $\bar{A}$ are linearly independent, the solution is unique and can still be expressed as (see Appendix)

$$\bar{X} = (\bar{A}^T\bar{A})^{-1}\bar{A}^T\bar{Y}. \tag{4.16}$$

Then, a bound on the norm of the vector $[\widehat{X}_w - \bar{X}]$ can be established as

$$\left\|\widehat{X}_w - \bar{X}\right\| \le (f_1 + f_2 + f_3) \tag{4.17}$$

where

$$\begin{aligned} f_1 &= \left\| \left\{ (\bar{A}^T\bar{A}) + f_{11} + f_{12} \right\}^{-1} \bar{A}^T - (\bar{A}^T\bar{A})^{-1}\bar{A}^T + f_{13} + f_{14} \right\| \left\|\bar{Y}\right\| \\ f_2 &= \left\| [(\bar{A} + \Delta\bar{A})^T (I + \Delta W)^2 (\bar{A} + \Delta\bar{A})]^{-1} \right\| \left\| \Delta\bar{A}^T \right\| \left\| (I + \Delta W)^2 \bar{Y} \right\| \\ f_3 &= \left\| [(\bar{A} + \Delta\bar{A})^T (I + \Delta W)^2 (\bar{A} + \Delta\bar{A})]^{-1} (\bar{A} + \Delta\bar{A})^T (I + \Delta W)^2 \right\| \left\| \Delta\bar{Y} \right\| \end{aligned} \tag{4.18}$$

and

$$\begin{aligned} f_{11} &= 2\bar{A}^T \Delta W \bar{A} + \bar{A}^T \Delta W^2 \bar{A} \\ f_{12} &= \Delta\bar{A}^T (I + \Delta W)^2 \bar{A} + \bar{A}^T (I + \Delta W)^2 \Delta\bar{A} + \Delta\bar{A}^T (I + \Delta W)^2 \Delta\bar{A} \\ f_{13} &= 2\left\{ (\bar{A}^T\bar{A}) + f_{11} + f_{12} \right\}^{-1} \bar{A}^T \Delta W \\ f_{14} &= \left\{ (\bar{A}^T\bar{A}) + f_{11} + f_{12} \right\}^{-1} \bar{A}^T \Delta W^2 . \end{aligned} \tag{4.19}$$

Therefore, from (4.17) and (4.18), the following holds:

i) Since $\lim_{T \to 0} \Delta\bar{A} = 0$, then $\lim_{T \to 0} f_2 = 0$.

ii) Since $\lim_{T \to 0} \Delta\bar{Y} = 0$, then $\lim_{T \to 0} f_3 = 0$.

iii) Concerning $\lim_{T \to 0} f_1$, from (4.19),

a) Since $\lim_{T \to 0} \Delta W = 0$, then $\lim_{T \to 0} f_{11} = 0$.

b) Since $\lim_{T \to 0} \Delta\bar{A} = 0$ and $\lim_{T \to 0} \Delta W = 0$, then $\lim_{T \to 0} f_{12} = 0$.

c) Since $\lim_{T \to 0} \Delta W = 0$, then $\lim_{T \to 0} f_{13} = 0$ and $\lim_{T \to 0} f_{14} = 0$.

In reference to (4.18), (a), (b) and (c) imply $\lim_{T \to 0} f_1 = 0$.

Finally, the lemma follows by applying (i), (ii) and (iii) to (4.17).B

Lemma 4.3

Let $\widehat{\Phi}_w(\varepsilon)$ be the discrete-time PITF formed using the solution from weighted least-square method for a stable $\overline{\Phi}(s) \in RH_\infty$ and let (4.11) hold. There exists a $T^* > 0$ such that $\widehat{\Phi}_w(\varepsilon)$ is stable for $0 < T < T^*$.D

Proof

Suppose that there does *not* exist a $\alpha > 0$ such that for any $T \in (0, \alpha)$ $\widehat{\Phi}_w(\varepsilon) \in RH_\infty$. To this $\widehat{\Phi}_w(\varepsilon)$, apply the w-transformation

$$\varepsilon = \frac{w}{1 - Tw/2}, \tag{4.20}$$

which yields $\Phi(w) \notin RH_\infty$, $\forall\, T \in (0, \alpha)$, $\forall\, \alpha \in \mathrm{R}^+$. Specifically consider an infinitesimal $T = \delta$, $\delta \in (0, \alpha)$, $\alpha \in \mathrm{R}^+$. The hypothesis then also gives $\widehat{\Phi}_w(w) \notin RH_\infty$. However, this violates the continuity property of the mapping of poles of the MPZ model. Therefore the theorem holds.B

Lemma 4.4

$\widehat{\Phi}_w(\varepsilon)\Big|_{\varepsilon = \frac{e^{sT} - 1}{T}} \cdot K_w$ converges to $\overline{H}(s)$, pointwise in s, as $T \to 0$.D

Proof

From Lemma 4.3, and the facts that, i) the zeros of $\widehat{\Phi}_w(\varepsilon)$ equal those of $\widehat{\Phi}(\varepsilon)$ and $\Phi(\varepsilon)$, and ii) K_w is calculated from (4.10).

Remarks 4.2, 4.3, 4.4

It is important for W to satisfy (4.11) in order to demonstrate the rapprochement property for the weighted least-square solution $\widehat{X}_w$ and discrete-time transfer function $\widehat{\Phi}_w(\varepsilon)$ detailed in Lemmas 4.2 to 4.4. As described later in this section, in the general weighted least-square problem formulation, W is usually set by the designer heuristically based on practical experience. Having said that however, for the present purpose of sampled-data system design, it is possible to

obtain a W such that it satisfies (4.11) and performs the required function.c

Now the rationale and how this modification can be applied is given. There are two motivations for attaching a weighting matrix W to (4.1) to form a system of equations given by (4.7). First, suppose for a particular sampling period T, a least-square solution $\widehat{X}$ is obtained in (4.2). The ensuing controller synthesis results in a discrete-time PITF whose denominator coefficients are given by $\widehat{Y}$ in (4.3). In least-square curve fitting, $\widehat{X}$ is viewed as the coefficients to be determined for a "best fit" polynomial and Y is viewed as the y-value of data points. The least-square formulation minimizes the error $\left\| \widehat{Y} - Y \right\|^2$ by calculating a "line of best fit." Now through the addition of a diagonal weighting matrix W, more emphasis can be put on certain y-values than others in obtaining a least-square solution $\widehat{X}$. At the same time, in the context of classical control system design, typically a controller is used to alter the modelled lower-order dynamics part of a plant. If its un-modelled higher order dynamics does not couple erroneously with the lower-order dynamics, satisfactory behaviour is usually obtained. This is indeed how PID controllers have been successful in industry. A combined idea can be applied in (4.7) to weight the lower-order dynamics of the desired discrete-time PITF heavier than higher-order ones in the least-square formulation. This is explained in a little more detail as follows: In the least-square formulation, since Y is composed of coefficients of the desired closed loop PITF denominator, such that

$$Y = \left[d_p \; d_{p-1} \; \cdots \; d_1 \; d_0 \right]^T \tag{4.21}$$

where $d_k, k = 0, 1, 2, ..., p$ represents the denominator coefficients, a weighting matrix W can be used to progressively weigh the importance of matching the lower-order dynamics of the sampled-data system in finding a least-square solution for the system of equations given by (4.7). This is done by assigning the following structure for W

$$W = \begin{bmatrix} w_p & 0 & \cdots & \cdots & 0 \\ 0 & w_{p-1} & 0 & & \vdots \\ \vdots & 0 & \ddots & \ddots & \vdots \\ \vdots & & \ddots & \ddots & 0 \\ 0 & \cdots & \cdots & 0 & w_0 \end{bmatrix} \tag{4.22}$$

where $w_p < w_{p-1} < \ldots < w_0$. Now, there are many different ways for W to satisfy (4.1) as well, although this may involve considering a coarse range of sampling period T that the discrete-time control system is designed to operate with. As an example, suppose that in a sampled-data system design using the modified PIM method, the desired discrete-time PITF denominator has a degree of 4. Assume the system is designed to operate approximately between $T = 0.1$ sec. and 0.02 sec. Then the following W can be proposed

$$W = \begin{bmatrix} 1-10T & 0 & \ldots & \ldots & 0 \\ 0 & 1-5T & 0 & & \cdot \\ \vdots & 0 & 1+T & 0 & \vdots \\ \cdot & & 0 & 1+5T & 0 \\ 0 & \ldots & \ldots & 0 & 1+10T \end{bmatrix}. \tag{4.23}$$

It can be seen from (4.23) that, i) W approaches $I_{5\times5}$ as T approaches zero, and ii) in reference to (4.22), $w_4 < w_3 < \ldots < w_0$. It is foreseeable that successful selection of the weighting matrix W can be versatile in the sampled-data system design.

To appreciate the difference in solutions obtained using the two different least-square methods, observe that $\widehat{X}$ and $\widehat{X}_w$ satisfy [56]

$$\widehat{X}_w - \widehat{X} = (A^T W^2 A)^{-1} A^T (W^2 - I)\left(Y - A\widehat{X}\right). \tag{4.24}$$

Using (4.4), this implies

$$\widehat{X}_w - \widehat{X} = (A^T W^2 A)^{-1} A^T (W^2 - I)\,\widehat{e}\,. \tag{4.25}$$

To examine what this difference makes in the resultant discrete-time PITF denominator

$$\begin{aligned} \left\|\widehat{e_w}\right\| = \left\|\widehat{Y}_w - Y\right\| &= \left\|\{(WA)[(WA)^T(WA)]^{-1}(WA)^T W - I\}Y\right\| \\ &\le \left\|\{(WA)[(WA)^T(WA)]^{-1}(WA)^T W - I\}\right\|\|Y\|\,. \end{aligned} \tag{4.26}$$

Define

$$\Psi_w = \{(WA)[(WA)^T(WA)]^{-1}(WA)^T W - I\} \tag{4.27}$$

such that

$$\left\|\widehat{e_w}\right\| = \|\Psi_w Y\| \le \|\Psi_w\|\|Y\| . \tag{4.28}$$

Then,

$$\begin{aligned}\|\Psi_w\| &= \left\|\{(WA)[(WA)^T(WA)]^{-1}(WA)^T W - I\}\right\| \\ &\le \left\|(WA)[(WA)^T(WA)]^{-1}(WA)^T W\right\| + 1 \\ &\le w_{\max}\|A\|\left\|(A^T W^2 A)^{-1}\right\| w_{\max}\|A^T\| w_{\max} + 1 \\ &= (w_{\max})^3\|A\|\left\|(A^T W^2 A)^{-1}\right\|\|A^T\| + 1\end{aligned} \tag{4.29}$$

where $w_{\max}$ is the maximum diagonal entry in W. In comparison, examining the expression for Ψ in (4.5) and (4.6),

$$\begin{aligned}\|\Psi\| &= \left\|A(A^T A)^{-1}A^T - I\right\| \\ &\le \left\|A(A^T A)^{-1}A^T\right\| + 1 \\ &\le \|A\|\left\|(A^T A)^{-1}\right\|\|A^T\| + 1 .\end{aligned} \tag{4.30}$$

It is seen from (4.29) and (4.30) that a comparison of solutions obtained using the two methods is dependent on the weighting used in W. In fact, in consideration of (4.29), in order to minimize $\|\Psi_w\|$, W in (4.23) should in fact be set to the following

$$W = \begin{bmatrix} 1-50T & 0 & \cdots & \cdots & 0 \\ 0 & 1-30T & 0 & & \vdots \\ \vdots & 0 & 1-20T & 0 & \vdots \\ \vdots & & 0 & 1-10T & 0 \\ 0 & \cdots & \cdots & 0 & 1-5T \end{bmatrix} \tag{4.31}$$

such that $w_{\max} < 1$. In practice, different relative weightings w_{ii} will result in different system response, particularly if considered in the context of discrete-time PITF. Therefore this is an extra degree of freedom that designers will have available for the tuning of controllers in the sampled-data system design using the reduced-order PIM method.

Closely related to the above is the second motivation for proposing the weighted least-square method. During the sampled-data system design process, if it is desirable to obtain controllers with a certain order number, but the reduced-order PIM method does not yield a set of stabilizing

controllers, then this modified procedure can be used in an attempt to overcome the problem. In fact, the set of stabilizing controllers obtained using this modified, or *weighted* reduced-order PIM method is a superset of those obtained using the "regular" reduced-order PIM method. This is formally stated in Theorem 4.12. The construction of ideas leading up to Theorem 4.12 is given below.

Theorem 4.5

Let Λ denote the set of all solutions $\widehat{X}$ obtained by solving the least-square problem given by (4.1), which is associated with the digital re-design of a proper LTI finite dimensional continuous-time SISO feedback control system using the reduced-order PIM method for a non-pathological sampling period T, as detailed in Section 2.6.5. Then, Λ is a closed set.D

Proof

Consider the plant of such a SISO analogue feedback control system where the degree of the plant's numerator and denominator polynomials are m and n, respectively. Let p be the degree of the denominator polynomial of the desired discrete-time PITF. Then from the Diophantine equation in (2.72) to (2.74), there are only a finite possible number of solution $\widehat{X}$ that will result by varying l and k in solving the least-square problem.

Since m, n, p are assumed to be finite, the number of possible solutions of $\widehat{X}$ are also limited and finite. This implies Λ being a closed set.B

Theorem 4.6

Let Λ_w denote the set of all solutions $\widehat{X_w}$ obtained by solving the weighted least-square problem given by (4.7) which is associated with the digital re-design of a proper LTI finite dimensional continuous-time SISO control system using the Weighted reduced-order PIM method proposed in Section 4.2 for a non-pathological T. Then, Λ_w is an open set.D

Proof

Let $W, \Delta W$ be diagonal with non-zero entries such that it has full rank and its inverse is uniquely defined. For all $\widehat{X_w} \in \Lambda_w$ obtained using a W, there exists diagonal $W' = W + \Delta W$ where

$\Delta W \neq 0$ and $\Delta W \to 0$ as $T \to 0$ with non-zero entries $(w_{ii}' \neq 0) \in R$ such that all elements $\widehat{X}_w$ obtained using W and contained in the ball $[\widehat{X}_w; r > 0]$ are also contained in Λ_w.B

Theorem 4.7

Denote a subset $\lambda \subset \Lambda$ such that, $\forall\ \widehat{X} \in \lambda$, $\widehat{Y} = A\widehat{X}$ yields a set of coefficients for the denominator polynomial of a discrete-time PITF as in (4.21) such that its roots lie in the domain of stability given in Table 2.1 for a non-pathological T. Then, λ is a closed set.D

Proof

From Theorem 4.5, since only a limited number of solutions $\widehat{X}$ to the least-square problem exist, the possible sets of digital controllers that will bring closed loop stability to the sampled-data system using these least-square solution is also limited. Therefore λ is a closed set.B

Theorem 4.8

Define a subset $\lambda_w \subset \Lambda_w$ such that, $\forall\ \widehat{X}_w \in \lambda_w$, $\widehat{Y}_w = A\widehat{X}_w$ yields a set of coefficients for the denominator polynomial of a PITF as in (4.21) whose roots lie in the domain of stability given in Table 2.1 for a non-pathological T. Then from the definitions of λ in Theorem 4.7, $\lambda \subset \lambda_w$.D

Proof

It is only necessary to show that the set of solutions $\widehat{X}$ contained in λ is in fact obtained as a special case of those in λ_w, by setting $W = I$.B

Remark 4.8

This shows that a larger set of solutions λ_w that brings closed loop stability to the sampled-data system can be found by adding W to (4.1) in forming the weighted least-square problem. This has special connection with Theorem 4.12.c

Theorem 4.9

A sampled-data system which is digitally re-designed by applying the weighted reduced-order PIM method to a proper LTI finite dimensional continuous-time SISO feedback control system using a non-pathological T is stable, if there exist a W for solving (4.7) such that λ_w is open and

$(\lambda_w \bigcap \Lambda_w) = \Lambda_w$.

Proof

If $\exists$ W in (4.8) such that $(\lambda_w \bigcap \Lambda_w) = \Lambda_w$, then $\forall$ $\widehat{X}_w \in \Lambda_w$, a set of stabilizing digital controllers can be formed for the particular T.B

Remark 4.9

The above can be strengthened if W can be found to satisfy Theorem 4.9 for *any* non-pathological T.c

Lemma 4.10

Assume that λ as defined in Theorem 4.9 is non-empty. Let Π denote the set of proper, rational, LTI digital controllers that results from the digital re-design of a proper, LTI finite dimensional continuous-time SISO control systems for a particular non-pathological T using the reduced-order PIM method described in Section 2.6.5. Then Π is an open set.D

Proof

If $\lambda \neq \emptyset$, then there exists at least one least-square solution $\widehat{X}$ of (4.1) that can be used to form a set of digital controllers that leads to closed loop stability for the sampled-data system. From the procedure described in (2.77) to (2.80) for constructing the transfer functions of the required digital controllers, *any* polynomial μ with its roots inside the domain of stability described in Table 2.1 will suffice in setting up a general 3-controller stable closed loop system.

Now, for all $\pi_{\widehat{x},\mu} \in \Pi$ obtained using μ, $\exists$ $\mu' = \mu + \Delta\mu$ also with roots inside the domain of stability described in Table 2.1, such that all elements $\pi_{\widehat{x},\mu'}$ obtained using μ' and contained in the ball $[\pi_{\widehat{x},\mu}; r > 0]$ are also contained in Π.B

Remark 4.10

Note that from the formulation of the discrete-time control system described in Section 2.6.5, the discrete-time PITF of the sampled-data system does not depend on the selection of μ.c

Lemma 4.11

Assume that $\lambda_w \neq \emptyset$. Let Π_w denote the set of proper, rational, LTI digital controllers that results from the digital re-design of the same continuous-time control system using the weighted reduced-order PIM method proposed in Section 4.3. Then Π_w is an open set.□

Proof

This is identical to the proof of Lemma 4.10, with λ and Π replaced by λ_w and Π_w respectively.■

Theorem 4.12

From the definitions of Π in Lemma 4.10 and Π_w in Lemma 4.11, $\Pi \subset \Pi_w$.□

Proof

It is suffice to show that the set of controllers obtained in Π is a special case of Π_w when $W = I$.■

Remark 4.12

What this represents is that the weighted reduced-order PIM method in general gives a larger set of stabilizing digital controllers for a particular T which a designer may employ. This is illustrated below in Figure 4.2

Figure 4.2: The sets Π and Π_w where $\Pi \subset \Pi_w$.

In light of Theorem 4.9, if a W can be found systematically for any non-pathological T such that the resultant sampled-data system is stable, then this bypass the need to find a range for T that guarantees closed loop stability as in Lemma 4.3.c

4.3 Consideration for reduced-order Controller Design

There are mainly three scenarios to consider during the design of closed loop sampled-data control systems using PIM methods.

a) Low Order Plant

In such a case, the order of digital controllers from applying the regular PIM digital re-design will also be low, though perhaps not as low as the designed analogue ones. In any rate, the order number is considered low enough such that using measures described in Section 2.7, it is possible to avoid much FWL effects in practical implementation. Is it still then justified to use the reduced-order PIM method? Section 4.2 showed that the application of reduced-order PIM method in general represents a deviation of the closed loop system performance from ones obtained by the PIM method. This can translate into having larger overshoots, more oscillatory motion and longer settling time for plant input and closed loop system output signals. Since in this case, in the absence of significant finite word length effect, the PIM method gives desirable sampled-data system performance, the simple verdict is: use the regular PIM method.

The example of the missile control system shown in Chapter 3 is used to illustrate the point: Figure 4.3 compares the step response of the continuous-time missile control system with that obtained by applying the PIM digital re-design method to the re-structured multi-loop system shown in Section 3.4.3. Recall that the analogue missile control system has a fourth-order plant and two first-order controllers, and the PIM digital re-design of the re-structured multi-loop system results in having four fifth-order controllers. In Figure 4.4 & Figure 4.5, the comparison is repeated with sampled-data systems employing lower-order digital controllers. These systems are designed using the reduced-order PIM method for multi-loop systems, illustrated in Section 3.4.4. An examination of the three figures reveals that the system response progressively deviates from the continuous-time design as the controller-orders decrease to attain those of the analogue ones. Therefore, in fact the regular PIM method gives the best performance in this case.

In practice, a designer will be able to know how high or low the plant order is from experience and more reliably, from computer simulation using softwares such as Fixed-Point Blocksets in

Simulink that allows the users to investigate the effect of FWL.

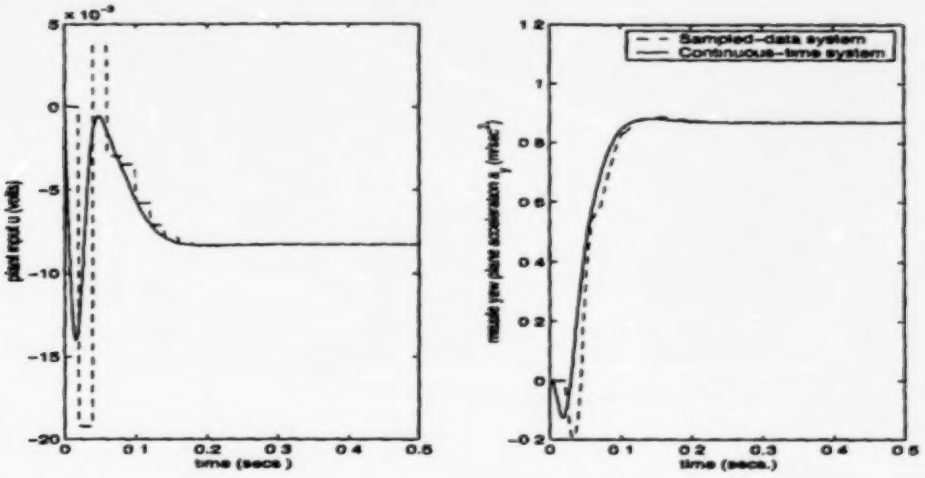

Figure 4.3: Step response of the sampled-data system obtained for $T = 0.02$ secs. using multi-loop PIM digital re-design, (a) plant input signal $\bar{u}$, (b) lateral acceleration of missile $\bar{a}_y$.

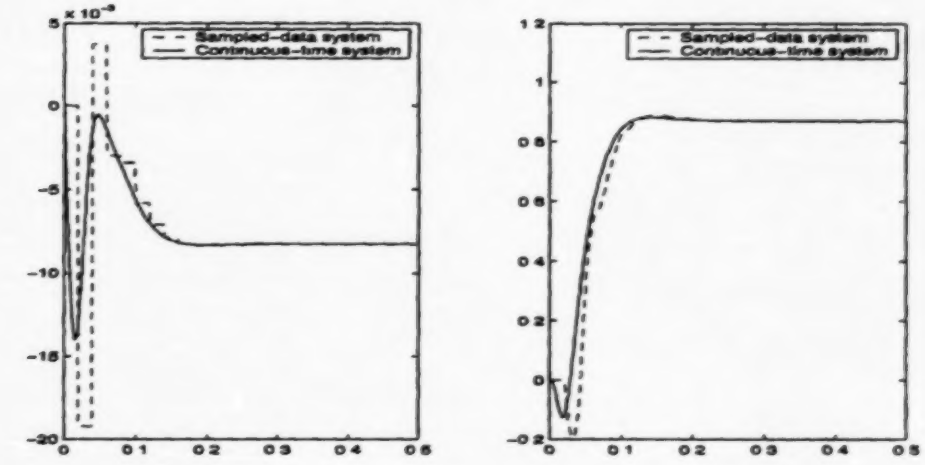

Figure 4.4: With $n = 2$, (a) plant input signal $\bar{u}$, (b) lateral acceleration of missile $\bar{a}_y$.

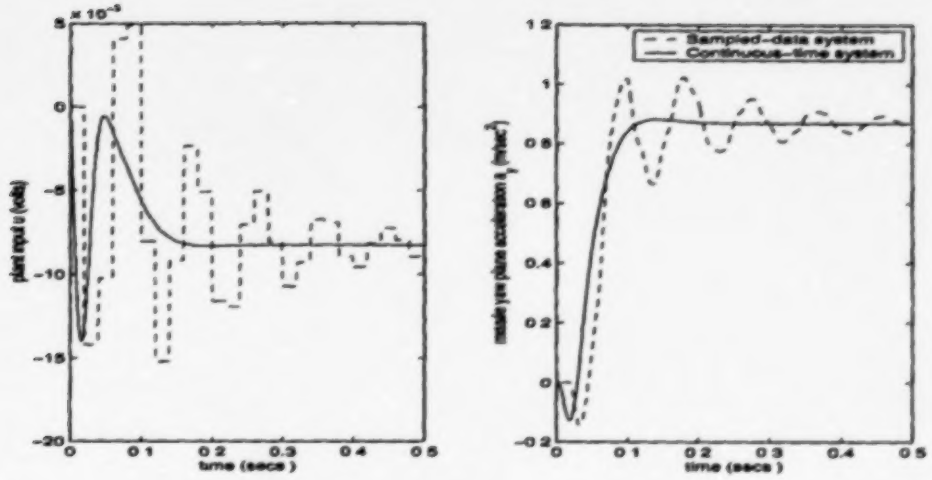

Figure 4.5: With $n = 1$, i.e. order of digital controllers is the same as continuous-time system, (a) plant input signal $\bar{u}$, (b) lateral acceleration of missile $\bar{a}_y$.

b) High Order Plant

In this situation, the order of controllers that result from applying the PIM method will also be high. This indicates a strong presence of finite word length effect in control algorithm calculation. Therefore, the choice is clear-It is necessary to use the reduced-order or weighted reduced-order PIM method to design lower-order controllers for the sampled-data system. The reason for this is that, while reduced-order controllers do result in less than desirable performance than what the full order controllers theoretically and ideally offer, when designed successfully with closed loop stability inherited and measures applied to reduce FWL effects in the implementation of reduced-order digital controllers, the resultant system response can be calculated by virtue of knowing the representation of the actual controllers, albeit reduced-order ones. In contrast, if the full order controllers are used, the FWL effect may be severe enough to sufficiently degrade the performance of the system, but the worst is that this performance is essentially unpredictable. This justifies the need for carrying out an order reduction.

c) Intermediate Order Plant

If the analogue plant under consideration falls into this category, then following arguments from the previous two cases, a course of action is not so immediately transparent. Instead, an iterative

procedure can be used to design the digital controllers step by step. If one considers carefully at the reduced-order PIM method, (4.1) reveals indirectly that the indices i and j, and as a result the order of controllers, can in fact be set arbitrarily so long as $(i+j+2)<(p+1)$ is satisfied. This is a nice incurred flexibility. Making use of this, the following design procedure is proposed: reduced the order of digital controllers from the full order ones in stages. In each step, calculate a new set of digital controllers by re-carrying out a reduced-order PIM digital re-design. In doing so, the resultant system response will differ increasingly from the desired ones. Therefore, check the FWL properties of the sampled-data system during each step. This repetitive procedure terminates when the designer decides a compromise between performance and acceptable FWL effect is reached.

The weighted reduced-order PIM method can play a significant role in this case in view of Theorem 4.12. In cases when the reduced-order PIM method fails to deliver stable closed loop controllers with a particular low order number, it is foreseeable that the weighted method may be able to solve the problem by proper selection of the weighting matrix. Therefore the set of digital controllers obtained using the weighted reduced-order PIM method can have lower-order than those obtained using the reduced-order PIM method as proposed by Rabbath et al in [32]. More research needs to be done on this topic.

4.4 Further Comments

Following discussions in Section 4.3 and referring to Figure 4.1, it is possible to infer that, the weighted reduced-order PIM method together with the regular PIM method forms a class of direct and systematic digital re-design method for high and low order plants that offers a range of closed loop digital controllers with varying order and thus closed loop performance. Depending on the specific performance criteron, the engineer can design a set of digital controllers in accordance with procedure described in Section 4.3. It remains, however, to formulate a reduced-order PIM method that would apply for MIMO systems. A partial remedy exists for the class of MIMO systems considered by Lemma 3.2, which shows that systems can be re-formulated as multi-loop systems and, thereafter, the reduced-order PIM method can be applied to the re-structured system

loop-by-loop, in the same spirit as the reduced-ordered multi-loop PIM method described in Section 3.4.4.

As a concluding remark, the need for performing controller order reduction or designing lower-order controllers for the PIM method is largest when the control algorithm calculation is to be carried out using fixed point arithmetic. If the specification of the sophisticated or mission critical control system calls for the budget to employ high-end floating point calculation units with a short computation time in comparison with the sampling interval, then following the above discussion, it is best to stick with the PIM method that are likely to produce sampled-data system with much closer characteristics to the designed continuous-time system performance.

Chapter 5

Conclusion

5.1 Research Contribution

This thesis examined several issues that contributed to the knowledge of continuous-time and discrete-time control system design. In sections of Chapters 2 and 3, the relationship between the sampling frequency and bandwidth of a MIMO system was clarified for employing local discretization on MIMO feedback system in the classical sense. For the design of SIMO systems, Chapter 3 investigated several properties related to SIMO continuous-time control system design. The procedure and usefulness for re-structuring a specific class of closed loop MIMO systems to multi-loop systems is shown. The research then focused on the indirect design of sampled-data system using PIM methods with particular reference to the control of yaw plane dynamics of an air-to-air missile model, which also belonged to the aforementioned class of MIMO systems. Section 3.3 illustrated that the application of MIMO PIM method on the aforementioned class of MIMO systems in general gave to different sampled-data systems in comparison to those obtained by applying the multi-loop PIM method on the re-structured mutli-loop system. Results from computer simulation displayed in Section 3.5 verified the Lemma. A framework was established in Section 3.4 that combined the mutli-loop and reduced order PIM method together into a single formulation. A simple extension as it was, the proposed scheme allows the direct design of low order digital controllers for the aforementioned class of analogue MIMO feedback systems.

Chapter 4 considered the issue of controller order reduction with particular consideration of the PIM digital re-design of analogue feedback systems. A weighted reduced order PIM formulation

was proposed, and the rapprochement property of the modified method in the time domain was ascertained and proven. The theoretical development showed that the proposed method enlarged the set of closed loop stabilizing low order digital controllers that a designer may employ for the PIM method. This in fact corresponded to an extra degree of freedom that an engineer may have available in sampled-data system design. Finally, some guidelines and practical consideration for the design of lower order controllers were given in reference to the PIM methods.

5.2 Future Research Work

Finding interesting research problems and topics is a challenging and yet rewarding exercise. During the course of this thesis, several related issues surfaced and they may be of interest. Relating to continuous-time SIMO systems, following work in Section 3.3, much remain to be done to extend design and analysis tool already available for MIMO systems, such as the characteristics-locus method, Nyquist-array method, direct sequential loop closing in controller design etc., to the SIMO setting. By treading on this dividing ridge between the SISO realm and MIMO realm, the effort would only serve to better understand how SISO and MIMO systems relate to one another.

As far as PIM method goes, there are several fronts that can be explored. First, related to SIMO systems as in Section 3.3, more analysis can be carried out to look into the frequency response of sampled-data system designed using the MIMO PIM and multi-loop PIM method, their sensitivity to disturbance, as well as effects of FWL on the *closed loop* system. In fact, all of these can be done for the different variants of PIM method. Studies in the past have compared local discretization with PIM methods qualitatively and quantitatively in the time domain; a frequency domain analysis would compliment the knowledge already obtained.

In the topic of controller order reduction relating to PIM methods, much further research is needed for the direct design of lower order digital controllers using the reduced order PIM method and its modification proposed in this thesis. The activity should be directed to focus on ways to guarantee the stability of the ensuing sampled-data system, by finding a T^* such that the stability

for all lesser non-pathological T is guaranteed, and in the case of the weighted reduced order PIM method, by formulating a weighting matrix as a function of T such that the resultant sampled-data system stability is guaranteed for all non-pathological T, therefore bypassing the need to find a T^* as above. All these previous discussions are, however, limited to SISO systems and the class of MIMO systems that can be re-structured as a multi-loop system, shown in Lemma 3.2. The case for MIMO system is yet to be addressed. The study can also be extended for *continuous-time* systems. These are large areas that require much investigation.

5.3 Epilogue

By its very nature, control engineering is a multi-disciplinary subject, and its development will always be tightly knitted to other branches of applied science. The success of control system design depends sound knowledge of control methodology and theory, but the importance of accurate and adequate system modelling cannot be neglected. It will be certainly be interesting to see how the research community carries this philosophy.

Blibliography

[1] W. Albanes (1981). "Design of Guidance and Control Digital Autopilots." *AIAA Journal of Guidance and Control*, Vol. 4, No.2, pages 126-133, March-April 1978.

[2] B.D.O. Anderson and Y. Liu (1989). "Controller Reduction: Concepts and Approaches." *IEEE Transactions on Automatic Control*, Vol. 34, No.8, pages 802-812, August 1989.

[3] B.D.O. Anderson (1993). "1992 Bode Prize Lecture—Controller Design: Moving from Theory to Practice." *IEEE Control Systems Magazine*, Vol. 13, No.4, pages 16-25, August 1993.

[4] A. Arrow (1985). "Status and Concerns for Bank-to-Turn Control of Tactical Missiles." *AIAA Journal of Guidance, Control and Dynamics*, Vol. 8, No.2, pages 267-274, March-April 1985.

[5] K.J. Åström, P. Hagander and J. Sternby (1984). "Zeros of Sampled Systems." *Automatica*, Vol.20, N0.1, pages 31-38, 1984.

[6] B.A. Bamieh and J.B. Pearson, Jr. (1092). "A General Framework for Linear Periodic Systems with Applications to H^∞ Sampled-Data Control." *IEEE Transactions on Automatic Control*, Vol. 37, No.4, pages 418-435, April 1992.

[7] T.Chen and B.A. Francis (1991). "Input-Output Stability of Sampled-Data Systems." *IEEE Transactions on Automatic Control*, Vol. 36, No.1, pages 50-58, January 1991.

[8] J.R. Cloutier, J.H. Evers and J.L. Feeley (1989). "Assessment of Air-to-Air Missile Guidance and Control Technology." *IEEE Control Systems Magazine*, Vol. 9, No.6, pages 27-34, October 1989.

[9] J.S. Freudenberg, R.H. Middleton and J.H. Braslavsky (1994). "Inherent Design Limitation for Linear Sampled-data Feedback Systems." In *Proceedings of the 1994 American Control Conference*, pages 3227-3231, Baltimore, Maryland.

[10] C. Ha and U.-L. Ly (1991). "Optimal Discrete-Time Static Output Feedback Design: A w'-Domain Approach." In *Proceedings of the 1991 American Control Conference*, pages 1269-1270, Boston, MA.

[11] H. Hanselmann (1987). "Implementation of Digital Controllers—A Survey." *Automatica*,

Vol. 23, No.1, pages 7-32, January 1987.

[12] J.P. Keller and B.D.O. Anderson (1990). "H_∞ Optimal Controller Discretization." In *Proceedings of the 29th Conference on Decision and Control*, pages 1781-1785, Honolulu, Hawaii.

[13] J.P. Keller and B.D.O. Anderson (1992). "A New Approach to the Discretization of Continuous-Time Controllers." *IEEE Transactions on Automatic Control*, Vol. 37, No.2, pages 214-223, February 1992.

[14] R.A. Kennedy and R.J. Evans (1990). "Digital Redesign of a Continuous Controller Based on Closed Loop Performance." In *Proceedings of the 29th Conference on Decision and Control*, pages 1898-1902, Honolulu, Hawaii.

[15] A.J. Koivo (1969). "Quantization Error and Design of Digital Control Systems." *IEEE Transactions on Automatic Control*, Vol. 14, No.1, pages 55-58, February 1969.

[16] V. Kucera (1993). "Diophantine Equation in Control—A Survey." *Automatica*, Vol.29, No.6, pages 1361-1375, 1993.

[17] R.H. Middleton and G.C. Goodwin (1986). "Improved Finite Word Length Characteristics in Digital Control Using Delta Operators." *IEEE Transactions on Automatic Control*, Vol. 31, No.11, pages 1015-1021, November 1986.

[18] Y. Liu, B.D.O. Anderson and U.-L. Ly (1990). "Coprime Factorization Controller Reduction with Bezout Identity Induced Frequency Weighting." *Automatica*, Vol. 26, No.2, pages 233-249, 1990.

[19] C.N. Nett, C.A. Jacobson and M.J. Balas (1984). "A Connection Between State-Space and Doubly Coprime Fractional Representations." *IEEE Transactions on Automatic Control*, Vol. 29, No.9, pages 831-832, September 1984.

[20] H. Öz, L. Meirovitch and C.R. Johnson (1980). "Some Problems Associated with Digital Control of Dynamical Systems." *AIAA Journal of Guidance and Control*, Vol. 3, No.6, pages 523-528, November-December 1980.

[21] K.S. Rattan (1984). "Digitalization of Existing Continuous Control Systems." *IEEE Transactions on Automatic Control*, Vol. 29, No.3, pages 282-285, March 1984.

[22] J.B. Slaughter (1964). "Quantization Errors in Digital Control Systems." *IEEE Transactions on Automatic Control*, Vol. 9, No.1, pages 70-74, January 1964.

[23] R.F. Whitbeck and L.G. Hofmann (1978). "Digital Control Law Synthesis in the *w'* Domain." *AIAA Journal of Guidance and Control*, Vol. 1, No.5, pages 319-326, September-October 1978.

[24] T. Mori, P.N. Nikiforuk, M.M. Gupta and N. Hori (1987). "A Class of Discrete time Models for a Continuous Time System." In *Proceedings of the 1987 American Control Conference*, pages 953-957, Minneapolis, MN.

[25] N. Hori, P.N. Nikiforuk and K. Kanai (1988). "On a Discrete-Time System Expressed In The Euler Operator." In *Proceedings of the 1988 American Control Conference*, pages 873-878, Atlanta, GA.

[26] N. Hori, T. Mori and P.N. Nikiforuk (1989). "A New Perspective for Discrete-Time Models of a Continuous-Time System." In *Proceedings of the 1989 American Control Conference*, pages 1659-1664, Pittsburgh, PA.

[27] N. Hori (1991). "On System Representations and Discrete-Time Models of a Multivariable System." In *Proceedings of the 1991 American Control Conference*, pages 2407-2412, Boston, MA.

[28] N. Hori, T. Mori and P.N. Nikiforuk (1992). "A New Perspective for Discrete-Time Models of a Continuous-Time System." *IEEE Transactions on Automatic Control*, Vol. 37, No.7, pages 1013-1017, July 1992.

[29] A.H.D. Markazi and N. Hori (1992). "A New Method with Guaranteed Stability for Discretization of Continuous-Time Control Systems." In *Proceedings of the 1992 American Control Conference*, pages 1397-1402, Chicago, IL.

[30] N. Hori, T. Mori and P.N. Nikiforuk (1994). "Discrete-Time Models of Continuous-Time Systems." In C.T. Leondes, editor, *Control and Dynamic Systems*, Vol. 66, pages 1-45. Academic Press, Toronto, ON.

[31] A.H.D. Markazi and N. Hori (1995). "Discretization of continuous-time control systems with guaranteed stability." In *IEE Proc.-Control Theory Appl.*, Vol. 142, No.4, pages 323-328, July 1995.

[32] C.A. Rabbath and N. Hori (1999). "Model Reduction of PIM-Based Digital Flight Control Systems." In *Proceedings of the 14th IFAC World Congress, preprint*, Vol. Q, pages 127-132, Beijing, China.

[33] C.A. Rabbath and N. Hori (1999). "Comparative Study of Digital Re-design Methods in the Control of a Fast Positioning Mechanism." In *Proceedings of the 17th Canadian Congress of Applied Mechanics*, pages 343-344, Hamilton, ON.

[34] N. Hori and C. Ng (1999). "On The Step Response of a Stable System With Distinct Poles." In *Proceedings of the 17th Canadian Congress of Applied Mechanics*, pages 345-346, Hamilton, ON.

[35] K.K. Ro and N. Hori (1999). "Digital Re-design of Multi-Loop Continuous-time Control Systems." In *Proceedings of the 17th Canadian Congress of Applied Mechanics*, pages 347-348, Hamilton, ON.

[36] R. Cormier Jr. (1989). "*Matched Z-Transform Models Under a New Classification Using the Euler Operator.*" Master's thesis. Department of Mechanical Engineering, McGill University, 1989.

[37] R. Comeau (1991). "*Numerical Properties of the Euler Operator in Digital Control.*" Mas-

ter thesis. Department of Mechanical Engineering, McGill University, 1991.

[38] A.H.D. Markazi (1994). *"A New Approach to the Digital Implementation of Analog Controllers and Continuous-time Reference Models."* Ph.D. thesis. Department of Mechanical Engineering, McGill University, 1994.

[39] C.A. Rabbath (1995). *"Sensitivity of the Discrete- to Continuous-Time Pole Transformation at Fast Sampling Rates."* Master thesis. Department of Mechanical Engineering, McGill University, 1995.

[40] R. Comeau (1997). *"Higher Order Discrete-Time Models with Applications to Multi-Rate Control."* Ph.D. thesis. Department of Mechanical Engineering, McGill University, 1997.

[41] C.A. Rabbath (1999). *"A Characterization and Performance Evaluation of Digitally Redesigned Control systems."* Ph.D. thesis. Department of Mechanical Engineering, McGill University, 1999.

[42] DERA (1996). *"Investigation of Digital Implementation Effects on a Missile Flight Control."* DERA/AS/FMC/WP97281/1.0, Defence Evaluation and Research Agency, Farnborough, Hampshire, England, U.K. Restricted.

[43] J. King (1997). *"Robust Multivariable Control Law Design For Missile Autopilots."* Ph.D. thesis, Department of Aerospace and Guidance Systems, School of Engineering and Applied Science, Royal Military College of Science, Shrivenham, U.K. Restricted.

[44] M. Lauzon and C. Ng (1998). *"A Vertical Launch Missile Optimized Autopilot Model."* DREV - TM - 9808, Research And Development Branch, Department of National Defence Canada. Restricted.

[45] P. Garnell (1980). *Guided Weapon Control Systems*, 2nd ed. Brassey's, U.K.

[46] J.H. Blakelock (1991). *Automatic Control of Aircraft and Missile*, 2nd ed. John Wiley, Toronto, ON.

[47] K.J. Åstrom, B. Wittenmark (1999). *Computer-Controlled Systems*, 3rd ed. Prentice Hall, Upper Saddle, N.J.

[48] P.R. Bélanger (1995). *Control Engineering*. Oxford University Press, New York.

[49] C.-T. Chen (1999). *Linear System Theory And Design*, 3rd ed. Oxford University Press, New York.

[50] T. Chen and B. Francis (1995). *Optimal Sampled-Data Control Systems*. Springer-Verlag, New York.

[51] R.V. Churchchill and J.W. Brown (1990). *Complex Variables and Applications*, 5th ed. McGraw-Hill, Toronto, ON.

[52] R.C.Dorf and R. Bishop (1998). *Modern Control Systems*, 8th ed. Addison-Wesley, Don Mills, ON.

[53] A. Feuer and G.C. Goodwin (1996). *Sampling in Digital Signal Processing and Control.* Birkhäuser, Boston, MA.

[54] G.F. Franklin, J.D. Powell and Emami-Naeini (1994). *Feedback Control of Dynamic Systems*, 3rd ed. Addison-Wesley, CA.

[55] G.F. Franklin, J.D. Powell and M. Workman (1998). *Digital Control of Dynamic Systems*, 3rd ed. Addison-Wesley, Don Mills, ON.

[56] G.H. Golub and C.F. Van Loan (1989). *Matrix Computations*, 2nd ed. The Johns Hopkins University Press, Baltimore, Maryland.

[57] T. Kailath (1980). *Linear Systems.* Prentice Hall, Englewood Cliffs, N.J.

[58] P. Katz (1981). *Digital Control Using Microprocessors.* Prentice Hall, Englewood Cliffs, N.J.

[59] D.C. Lay (1994). *Linear Algebra and Its Applications.* Addison-Wesley, Don Mills, ON.

[60] J.M. Maciejowski (1989). *Multivariable Feedback Design.* Addison-Wesley, Don Mills, ON.

[61] C.D. McGillem and G.R. Cooper (1991). *Continuous and Discrete Signal and System analysis*, 3rd ed. Saunders College Publishing, Toronto, ON.

[62] R.H. Middleton and G.C. Goodwin (1990). *Digital Control And Estimation.* Prentice Hall, Upper Saddle, N.J.

[63] P. Moroney (1983). *Issues in the Implementation of Digital Feedback Compensators.* The MIT Press, Cambridge, Massachusetts.

[64] B. Nobel (1969). *Applied Linear Algebra*, 2nd ed. Prentice Hall, Englewood Cliffs, N.J.

[65] J.G. Proakis and D.G. Manolakis (1996). *Digital Signal Processing*, 3rd ed. Prentice Hall, Upper Saddle, N.J.

[66] W.J. Ruge (1996). *Linear System Theory*, 2nd ed. Prentice Hall, Upper Saddle, N.J.

[67] G.B. Thomas, Jr. and R.L. Finney (1996). *Calculus and Analytic Geometry*, 9th ed. Addison-Wesley, Don Mills, ON.

[68] W.A. Wolovich (1974). *Linear Multivariable Systems.* Springer-Verlag, New York.

[69] W.A. Wolovich (1994). *Automatic Control Systems.* Saunders College Publishing, Toronto, ON.

[70] K. Zhou, J.C. Doyle and Keith Glover (1996). *Robust and Optimal Control.* Prentice Hall, Upper Saddle, N.J.

[71] *Fixed-Point Blockset User's Guide Version 1.0*, The MathWorks Inc.

[72] *Delta Toolbox Users Guide.*

Appendix

The bound on the error vector in Lemma 4.2

Since the discrete-time system associated with the "A" matrix is a SIM of the continuous-time system, and the desired discrete-time PITF is a MPZ model of the continuous-time PITF, one can write

$$\begin{aligned} A &= \bar{A} + \Delta\bar{A}, \text{ and} \\ Y &= \bar{Y} + \Delta\bar{Y} \end{aligned} \tag{A.1}$$

where

$$\lim_{T\to 0} \Delta\bar{A} = 0 \text{ and } \lim_{T\to 0} \Delta\bar{Y} = 0. \tag{A.2}$$

Further, knowing the solution $\bar{X}$ exists, if the columns of $\bar{A}$ are linearly independent, the solution is unique and can still be expressed as

$$\bar{X} = (\bar{A}^T\bar{A})^{-1}\bar{A}^T\bar{Y}. \tag{A.3}$$

Then, denote $(A^TW^2A)^{-1}$ as Ξ, a bound on the norm of the vector $[\widehat{X}_w - \bar{X}]$ can be established as

$$\left\|\widehat{X}_w - \bar{X}\right\| = \left\|(A^TW^2A)^{-1}A^TW^2Y - (A^TA)^{-1}A^TY\right\| \tag{A.4}$$

$$= \left\|\Xi(\bar{A}+\Delta\bar{A})^TW^2(\bar{Y}+\Delta\bar{Y}) - (\bar{A}^T\bar{A})^{-1}\bar{A}^T\bar{Y}\right\|$$

$$= \left\|\Xi\bar{A}^TW^2\bar{Y} - (\bar{A}^T\bar{A})^{-1}\bar{A}^T\bar{Y} + \Xi\Delta\bar{A}^TW^2\bar{Y} + \Xi(\bar{A}+\Delta\bar{A})^TW^2\Delta\bar{Y}\right\|$$

$$= \left\|\left[\Xi(\bar{A}+\Delta\bar{A})^TW^2(\bar{A}+\Delta\bar{A})\right]^{-1}(\bar{A}+\Delta\bar{A})^TW^2 - (\bar{A}^T\bar{A})^{-1}\bar{A}^T\right]\bar{Y} + \Xi\Delta\bar{A}^TW^2\bar{Y}\right\|$$

where

$$
\begin{aligned}
f_1 &= \left\| [(\bar{A}+\Delta\bar{A})^T W^2 (\bar{A}+\Delta\bar{A})]^{-1} \bar{A}^T W^2 - (\bar{A}^T\bar{A})^{-1}\bar{A}^T \right\| \left\| \bar{Y} \right\| \\
f_2 &= \left\| \Xi \right\| \left\| \Delta\bar{A}^T \right\| \left\| W^2 \bar{Y} \right\| \\
f_3 &= \left\| \Xi (\bar{A}+\Delta\bar{A})^T W^2 \right\| \left\| \Delta\bar{Y} \right\| .
\end{aligned}
\tag{A.5}
$$

From (4.11), one can express W as

$$
W = I + \Delta W \tag{A.6}
$$

where,

$$
\lim_{T \to 0} \Delta W = 0 . \tag{A.7}
$$

For the term f_1 in (A.5), using expression of W in (A.6) leads to

$$
\begin{aligned}
f_1 &= \left\| [(\bar{A}+\Delta\bar{A})^T W^2 (\bar{A}+\Delta\bar{A})]^{-1} \bar{A}^T W^2 - (\bar{A}^T\bar{A})^{-1}\bar{A}^T \right\| \left\| \bar{Y} \right\| \\
&= \left\| \left\{ [\bar{A}^T W^2 \bar{A}] + \Delta\bar{A}^T W^2 \bar{A} + \bar{A}^T W^2 \Delta\bar{A} + \Delta\bar{A}^T W^2 \Delta\bar{A} \right\}^{-1} \bar{A}^T W^2 - (\bar{A}^T\bar{A})^{-1}\bar{A}^T \right\| \left\| \bar{Y} \right\| \\
&= \left\| \left\{ (\bar{A}^T\bar{A}) + f_{11} + f_{12} \right\}^{-1} \bar{A}^T - (\bar{A}^T\bar{A})^{-1}\bar{A}^T + f_{13} + f_{14} \right\| \left\| \bar{Y} \right\|
\end{aligned}
\tag{A.8}
$$

where

$$
\begin{aligned}
f_{11} &= 2\bar{A}^T \Delta W \bar{A} + \bar{A}^T \Delta W^2 \bar{A} \\
f_{12} &= \Delta\bar{A}^T (I+\Delta W)^2 \bar{A} + \bar{A}^T (I+\Delta W)^2 \Delta\bar{A} + \Delta\bar{A}^T (I+\Delta W)^2 \Delta\bar{A} \\
f_{13} &= 2\left\{ (\bar{A}^T\bar{A}) + f_{11} + f_{12} \right\}^{-1} \bar{A}^T \Delta W \\
f_{14} &= \left\{ (\bar{A}^T\bar{A}) + f_{11} + f_{12} \right\}^{-1} \bar{A}^T \Delta W^2 .
\end{aligned}
\tag{A.9}
$$

The expressions for f_2 and f_3 can be obtained by substituting back Ξ for $(A^T W^2 A)^{-1}$ in (A.5). This gives

$$
\begin{aligned}
f_2 &= \left\| [(\bar{A}+\Delta\bar{A})^T (I+\Delta W)^2 (\bar{A}+\Delta\bar{A})]^{-1} \right\| \left\| \Delta\bar{A}^T \right\| \left\| (I+\Delta W)^2 \bar{Y} \right\| \\
f_3 &= \left\| [(\bar{A}+\Delta\bar{A})^T (I+\Delta W)^2 (\bar{A}+\Delta\bar{A})]^{-1} (\bar{A}+\Delta\bar{A})^T (I+\Delta W)^2 \right\| \left\| \Delta\bar{Y} \right\| .
\end{aligned}
\tag{A.10}
$$

Equations (A.8), (A.9) and (A.10) together give (4.19) and (4.20) in Chapter 4.